CRITICAL STUDY OF SHEAR CAPACITY OF REINFORCED CONCRETE BEAM HAVING FRP REINFORCEMENT

A Thesis submitted to Gujarat Technological University

for the Award of

Doctor of Philosophy

in

Civil Engineering

by

Tarak Prafulkumar Vora

[119997106010]

GUJARAT TECHNOLOGICAL UNIVERSITY
AHMEDABAD

[April – 2017]

CRITICAL STUDY OF SHEAR CAPACITY OF REINFORCED CONCRETE BEAM HAVING FRP REINFORCEMENT

A Thesis submitted to Gujarat Technological University

for the Award of

Doctor of Philosophy

in

Civil Engineering

by

Tarak Prafulkumar Vora

[119997106010]

under supervision of

Dr. Bharat J. Shah

GUJARAT TECHNOLOGICAL UNIVERSITY
AHMEDABAD

[April – 2017]

Declaration

I declare that the thesis entitled **"Critical Study of Shear Capacity of Reinforced Concrete Beam Having FRP Reinforcement"** submitted by me for the degree of Doctor of Philosophy, is the record of research work carried out by me during the period from October 2011 to September 2016 under the supervision of **Dr. Bharat J. Shah, Professor and Head, Applied Mechanics Department, Government Engineering College, Modasa** and this has not formed the basis for the award of any degree, diploma, associateship, fellowship, titles in this or any other University or other institution of higher learning.

I further declare that the material obtained from other sources has been duly acknowledged in the thesis. I shall be solely responsible for any plagiarism or other irregularities, if noticed in the thesis.

Signature of the Research Scholar Date: 15th April, 2017

Name of Research Scholar: **Tarak P. Vora**

Place: Ahmedabad

Certificate

I certify that the work incorporated in the thesis **"Critical Study of Shear Capacity of Reinforced Concrete Beam Having FRP Reinforcement"** submitted by **Tarak Prafulkumar Vora** was carried out by the candidate under my guidance. To the best of my knowledge: (i) the candidate has not submitted the same research work to any other institution for any degree, diploma, Associateship, Fellowship or other similar titles. (ii) the thesis submitted is a record of original research work done by Research Scholar during the period of study under my supervision, and (iii) the thesis represents independent research work on the part of the Research Scholar.

Signature of Supervisor Date: 15th April, 2017

Name of Supervisor: **Dr. Bharat J. Shah**
Professor & Head, Applied Mechanics Department,
Government Engineering College, Modasa

Place: Ahmedabad

Originality Report Certificate

It is certified that PhD Thesis titled **"Critical Study of Shear Capacity of Reinforced Concrete Beam Having FRP Reinforcement"** by **Tarak P. Vora** has been examined by us. We undertake the following:

a. Thesis has significant new work / knowledge as compared already published or is under consideration to be published elsewhere. No sentence, equation, diagram, table, paragraph or section has been copied verbatim from previous work unless it is placed under quotation marks and duly referenced.
b. The work presented is original and own work of the author (i.e. there is no plagiarism). No ideas, processes, results or words of others have been presented as Author own work.
c. There is no fabrication of data or results which have been compiled / analysed.
d. There is no falsification by manipulating research materials, equipment or processes, or changing or omitting data or results such that the research is not accurately represented in the research record.
e. The thesis has been checked using **<Turnitin>** (copy of originality report attached) and found within limits as per GTU Plagiarism Policy and instructions issued from time to time (i.e. permitted similarity index <=25%).

Signature of Research Scholar Date: 15th April, 2017

Name of Research Scholar: **Tarak P. Vora**

Place: Ahmedabad

Signature of Supervisor Date: 15th April, 2017

Name of Supervisor: **Dr. Bharat J. Shah**
Professor & Head, Applied Mechanics Department,
Government Engineering College, Modasa

Place: Ahmedabad

Turnitin – Report

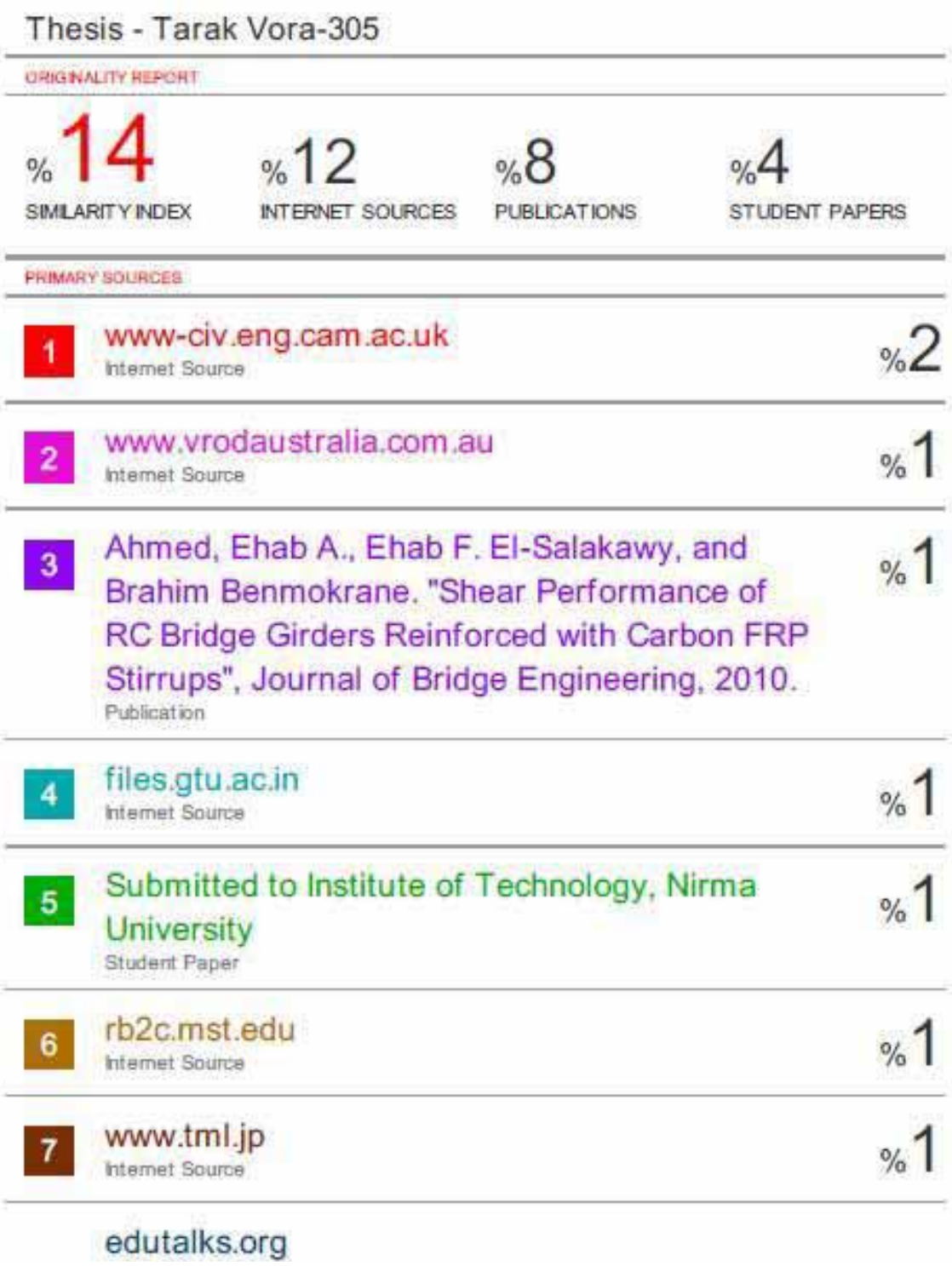

Thesis - Tarak Vora-305

ORIGINALITY REPORT

%14	%12	%8	%4
SIMILARITY INDEX	INTERNET SOURCES	PUBLICATIONS	STUDENT PAPERS

PRIMARY SOURCES

1	www-civ.eng.cam.ac.uk Internet Source	%2
2	www.vrodaustralia.com.au Internet Source	%1
3	Ahmed, Ehab A., Ehab F. El-Salakawy, and Brahim Benmokrane. "Shear Performance of RC Bridge Girders Reinforced with Carbon FRP Stirrups", Journal of Bridge Engineering, 2010. Publication	%1
4	files.gtu.ac.in Internet Source	%1
5	Submitted to Institute of Technology, Nirma University Student Paper	%1
6	rb2c.mst.edu Internet Source	%1
7	www.tml.jp Internet Source	%1
	edutalks.org	

PhD Thesis Non-Exclusive License to Gujarat Technological University

In consideration of being a PhD Research Scholar at GTU and in the interests of the facilitation of research at GTU and elsewhere, I, **Tarak Prafulkumar Vora**, having Enrollment No. **119997106010** hereby grant a non-exclusive, royalty free and perpetual license to GTU on the following terms:

a) GTU is permitted to archive, reproduce and distribute my thesis, in whole or in part, and / or my abstract, in whole or in part (referred to collectively as the "Work") anywhere in the world, for non-commercial purposes, in all forms of media;

b) GTU is permitted to authorize, sub-lease, sub-contract or procure any of the acts mentioned in paragraph (a);

c) GTU is authorized to submit the Work at any National / International Library, under the authority of their "Thesis Non-Exclusive License";

d) The University Copyright Notice © shall appear on all copies made under the authority of this license;

e) I undertake to submit my thesis, through my University, to any Library and Archives. Any abstract submitted with the thesis will be considered to form part of the thesis.

f) I represent that my thesis is my original work, does not infringe any rights of others, including privacy rights, and that I have the right to make the grant conferred by this nonexclusive license.

g) If third party copyrighted material was included in my thesis for which, under the terms of the Copyright Act, written permission from the copyright owners is required, I have obtained such permission from the copyright owners to do the acts mentioned in paragraph (a) above for the full term of copyright protection.

h) I retain copyright ownership and moral rights in my thesis, and may deal with the copyright in my thesis, in any way consistent with rights granted by me to my University in this non-exclusive license.

i) I further promise to inform any person to whom I may hereafter assign or license my copyright in my thesis of the rights granted by me to my University in this non-exclusive license.

j) I am aware of and agree to accept the conditions and regulations of PhD including all policy matters related to authorship and plagiarism.

Signature of Research Scholar Date: 15th April, 2017

Name of Research Scholar: **Tarak P. Vora**

Place: Ahmedabad

Signature of Supervisor Date: 15th April, 2017

Name of Supervisor: **Dr. Bharat J. Shah**
Professor & Head, Applied Mechanics Department,
Government Engineering College, Modasa

Place: Ahmedabad

Thesis Approval Form

The viva-voce of the PhD Thesis submitted by **Shri Tarak Prafulkumar Vora** (Enrollment No. 119997106010) entitled **"Critical Study of Shear Capacity of Reinforced Concrete Beam Having FRP Reinforcement"** was conducted on _____ at Gujarat Technological University.

(Please tick any one of the following option)

☐ The performance of the candidate was satisfactory. We recommend that he/she be awarded the PhD degree.

☐ Any further modifications in research work recommended by the panel after 3 months from the date of first viva-voce upon request of the Supervisor or request of Independent Research scholar after which viva-voce can be re-conducted by the same panel again.

(briefly specify the modifications suggested by the panel)

☐ The performance of the candidate was unsatisfactory. We recommend that he/she should not be awarded the PhD degree.

(The panel must give justifications for rejecting the research work)

Dr. Bharat J. Shah (Supervisor)
Professor & Head, Applied Mechanics Department,
Government Engineering College, Modasa

1) (External Examiner 1) Name and Signature

2) (External Examiner 2) Name and Signature

3) (External Examiner 3) Name and Signature

Abstract

Sustainable structures are the need of today where the root cause of deterioration of the structures is corrosion of steel reinforcement. Different forms of FRPs have proved to be a good alternative to the conventional steel reinforcement because of the properties like high tensile strength, noncorrosive, nonmagnetic and light weight. Extensive research is ongoing worldwide and design recommendations are produced by various standards; even though, there are many challenges for using FRPs as primary reinforcement. This study is concentrated on shear capacity of RC beam elements using FRP reinforcement, specifically shear contribution made by FRP shear reinforcement.

Various design standards adopt different approaches to predict shear contribution made by the stirrups by keeping permissible strain limit or bend strength as upper limit. The range of permissible strain in FRPs is from 0.0025 to 0.004 in different standards (i.e. ISIS Canada, JSCE and ACI) which are very close to strain limit of steel reinforcement. Marginal difference between theoretical predictions and experimental results in the literature motivated to investigate the shear capacity of the beams with FRP reinforcement in flexure as well as shear.

Advance testing on thirteen RC beams of size 230 x 300 x 2000 mm with GFRP as flexural and shear reinforcement is done by data observation of strain development at critical locations as well as deflection at midspan. Different strain gauges like PL-90-11-3L for concrete (surface), BFLA-5-5-3L for composite reinforcement (GFRP) and FLA-3-11-1L for steel made by TML, Japan are used for strain measurement. Multi channel data acquisition system TMR-200 is used for data recording, where the midspan displacement is observed by displacement transducers CDP – 100. Perfect beam action was observed as well as all the type of shear failure like diagonal tension, shear compression, shear tension and stirrup failure were observed depending on the reinforcement and loading configuration. It is observed that average ultimate strains as well as at 0.5 mm crack width are considerably higher than the permissible limits prescribed in above mentioned standards.

The study concluded with recommendation to increase permissible strain limit of shear reinforcement specified by ISIS Canada, JSCE and ACI to improve the efficiency of the design recommendations.

Acknowledgement

It is pleasure to me to express deep sense of gratitude to my honorable supervisor **Dr. Bharat J. Shah**, Professor & Head, Applied Mechanics Department, Government Engineering College, Modasa, Gujarat, India. His valuable guidance, ever enthusiasm and parental care have been my invaluable assets for this research work.

My special thanks to my overseas supervisor **Dr. Vinay Dayal**, Associate Professor, Iowa State University, Ames, Iowa, US for extending his pin pointed guidance and moral support; he has provided to me during my present.

I am very much thankful and grateful to my Doctoral Progress Committee members **Dr. Hemant S. Patil**, Professor, Applied Mechanics Department, SVNIT, Surat and **Dr. Urmil V. Dave**, Professor, Civil Engineering Department, Nirma University, Ahmedabad for mentoring me and providing me valuable guidance at every stage of this research work.

I shall take this opportunity to express my deep thanks to the **Management** and Dean **Dr. R. B. Jadeja** Marwadi Education Foundation, Rajkot for providing laboratory facilities for the experimental work and continuous moral support to complete this research work.

My heartily thanks and gratitude to **Dr. Chaitanya S. Sanghvi**, Professor, Applied Mechanics Department, L. D. College of Engineering, Ahmvedabad and **Dr. Vasant Matsagar**, Associate Professor, Department of Civil Engineering, IIT Delhi, New Delhi for their motivation and moral support throughout this work.

I would like to pay my sincere thanks to my dear friends **Mazhar Dhankot**, **Ankit Rathod** and **Departmental Colleagues** for continuous support in accomplishing this experimental work.

I am deeply grateful to my wife **Nancy**, daughter **Mrinal** and son **Shreyansh**; their encouragement, love, patience and understanding have remained source of inspiration and motivation throughout.

Any word of acknowledgment to my **parents, Urmilaben** and **Prafulkumar** may not be sufficient; I dedicate these work and thesis to my parents.

Tarak Prafulkumar Vora

Table of Contents

List of Abbreviations

FRP	: Fiber Reinforced Polymer
GFRP	: Glass Fiber Reinforced Polymer
CFRP	: Carbon Fiber Reinforced Polymer
AFRP	: Aramid Fiber Reinforced Polymer
ISIS	: Intelligent Sensing for Innovative Structures, Canda
JSCE	: Japan Society of Civil Engineering standard
ACI	: American Concrete Institute
CSA	: Canadian Standards Association standards
RC	: Reinforced Concrete
FRP-RC	: FRP – Reinforced Concrete
UP	: Unsaturated Polyester
MCFT	: Modified Compression Field Theory
SCFT	: Simplified Compression Field Theory
STM	: Strut and Tie Model
HSC	: High Strength Concrete
SCC	: Self-Compacting Concrete

List of Notations

A_{fv} : Total cross-sectional area of shear reinforcement (mm^2)

A_g : Total cross-sectional area of the member (mm^2)

A_s : Area of cross section of steel or FRP reinforcing bars (mm^2)

b : Beam width (mm)

c : Neutral axis depth (mm)

d : Distance from extreme comp. fiber to centroid of tension r/f (mm)

d_b : Bar diameter (mm)

d_v : Effective shear depth for longitudinal reinforcement (mm)

E_{fl} : Modulus of elasticity of longitudinal reinforcement (MPa)

E_{fv} : Modulus of elasticity of the shear reinforcement (MPa)

E_s : Modulus of elasticity of steel (MPa)

f_c : Compressive strength of the concrete (MPa)

f_{cr} : Cracking strength of the concrete (MPa)

$f_{FRPbend}$: Strength of bent portion of FRP bar (MPa)

f_{FRPu} : Design tensile strength of FRP (MPa)

f_{fuv} : Tensile strength of the straight portion of the shear reinforcement (MPa)

f_{mcd} : Design compressive strength of concrete allowing for size effect (MPa)

h : Total depth of the member (mm)

M_d : Design bending moment (N/mm)

M_f : Factored moment at a section (N/mm)

M_o : Decompression moment (N/mm)

N_f : Factored axial load occurring simultaneously with V_f (N)

n_f : Modular ratio

r_b : Internal bend radius of the FRP stirrups (mm)

s : Spacing of shear reinforcement (mm)

s_z : Crack spacing parameter

s_{ze} : Equivalent crack spacing parameter; shall not be taken less than $0.85s_z$

V_c : Factored shear resistance provided by tensile forces in concrete (N)

V_f : Factored shear force at a section (N)

V_{FRP} : Factored shear resistance provided by the FRP shear reinforcement (N)

V_r : Factored shear resistance (N)

α_s : Angle between the shear reinforcement and axis of the beam

β : Factor used to account for the shear resistance of cracked concrete

ε_{fv} : Strain in an FRP stirrup

ε_x : Longitudinal strain at midheight of the cross section

θ : Angle of inclination of the principal diagonal comp.stress (in degrees)

γ_b : Safety factor=1.3

γ_{mfb} : Safety factor for the bent portion=1.3

ρ_{fl} : Flexural reinforcement ratio

ρ_{fv} : Shear reinforcement ratio

σ_{fv} : Vertical stress in the FRP stirrups (MPa)

σ_N : Stress in concrete due to axial loads (MPa)

List of Figures

List of Tables

.

List of Appendices

CHAPTER : 1

Introduction

1.1 General

Service life of the structures has remained a great concern for the growing as well as the stable economy. Major cause of deterioration of the structure are corrosion of steel, fatigue, and increase in service loads, which in result produces the reduced life of the structures[1]. With the advent of the technological revolution, it is equally important to explore and acknowledge the novel material to suit to the current state of affairs. Due to non-corrosive nature, different forms of FRPs have gained the acceptance as an alternative to the steel reinforcement. However, anisotropic, brittle elastic behavior, low modulus of elasticity, bend strength and bond characteristics make the FRPs different from steel reinforcement[2-10]. Even due to high strength and stiffness-to-weight ratio, FRPs have gain attraction in repair, retrofitting and strengthening of damaged structures also[11-13]. Glass Fiber Reinforced Polymer (GFRP) has no significant effect of harsh environmental condition of bond behavior[14]. Number of guidelines and standards are produced for the safe design using FRP reinforcement by various agencies like Intelligent Sensing for Innovative Structures, Canadian Network of Excellence (ISIS Canada 2007)[15]; Japan Society of Civil Engineering standard (JSCE 1997)[16]; International Federation for Structural Concrete standard (fib 2007)[17]; American Concrete Institute ; ACI 440.1R-06 (ACI 2006)[18] and Canadian Standards Association standards CSA S6-06 (CSA 2006)[19] and CSA S806-12 (CSA 2012)[20] worldwide. Behavior of the beam in shear is found complex. Shear failure of an RC beam is a type of failure mode that has a catastrophic effect and occurs with no advance warning of distress[21,22]. Almost all the recommendations are following same format $V_r = V_c + V_s$, where total shear capacity (V_r) is the individual contribution of concrete (V_c) and stirrups (V_s). However, all the standards have adopted different approaches to derive individual contributions, which provide conservative results in overall.

Total five mechanisms for the concrete contribution (V_c) are reported by ACI-ASCE Committee 445 (1998)[23] for the beams without shear reinforcement as shear resistance of (1) uncracked concrete in compression zone, (2) aggregate interlock, (3) residual tensile stress across the shear cracks, (4) dowel action, and (5) arch action. Variety of experimentation have been done on the FRP-reinforced concrete (FRP-RC) beams without shear reinforcement to evaluate V_c[24-42], whereas limited experimentation is done to evaluate V_s on FRP-RC beams.

To quantify stirrups contribution V_s, similar relationship in FRP-RC elements is used as for steel reinforced concrete elements just by changing the stress level at failure in almost all the current recommendations. Different recommendations provide limiting strain value for the FRP stirrups to avoid stirrup rupture in bent portion and to control crack width in the shear zone. From the literature, it is found that the tensile strength and stiffness of FRP stirrups are lesser than the straight element because of manufacturing of FRPs. Bend strength is also governed by manufacturing process, bend radius, bar diameter and type of reinforcing bar[43-46]. Kinking of the innermost fibers would take place because of reduced strength of bend portion compared to straight portion. Collectively, bend strength is governed by manufacturing process, bend radius, bar diameter and type of reinforcing bar (ACI 2006).

In addition, it was observed that concrete contribution enhances after the formation of the first shear crack in FRP-RC elements. Even lower spacing of FRP stirrups enhances the shear capacity due to confinement of concrete. This helps in improving aggregate interlock and also controls the shear cracks. The strain limit in FRP stirrups, as specified in different codes and guidelines, enables better, but still conservative in predictions of shear strength of concrete members reinforced with GFRP stirrups[46].

Permissible strain limits in the stirrups from 0.002 to 0.004 in different recommendations is one of the significant parameter to quantify the shear contribution in FRP-RC elements. The objective of the research is to perform advanced testing on the beams by varying most influencing parameters to ascertain the strain level in the FRP rebars and to explore the scope of improving efficiency of the current design recommendations related to shear capacity of FRP reinforcement.

1.2 Objectives and Scope of Work

The research work focused on, experimental investigation of RC beams having FRP reinforcement in shear as well as in flexure and to explore the possibility of improving shear capacity considering FRP as an alternative to the steel reinforcement for sustainable structures.

1.2.1 Objective of Work

The main objective of the work is to investigate the shear behavior of RC beams with FRP reinforcement experimentally. It is aimed to determine strain level in the FRP stirrups at various stages of loading and the gap between theoretical predications for shear strength by various design standards and experimental behavior. It is also aimed to explore the scope for increase in strain limit in the FRP stirrups recommended by various design standards for determination of shear contribution made by FRP stirrups.

1.2.2 Scope of Work

The scope of the study involves the following stages by having full scale testing of real size beams.

- Review of current design standards (ISIS Canada, JSCE and ACI) related to shear contribution made by concrete and FRP reinforcement.
- To perform parametric investigation to determine the most influencing parameters contributing the shear capacity of the beam. It helps to decide the sample size which covers whole range of shear failure.
- To finalize the experimental program for materials to be used and cross verification of their properties as well as to define testing procedure and advanced instrumentation for the observation of experimental data.
- Data analysis and result interpretation to derive some conclusions compatible with the objective of the study.

1.3 Methodology

For achieving objectives of the research, parametric study, design of elements, experimental work, analytical study and behavioral study is done. Research methodology consists of review of various design recommendations like Canadian, Japanese and

American standards. Parametric study of the RC beam reinforced with FRP reinforcement is made to determine most influencing parameters which affects on shear capacity. Analytical study of beams experimented with GFRP reinforcement with variations in loading positions and reinforcement detailing is done. Behavioral study is made in terms of crack development and bond characteristic at ultimate stage to check feasibilty of FRP as an alternative to steel reinforcement. A parametric formulation is derived for shear capacity of beam with FRP reinforcement.

1.3.1 Research Hypothesis

Literature has shown that analytical and experimental results are not matching for the shear capacity of the FRP RC beams. Strain limit for FRP reinforcement specified by various standards are close to the steel reinforcement. If strain limit is changed as per the behavior and property of FRP reinforcement, gap of the analytical and experimental results can be reduced. Hence, following is hypothesis of the study.

"The range of permissible strain limit in various design standards is from 0.025 to 0.004 which is after stage wise modification from 0.002 specifically used for steel reinforcement. The range of actual strain at ultimate stage is from 0.012 to 0.03, which is considerably higher than the permissible. If permissible strain limit is increased depending on experimental behavior, effective utilization of the FRP reinforcement can be increased which leads to economical design."

1.4 Organization of Thesis

This thesis consists of six chapters.

Chapter 1 provides the outline of the research conducted with its objective, scope and approach adopted.

Chapter 2 contains a brief review of FRP materials and their applications in the structural engineering field. Shear capacity evaluation of reinforced concrete sections and type of failures are also discussed in this chapter. In addition, research programs conducted to investigate the shear capacity and its performance of FRP reinforced concrete sections are mentioned.

Chapter 3 describes the experimental program of the proposed study. Details of beam, specimens, constituent materials, instrumentation, test setup and brief description of test procedure are given.

Chapter 4 presents the observed data in the form of test result like crack load, ultimate load, strain values, type of failure and various chart like shear force verses strain, deflection, crack width, etc.

Chapter 5 deals with the design approach for computing the shear capacity of FRP reinforced beam adopted by ISIS Canada, JSCE, Japan and ACI with analytical justification for the improvement of design recommendations. This also includes the modification suggested for the improvement of design recommendation to reduce the gap between experimental and predicted values.

At the end, Chapter 6 provides emerged conclusions and recommendations for future research work.

CHAPTER : 2

Literature Review

2.1 General

The application of Fiber Reinforced Polymer (FRP) as primary reinforcement is becoming increasingly popular and accepted by owners, designers, and contractors due to outstanding combinations of their unique characteristics compared to any other construction materials. Strength-to-weight ratio of FRP composites is significantly higher than metals and other materials in construction industry. Additionally, these are non-magnetic, resistant to chemicals and non-corrosive. This is attractive and highly cost effective due to improved durability, easier handling & transportation, higher fatigue resistance, and lower maintenance costs with improved on-site productivity. FRPs have made their position in various construction applications because of such advantageous characteristics[47,48]. Various forms of FRPs have been also accepted as one of the reliable options in rehabilitation of structures also. This section provides brief details on FRP composites and their applications in the field of structural engineering. The main focus of this section is shear capacity of RC beams fully reinforced with FRP composites. The research investigations for evaluation of shear performance of FRP reinforced beams are reviewed.

2.2 Fiber Reinforced Polymer (FRP) Composites

Usually, two or more dissimilar materials form a composite, where the property of composite is completely different from those of their constituents. The major advantage of composite is the complementary nature of their constituents. For example, glass fibers having high tensile strength are subjected to environmental damage and bending, where counterpart polymers are malleable, protective to fiber surface and weak in tension.

FRP composite contains three main elements high strength fibers, polymer resin and additives. The additives include heat stabilizers, impact modifiers, plasticizers, flame retarders, light stabilizers, antistatic agents, blowing agents, and others, which shall be used as per the specific use. The major affecting factors on the performance of FRP

composite are fiber orientation, fiber mechanical properties, composition, length, and shape of the fibers, mechanical properties of resin matrix, and finally adhesive bond between fibers and matrix.

High strength fibers are oriented unidirectional and embedded in a polymer resin. Different types of fibers like carbon, glass, and aramid are the main load-carrying elements having wide range of strengths and stiffness. They have linear stress-strain relationship up to failure. These fibers are commercially available in continuous filaments.

The fibers are encapsulated and surrounded by polymer resin to bind them together. Importantly, this is the medium to distribute the load evenly in all the fibers of the section. Also, it protects the fibers from damage and maintain their alignment. Two types of polymers are available; thermosetting (e.g. epoxy and polyester) and thermoplastic (e.g. nylon) polymers. The mechanical properties and chemical compositions would be supplied by the manufacture; even reference details are currently available in many textbooks[49,50].

2.2.1 Fibers (Reinforcement)

Fibers are the main constituent of the composite to carry load and occupy the largest area in the cross section of the composite. Principal fibers for the various applications in the field of civil engineering are glass, carbon and aramid. Even the fibers are made from natural material jute. The major factors affects on the performance of composite are; type, orientation, length, shape, composition of fibers, and bond between fibers and matrix. A unidirectional fiber orientation is anisotropic. This results in maximum strength and modulus along the fiber axis. A planar arrangement of fibers along two directions has different strengths at various angle of fiber orientation. Where, the three dimensional array is isotropic, however, strength is substantially lower than the one-dimensional arrangement. Mechanical properties in unidirectional arrangement are proportional to the percentage fibers by volume oriented in the same direction as shown in Fig. 2.1. Mechanical properties and chemical resistance of different fibers are listed in Table 2.1 and 2.2[52] respectively.

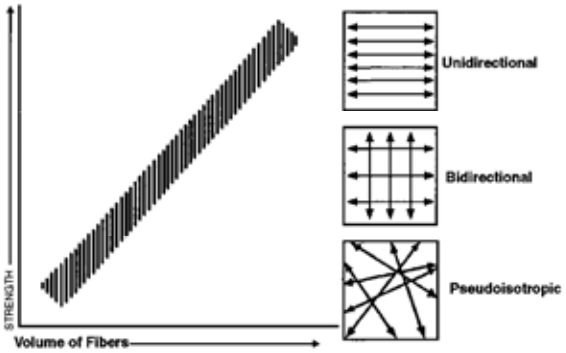

FIGURE 2.1 Strength relation to fiber orientation[50]

TABLE 2.1 Mechanical properties of fibers

Fiber Type		Tensile Strength [MPa]	Modulus of Elasticity [GPa]	Elongation [%]	Coefficient of Thermal Expansion [x10^{-6}]	Poisson's Ratio
CARBON						
PAN	**High Strength**	3500	200-240	1.3-1.8	-1.2 to -0.1 (α_{frpL}) 7 to 12 (α_{frpT})	-0.2
	High Modulus	2500-4000	350-650	0.4-0.8		
Pitch	**Ordinary**	780-1000	38-40	2.1-2.5	-1.6 to -0.9 (α_{frpL})	N/A
	High Modulus	3000-3500	400-800	0.4-1.5		
ARAMID						
Kevlar 29		3620	82.7	4.4	N/A	0.35
Kevlar 49		2800	130	2.3	-2.0 (α_{frpL}), 59 (α_{frpT})	
Kevlar 129		4210 (est.)	110 (est.)	--	N/A	
Kevlar 149		3450	172-179	1.9	N/A	
Twaron		2800	130	2.3	-2.0 (α_{frpL}), 59 (α_{frpT})	
Technora		3500	74	4.6	N/A	
GLASS						
E-Glass		3500-3600	74-75	4.8	5.0	0.2
S-Glass		4900	87	5.6	2.9	0.22
Alkali Resistant Glass		1800-3500	70-76	2.0-3.0	N/A	N/A

- **Glass Fibers :** Glass is the predominant fiber for various applications in civil engineering **because** of the proper economic balance between strength and cost properties. They are made from molten glass spun from electrically heated platinum rhodium alloy bushings at very high speed. These filaments are cooled from 1260°C to room temperature within a very short span of 10-5 seconds. Different commercially available glass fibers like E-glass, Z–glass, A–glass, C–glass and S–glass are used specifically as per their properties[49]. Glass fibers are having high tensile strength (1800–4900 MPa) with high chemical resistance, lower cost and excellent insulating properties. In addition, glass fibers are insulators of heat as well as electricity.

- **Carbon Fibers :** Carbon fibers contain 90% carbon by weight obtained by controlled pyrolysis of appropriate fibers. The term Graphite Fiber is used if carbon content is above 95%. Mainly two types of carbon fibers are there, namely polyacrylonitrile fibers (PAN) and Pitch-based fibers. PAN fibers are having high modulus of elasticity (350–650 GPa) and high strength (1500–5600 MPa). Where, the pitch-based fibers are made from coal or petroleum with lower strength and modulus of elasticity. Pitch-based fibers are cheaper than PAN based fibers. They are ideally suitable where strength, stiffness, outstanding fatigue resistance and lower weight constitute critical requirement. Even they perform well in temperature resistance, damping and chemical action[49].

- **Aramid Fibers :** Aramid fibers are aromatic compound of carbon, oxygen, hydrogen, and nitrogen. It is produced from para-phenylene diamine and terephthaloyl chloride. They are manufactured first in Germany with the brand name “Kevlar”. The aromatic ring structure provides higher thermal stability and para-configuration contributes to rigid and stiff molecules that lead to higher impact resistance, tensile strength and about 50% higher modulus than glass. However, compressive strength of aramid fibers remains very low. The density of aramid fibers is also very low in comparison to glass and carbon[49,51].

TABLE 2.2 Chemical resistance of fibers

Fiber Type		Acid Resistance	Alkali Resistance	Organic Solvent Resistance
CARBON				
PAN	**High Strength**	Good	Excellent	Excellent
	High Modulus	Excellent	Excellent	Excellent
Pitch	**Ordinary**	Excellent	Excellent	Excellent
	High Modulus	Excellent	Excellent	Excellent
ARAMID				
Kevlar 49		Poor	Good	Excellent
Technora		Good	Good	Good
GLASS				
E-Glass		Poor	Fair	Excellent
S-Glass		Good	Poor	N/A
Alkali Resistant Glass		Good	Good	N/A
OTHERS				
EC-Polyethylene		Excellent	Excellent	Excellent
Polyvinyl Alcohol Fibre		Good	Good	Good
Steel Fibre		Poor	Excellent (Sodium) Poor (Brine)	Excellent

2.2.2 Polymers

Polymers can be in liquid or solid state, where the cured polymer is called as matrix. Matrixes individually do not contribute in carrying load. They contribute in transferring the loads between the fibers. Additionally, they protect the fibers from the environmental attack and mechanical abrasion. The matrix also provides lateral stability in buckling of fibers under compressive load[50]. Overall performance of the composite depends on constituent materials, arrangement of primary load-bearing element of composite (reinforcing fibers), and interaction between them (fibers and matrix).

- **Thermoset versus Thermoplastic Matrix :** These matrixes can be classified in two categories, thermosets and thermoplastics based on their reaction on heating and cooling. Selection of matrix is important because each of them will have different in-plane or inter-laminar shear properties. In-plane shear strength is useful for components under torsion or in-plane shear, where inter-laminar shear strength is important in bending. Some of the advantages of thermosets against thermoplastics are better creep resistance, thermal stability, chemical resistance, and improved stress relaxation; whereas, thermosets have lower impact strength and strain at failure compared to thermoplastics.

2.2.3 Polyester Resin

Unsaturated polyester (UP) is most commonly used polymer resin to produce various composite structural parts. These resins remain in low viscosity liquid form during processing or until cured. Even, partially processed resins mixed with fibers can also be used at specific temperature and pressure. Various commercial unsaturated polyester resin used for various applications are orthophthalic polyester, isophthalic polyester, vinyl esters, bisphenol-A-fumarates, and chlorendics.

2.2.4 Epoxy Resin

Epoxy resins are used in advanced applications like aircraft, defense, aerospace, and many first generation composite reinforcing concrete products. Epoxy resins are almost two times expensive than polyester resins. Following are the performance characteristics of epoxy resins compared to polyester resins.

- A range of mechanical and physical properties can be developed because of diversity of constituent materials.
- No emission of volatile monomers during processing and curing.
- Low shrinkage during curing.
- Excellent resistance to chemicals and solvents.
- Good adhesion with number of fillers, fibers, and substrates.

TABLE 2.3 Properties of thermosetting resins

Resin	Specific Gravity	Tensile Strength [MPa]	Tensile Modulus [GPa]	Cure Shrinkage [%]
Epoxy	1.20 - 1.30	55.00 - 130.00	2.75 - 4.10	1.00 - 5.00
Polyester	1.10 - 1.40	34.50 - 103.50	2.10 - 3.45	5.00 - 12.00
Vinyl Ester	1.12 - 1.32	73.00 - 81.00	3.00 - 3.35	5.40 - 10.30

2.2.5 FRP Reinforcement

FRP reinforcement is an anisotropic material characterized by high tensile strength without yielding along the direction of the reinforcing fibers. This anisotropic characteristic affects on shear strength and dowel action of FRP bars. Lack of deformability shall be considered in the design procedure. The RC member reinforced with FRP bars is for required strength and checked for ultimate state criteria and serviceability (e.g. fatigue, creep rupture endurance, crack width, and deflection); however, serviceability criteria control the design in majority. The differences in mechanical characteristic like linear elastic stress-strain behavior up to rupture, higher ultimate strength, and lower modulus of elasticity, resulting in different damping, stiffness and hysteretic behavior of steel and FRP have to be considered specifically in the cases of wind and earthquake loadings. Even brittle failure may occur due to higher amount of FRP which is unfavorable in reinforced concrete (RC) elements[48].

FRP reinforcements are manufactured from continuous glass, carbon, or aramid fibers embedded in matrices. FRP bars are also produced in different diameters similar to steel reinforcement. Different types of surface can be produced like straight-plane, spiral, deformed, sanded-straight and sanded-braided. The bond between these FRP reinforcement and concrete may be either same or even better than the bond of steel reinforcement. Various forms of FRPs used as reinforcement in concrete structures are shown in Fig. 2.2.

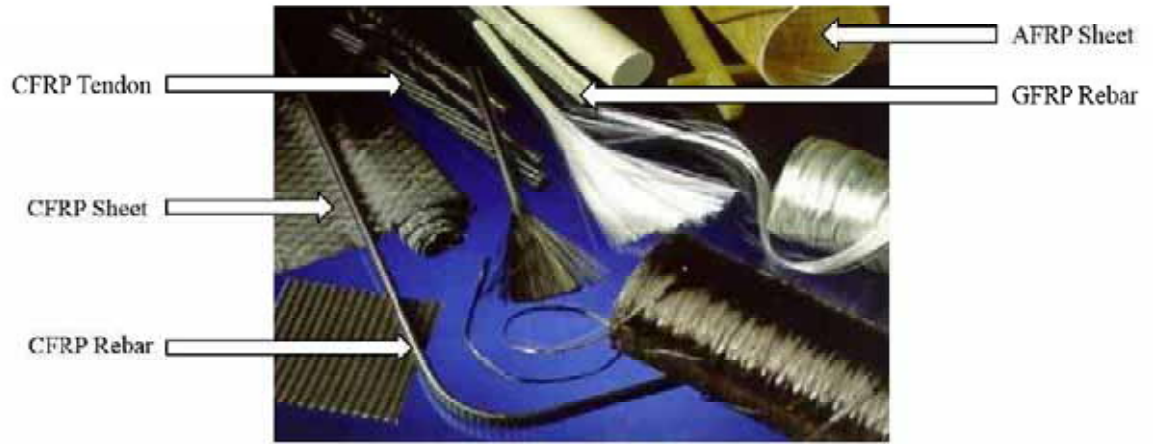

FIGURE 2.2 Various FRPs as reinforcement in concrete structures[53].

- **Material Properties of FRP :** Unlike steel reinforcement, there isn't any governing standard for the requirement of mechanical properties or production of FRP reinforcement. Few institutions are working with the industry to develop the draft standard; however, it may still take several years to be accepted by the regulatory bodies. The range of commercially-available FRP products and their material properties are quite large; however, it is advantageous for the designer in selection of different products depending on required strength and stiffness for his design application. The user is encouraged to consult commercial suppliers for the most up-to-date mechanical properties of their products as they can change when new versions of the product are produced. Mechanical properties of FRP reinforcing bars available commercially are given in Table 2.2[52].

TABLE 2.4 Typical mechanical properties of FRP reinforcing bars

Trade Name	Tensile Strength [MPa]	Modulus of Elasticity [GPa]	Ultimate Tensile Strain
Carbon Fiber			
V-ROD	1596	120.0	0.013
Aslan	2068	124.0	0.017
Leadline	2250	147.0	0.015
NEFMAC	1200	100.0	0.012
Glass Fiber			
V-ROD	710	46.4	0.015
Aslan	690	40.8	0.017
NEFMAC	600	30.0	0.020

Strength properties of the FRPs are different along each axis, characterized by a high tensile strength along the direction of the reinforcing fibers. As shown in Fig. 2.3, fibers are typically wound together in the longitudinal direction and bonded through a high-strength matrix (polymer resin). This fashion of manufacturing results in a highly anisotropic material having high and low strength along longitudinal and transverse directions respectively. This characteristic highly affects the shear strength, bond performance and dowel action of FRP bar reinforced with concrete. Even the performance of FRP reinforced elements can vary significantly depending on its shape (e.g. straight and/or bent bar).

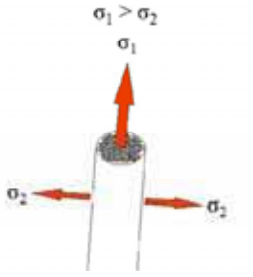

FIGURE 2.3 Anisotropic characteristics of FRPs[53]

Typically, FRPs are more effective in tension; they are used as tensile reinforcement along with concrete. Even, the mechanical properties of FRP bars can vary significantly by fiber content (percentage by weight) in cross section and manufacturing method. In contrast to its counterpart steel, FRPs exhibit linear-elastic tensile stress-strain behavior along the fibers orientation without yielding or abrupt failure. Generally, GFRP is cheaper than CFRP and AFRP. Except few CFRP systems, majority FRPs have a lower elastic modulus than steel.

The linear elastic stress-strain relationship of FRP composites along with steel are shown in Fig. 2.4, which depends on the failure strain of constituent fibers and the matrix. Stress-strain relationship of FRPs are only been modeled up to maximum 0.4 percent of its ultimate tensile strain as per various current design guidelines (ACI-440, 2006). This limitation results in excessive usage of material consequently increases project cost.

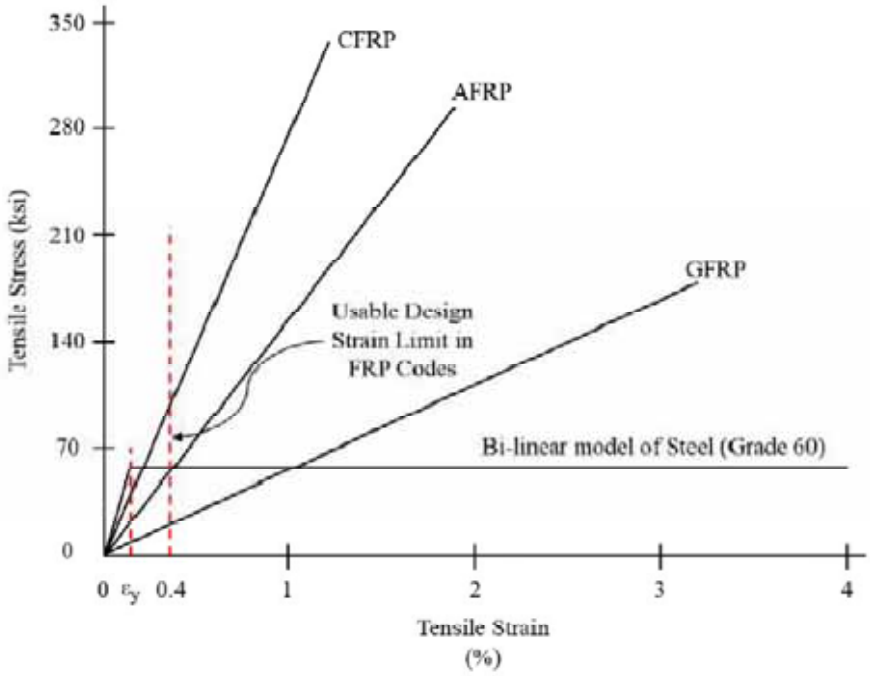

FIGURE 2.4 Stress-strain response of FRPs compared to steel[53].

2.2.6 Advantages and Disadvantages of FRP Reinforcement

Comparison of advantages and disadvantages of the FRP reinforcement are tabulated in Table 2.3.

TABLE 2.5 Advantages and disadvantages of FRP reinforcement

Advantages of FRP reinforcement	Disadvantages of FRP reinforcement
• High longitudinal tensile strength (varies with sign and direction of loading relative to fibers) • Corrosion resistance (not dependent on a coating) • Nonmagnetic • High fatigue endurance (varies with type of reinforcing fiber) • Lightweight (about 1/5 to 1/4 the density of steel) • Low thermal and electric conductivity (for glass and aramid fibers) • May be susceptible to fire depending on matrix type and concrete cover thickness	• No yielding before brittle rupture • Low transverse strength (varies with sign and direction of loading relative to fibers) • Low modulus of elasticity (varies with type of reinforcing fiber) • Susceptibility of damage to polymeric resins and fibers under ultraviolet radiation exposure • Low durability of glass fibers in a moist environment • Low durability of some glass and aramid fibers in an alkaline environment • High coefficient of thermal expansion perpendicular to the fibers, relative to concrete • May be susceptible to fire depending on matrix type and concrete cover thickness

2.2.7 Manufacturing Process

Three common manufacturing processes are there for production of FRP materials like pultrution, braiding, and filament winding. In pultrution technique FRP bars of continuous lengths of constant or nearly constant profile are manufactured. Fig. 2.5 shows a schematic representation of important stages of pultrution process. In the process, continuous strands of reinforcing fibers are drawn from creels and moved to the resin tank, where they are completely saturated with resin. Then they are passed through the number of wiper rings and moved into the mouth of a heated die to provide the shape and curing. Predetermined speed of pulling through die is maintained as per the curing time required. Various surface configurations are developed like straight-plane, spiral, deformed, sanded-straight or sanded-braided to ensure strong bond with concrete as per requirement.

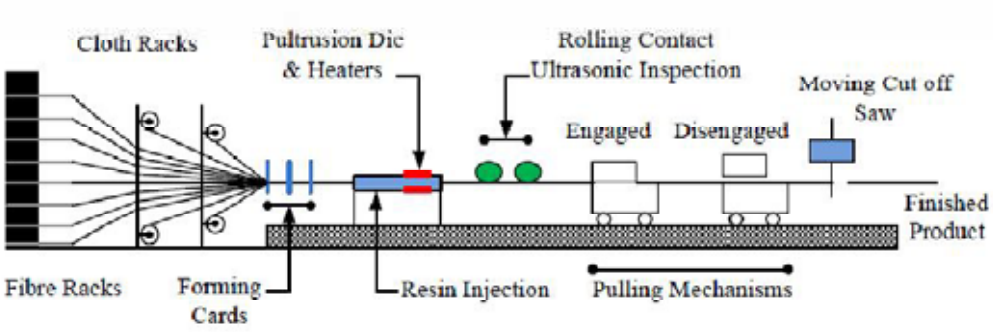

FIGURE 2.5 Pultrution process[51].

The term braiding is used for interlocking two or more yarns to form the integrity in the structure. In filament winding continuous fibers are impregnated with matrix resin and wrapped around a mandrel. In this process, fiber-volume fraction, thickness, and wind angle are controlled. Finally, they are cured using heat lamps. Mostly rods, pipes, tubes, and storage tanks are manufactured using this process.

2.2.8 Coefficient of Thermal Expansion of FRP

Fibers are having substantially different thermal properties in longitudinal and transverse directions. Accordingly, FRP reinforcement manufactured from these fibers would have different thermal expansion in both the directions.

Thermal characteristic depends on fiber type, type of matrix and fiber-volume ratio. The coefficient of thermal expansion of CFRP is close to zero in longitudinal direction[47,54]. AFRP is having negative coefficient of thermal expansion in longitudinal direction, indicates that AFRPs expands with decrease in temperature and contracts with increase in temperature. In case of GFRP, coefficient of thermal expansion in longitudinal direction is comparable to concrete; however, it is five times greater in transverse direction[55]. Coefficients of thermal expansion of GFRP, CFRP, and AFRP along with steel are shown in Table 2.4 (ACI 2000)[52].

TABLE 2.6 Typical coefficients of thermal expansion for FRP reinforcing bars

Coefficient of Thermal Expansion (x 10^{-6}/°C)				
Direction	**Steel**	**GFRP**	**CFRP**	**AFRP**
Longitudinal	11.7	6 to 10	-1 to 0	-6 to -2
Transverse	11.7	21 to 23	22 to 23	60 to 80

2.2.9 Effect of High Temperature

High temperatures would have adverse effect on the performance of FRP. Hence, precautionary measures should be taken where fire resistance is a significant design factor using FRPs. FRP will not burn due to a lack of oxygen in the embedded concrete; however, the epoxy will soften at elevated temperature. This is referred as the glass transition temperature, T_g. The T_g is a function of resin type and it remains around 110°C; where, both the strength flexural as well as bond of FRPs will be affected at this temperature.

The effect of T_g is much more theatrical for thermoplastics than for thermosets. Like in vinyl ester resin molecular chains of thermoplastics are not cross-linked; hence, they are much more mobile than thermoset resins. As an effect, flexural modulus of bar having thermoset before and after Tg will be to 50 and 20 GPa respectively, whereas it is 40 and 0.4 GPa with the thermoplastic resins.

Few researchers only have explored this area. It was observed that the surface became dark and some resin lost after 24 hours at 200C° and 300°C in the study carried Leadline products by Sayed-Ahmed and Shrive (1999). Some of the fibers became loose at 400°C after twenty four hours of exposure. Evaporation of resin is observed within one hour only at 500°C and bar became the bundle of loose fibers. This study was made specifically for Leadline products only and observed behavior is shown is Fig. 2.6.

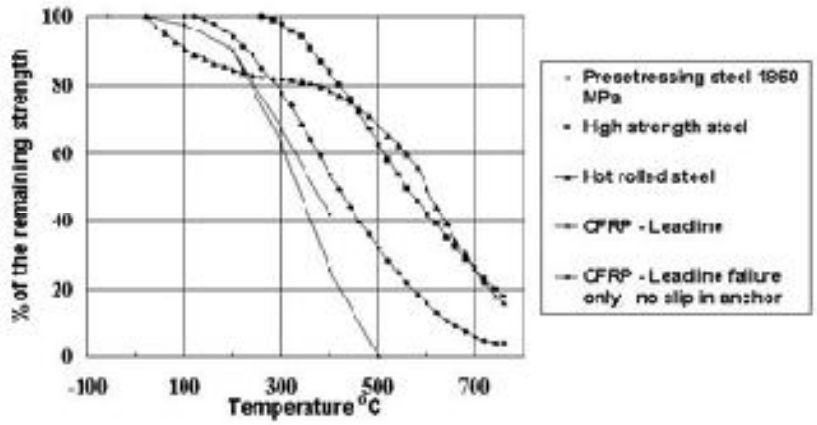

FIGURE 2.6 Effect of temperature on strength of Leadline[52].

2.2.10 Bond Properties of FRP Reinforcing Bars

Major influencing parameters affecting bond of FRPs are mechanical properties of FRP bars and environmental conditions[57]. Even different types of surfaces like straight-plane, spiral, deformed, sanded-straight and sanded-braided will also affect the bond properties of FRP bars. Friction, mechanical interlock, and adhesion transfer the bond forces to concrete. Unlike steel-reinforced concrete, there is no influence of compressive strength of concrete on bond of FRP bars[57].

2.2.11 Fatigue of FRP Reinforcing Bars

Tensile fatigue of FRP reinforcing bars has not been thoroughly investigated yet. There is no testing method accepted universally for FRP products; hence, all the test result must be supplemented by the testing method used.

AFRP bars named as FiBRA of typical tensile strength 1255 MPa were investigated for partial pulsating tensile fatigue tests at room temperatures. The test was carried out at 50 percent lower limit of tensile stress and varying upper limit was adopted. As tabulated in Table 2.5, rupture does not occur under two million cycles if upper limit doesn't exceed 80 percent of ultimate tensile strength[58].

TABLE 2.7 Tensile fatigue strength of FiBRA

Test	Lower Limit		Upper Limit		Stress Range (MPa)	Cycle to Rupture (x 10^3)
	Load (kN)	Stress (MPa)	Load (kN)	Stress (MPa)		
1	32.36	645.3	46.97	939.5	294.2	> 2090
2	32.36	645.3	42.52	990.5	345.2	> 3577
3	32.36	645.3	50.99	1019.9	374.6	> 2063
4	32.36	645.3	54.43	1088.5	443.3	305

CFRP is having excellent fatigue resistances. For 2 x 10^6 cycles, Leadline has 1100 MPa endurance limit with stress ratio 0.1 for 2 x 10^6 cycles. In case of pultruded CFRP with stress ratio 0.1, observed the endurance limit of 1400 MPa for 2 x 10^6 cycles[59].

2.2.12 Creep and Relaxation of FRP Reinforcing Bars

Failure occurred under sustained load is referred as creep. Creep endurance remains small when the ratio sustained load stresses to the live load stresses is larger. FRPs also experience the creep rupture. Most FRPs undergo elastic response initially, which is followed by non-linear behavior up to failure. High temperature, ultraviolet radiation, weathering, and alkalinity also affects the creep rupture failure of FRPs.

CFRP and GFRP bars are least and most susceptible to creep rupture respectively; whereas, AFRP remains in-between of other two. Sustained service stress shall be kept limited to the fraction of its ultimate strength to avoid creep rupture failure. Few of the codes have defined limits for the allowable service stress which is partially achieved through load and resistance factors; however, some codes like CSA S6-00 and CSA S806-02 provide specific limits that need to be checked by designer during the design process.

2.2.13 Durability of FRP Reinforcing Bars

One of the major factor for considering FRP bars in place of steel bars as reinforcement in concrete structure is its noncorrosive nature. Steel bars would corrode embedded in concrete when subjected to harsh environments that result in a loss of strength and durability (ACI 2000). Concrete elements exposed to chlorides are prone to corrosion of steel reinforcement. Concrete is highly alkaline with the pH from 12.5 to 13.5, and this

alkalinity decreases due to carbonation[60]. It is important to determine the reduction in strength and stiffness due to ageing of FRP bars under service condition for 50 to 100 years of service life. Many researchers are working on durability test to derive these strength and stiffness reduction factors. Also, the investigation is going on to derive calibration factors on the basis of field results[52].

The results extrapolated from weathering exposure programs are definitely valuable; however, they are not sufficient to promote the FRP reinforcement to be used rapidly. In addition, accelerated ageing test and predictive method are required to estimate long-term strength. The designers are working through the existing literature in this area[60-63].

2.3 Applications of FRP in Structural Engineering

FRP rebar and reinforcing grids have been used successfully as internal reinforcement in concrete beams and slabs[27]. Because of its advantageous properties like high strength to weight ratios, high specific strength and stiffness, noncorrosive, nonconductive, nonmagnetic, low alkali and salts, higher resistant to de-icing chemicals, law maintenance, enhanced fatigue life, and durable made it a better choice to be used in bridges and roadways compare to steel[64]. FRPs are also ideal for. FRP material is nonconductive, hence, it is ideal for sensitive electromagnetically applications which will not allow transmission of current in nearby electronic devices. This is useful in hospitals, nuclear power plants, air traffic control towers, electrical/phone transmission towers and specialized military structures[65].

Generally initial cost of FRP reinforcement is higher than steel reinforcement; however, it is quite economical in lifecycle cost analysis. In spite of several disadvantages, FRP is successfully entered in various engineering and construction applications with conservative approach.

Several applications of FRP reinforcement in various demonstrating projects have been initiated in Japan in the early 90's like floating marine structures, pontoon bridges, non-magnetic structures such as tracks for linear motors, bridge decks and ground anchors which are shown in Fig. 2.7 to 2.12 respectively.

FIGURE 2.7 Use of Leadline elements for the tensioning of diagonals of a floating marine structure, Japan[66]

FIGURE 2.8 Use of FRP tendons in the pontoon bridge at Takahiko three country club, Japan[66]

FIGURE 2.9 Magnetic levitation railway system in Japan[66]

FIGURE 2.10 Use of CFRP bars in a stress ribbon bridge at the southern yard country club, Japan[66]

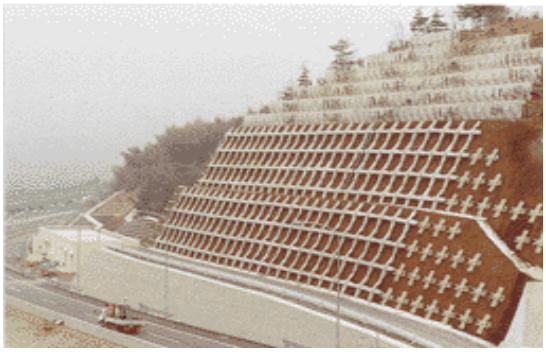

FIGURE 2.11 Use of Technora elements as ground anchors along the Meishin expressway, Japan[66]

FIGURE 2.12 The first concrete footbridge in Europe with only FRP reinforcement (EUROCRETE Project)[66]

Under different research and development programs in North America, Canada and Europe various FRP reinforced bridges have been constructed. Under the EUROCRETE project first FRP reinforced footbridge was constructed in Europe in 1996 as shown in Fig. 9. MRI

room in hospitals is becoming application nowadays. Fig. 2.13 to 2.16 shows some recent bridge applications in USA.

FIGURE 2.13 53rd Ave bridge, city of Bettendorf – Iowa (USA) [66]

FIGURE 2.14 GFRP bridge deck, Morristown – Vermont (USA) [66]

FIGURE 2.15 GFRP bridge deck, Cookshire-Eaton – Quebec[66]

FIGURE 2.16 GFRP bridge deck, Wotton, Quebec[66]

In addition, tunnel works the construction of soft-eye using FRP reinforcement to be excavated by tunnel boring machine (TBM) have become common in majority of the cases including Asia and Europe. Higher cost of FRP materials controls the use of FRPs limited to the applications where the unique characteristics are most appropriate; however, the scope of the application will expand with the improved efficiency of FRP in construction at reduced fabrication cost.

2.4 Discussion on Shear

Shear capacity of reinforced concrete beams having steel reinforcement has been subject of several debates and controversies from the beginning of 20th century. Exact analysis of shear capacity in reinforced concrete beam is quite complex. Reinforced concrete beams subjected to transverse load may fail in shear if designed inadequately before attaining the full flexural strength. Shear failures are unexpected, sudden, and sometimes violent as well

as catastrophic unlike its flexural failures. A thorough knowledge of various shear mechanism and different modes of shear failures is required to prevent them.

Shear force is the rate of change of bending moment at any section in the beam. A large number of experimentation has been carried out on the slender beams with and without shear reinforcement to understand the various failure modes that may happen due to various combinations of shear and bending moment acting at particular section.

The usually the shear capacity are investigated with two point load system loaded with concentrated loads 'P' placed symmetrically at distance 'a' (shear span) from the supports. It advantageous in generating two different test conditions, i.e. pure bending between two concentrated loads (as there is no shear force present) and constant shear force in the shear span 'a'.

The beam considered to be failed in shear when cracks are induced in the end region of the beam; Even though maximum bending moment is there in the central section. It is to be noted that the central section is subjected to pure bending (no shear force); hence, shear force or the shear stress present in the end zone must be responsible for such failure. Hence, the term 'shear failure' is opted.

It is believed that when principal tensile stress exceeds the tensile strength of concrete within the shear span the shear failure initiates in reinforced concrete members which results in development of diagonal cracks that propagates through the web of beam later. Means diagonal cracking strength depends on the tensile strength of concrete in reinforced concrete members which is dependent on compressive strength of concrete indirectly.

2.4.1 Shear Transfer Mechanisms

The evaluation of shear capacity of the reinforced concrete beam with ductile or brittle reinforcement must be on the basis of actual stress-state that satisfies the equilibrium as well as compatibility conditions both and which are linked with material constitutive laws. Hence, clear understanding about shear transfer mechanism through which the shear is resisted by the beam is required. Total six shear resisting mechanism are there for the beam as mentioned below. They are broadly divided into two parts like beams without and with shear reinforcement which are termed as "without stirrups" and "with stirrups" respectively[67,68]. Generally shear reinforcement is provided in the form of vertical stirrups that encircle tension reinforcement. It shall be confirmed that their free ends should

be anchored in the compression zone properly so that the vertical legs of the stirrups can resist tension without any slippage.

- The shear resistance of the uncracked concrete in compression zone
- Dowel action of the flexural reinforcement
- Aggregate interlock (shear friction) along the crack
- Arching action
- Residual tensile stresses across cracks
- Shear forces carried by shear reinforcement (stirrup)

A four-point simply supported beam would give the clear understanding of different shear mechanisms. The moment carried by the beam is represented by an internal force couple between the flexural reinforcement actions and compression-zone concrete. For equilibrium state in shear-span, the moment would vary as per V = dM/dx along the shear-span of the beam. Shear contribution of uncracked concrete depends on the depth of the concrete compressive zone and its strength. The shear contribution increases with deepening of the uncracked concrete zone or strength of concrete increases. Dowel action is the ability of longitudinal reinforcement to transfer shear forces near cracks. The aggregate interlock, also referred to as the shear friction, depends on maximum size of aggregate, compressive strength of concrete and the shear crack width. Wider cracks, smaller aggregate and higher concrete strength are less effective to this mechanism for shear resistance. In arch action vertical component of compressive strut formed in the uncracked concrete transfers the shear near the end of a beam, where the constant horizontal component is reacted by the tensile flexural reinforcement. In the case when, shear span to depth ratio is higher than 2.5, arching action remain negligible in slender beams. Residual tension in cracked concrete exists only up to the crack width of 0.15 mm.

- **Post-Cracking Behavior :** The mechanism of shear transfer in a cracked concrete beam is illustrated in a free body diagram as shown in Fig 2.17. The shear force V is resisted by the combined action of various forces as mentioned below.

$$\underline{V} = V_{cy} + V_{ay} + V_d \qquad (2.1)$$

where,

- V_{cy} = shear contribution from the uncracked concrete in compression zone.
- V_{ay} = shear contribution from vertical component of the force due to aggregate interlock or interface shear transfer.

- V_d = shear contribution from the dowel action of longitudinal reinforcement.

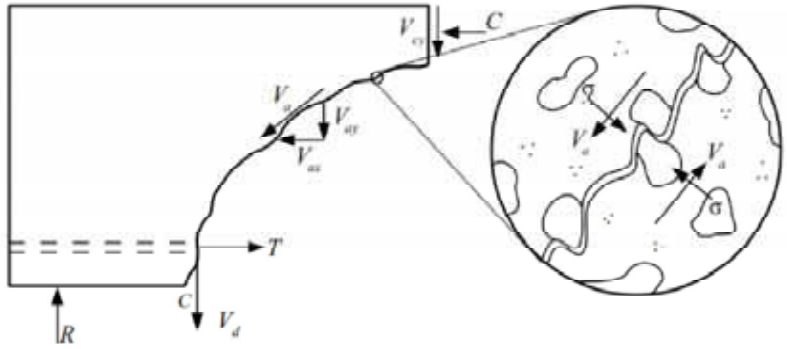

FIGURE 2.17 Mechanism of shear transfer in cracked concrete beam[53]

The approximate percentage contributions of above three components are

- Shear contribution from compression zone V_{cy} : 20 to 40%
- Shear contribution from aggregate interlock V_{ay} : 35 to 50%
- Shear contribution from dowel action V_d : 15 to 25%

With the initiation of shear displacement along the inclined shear crack, dowel action of reinforcements gets mobilized. When both the faces of flexural crack of moderate width are given a shear displacement relative to each other, large number of coarse aggregate elements projecting across the crack interlocks with each other and produces significant shear resistance.

In the process, dowel action is the first to reach its capacity with the increase in applied shear force. Subsequently proportionately large shear is carried by aggregate interlock which remain next to fail probably. As a consequence rapid transfer of a large shear force is required to be carried by uncracked concrete in compression zone. Sudden transfer of this large shear to the concrete often fails the beam abruptly and explosively. The shear reinforcement bridges the cracks and transfers shear forces of the crack. Truss analogy provides the understanding of shear carried by shear reinforcement.

2.4.2 Types of Shear Failure

Inclined cracks developed in the shear span determine the arch or beam mechanism to carry shear. Compatibility of each component of beam must be considered in conjunction with crack propagation. Different modes of shear failure describes the manner in which the compression-zone concrete fails

- Diagonal-tension failure
- Shear-compression failure
- Shear-tension failure
- Splitting or true shear failure

- **Diagonal-Tension Failure :** The concrete immediately in front of a crack is subjected to a tension field that causes the crack to propagate diagonally into the beam. In absence of shear-compression failure, the crack propagates towards the point where load is applied. The diagonal crack experiences the resistance as it moves up in the compression zone and becomes flatter where it stops at some point marked as 1 as shown in Fig. 2.18. With the further increase in load, this tensile crack extends gradually with the flat slope until sudden failure occurs at point 2. Meanwhile, more stipper crack as 3 and cracks nearby reinforcement will develop before ultimate failure at point 2. Because of that compatibility is not maintained between the compression zone concrete and flexural reinforcement across the crack, hence the beam action is not possible. An unstable diagonal-tension failure splits the beam into two pieces[69].

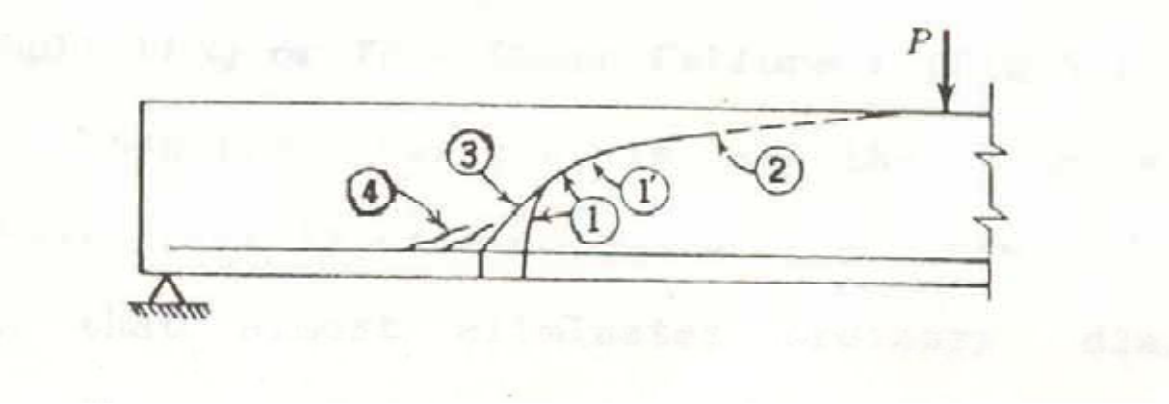

FIGURE 2.18 Diagonal tension failure[70]

- **Shear-Compression Failure :** Large shear force in the shear span a/d ranging from 1.0 to 2.5 would produce the diagonal cracks across the neutral axis at approximately 45° are called as web shear crack before the flexural cracks develop. Such a crack crowds the shear resistance (stresses) into a smaller depth and propagates until stopped by the load or reaction as shown in Fig. 2.19. Finally, compression failure takes place nearby the load in absence of triaxial confinement

of concrete. This type of failure is designated as shear compression failure as the failure is caused by combination of both. Shear-Compression failure is often described as "crushing of concrete". Sometimes, the ultimate load remains more than double compared to diagonal cracking.

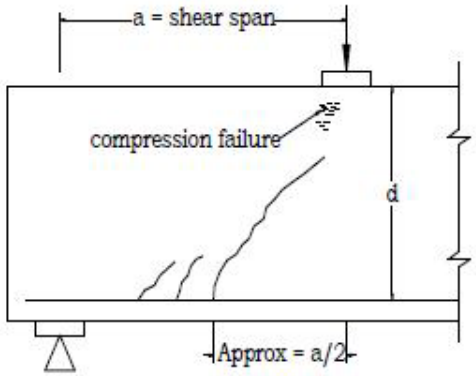

FIGURE 2.19 Shear-compression failure[70]

- **Shear-Tension Failure :** This type of failure is similar to diagonal tension failure. It is also common in short beams. Diagonal crack generates initially, which penetrates through the beam and leads towards the longitudinal reinforcement. Finally, beam fails in shear with the propagation of crack along the reinforcement.

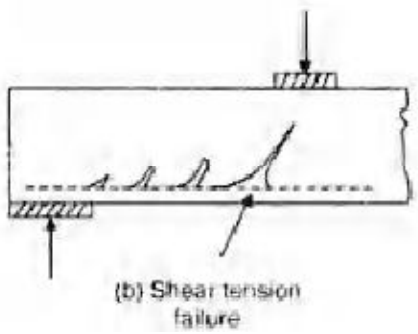

FIGURE 2.20. Shear tension failure[70]

- **Splitting or True Shear Failure :** This type of failure takes place when shear span to depth ratio is less than unity. An inclined shear crack develops between load and reaction which almost eliminates conventional diagonal tension concept. Much higher shear strength is observed in such cases. At ultimate stage, either it splitting failure may occur or compression failure near to the support may be observed as

shown in Fig. 2.21. Such an analysis of send section is closely related to the deep beam analysis.

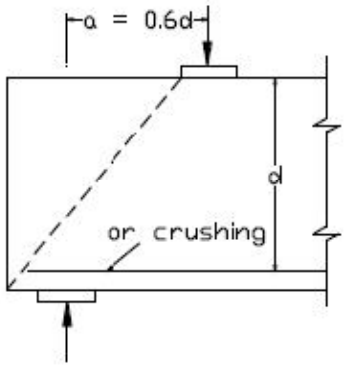

FIGURE 2.21 Splitting shear failure[70]

2.4.3 Compatibility of the Flexural Reinforcement

Compatibility of the flexural reinforcement with the concrete plays a crucial role in shear failure of concrete in compression-zone when it crosses a crack as shown in Fig. 2.22. The local crack opening will have both the components axial and shear in correlation with the reinforcement at the bottom of shear crack where it crosses. Stretching of unbonded reinforcement as well as slip of the bonded reinforcement, these two modes are responsible to achieve the compatibility across the crack[71]. Slip remains negligible in case of steel compare to plastic stretching. While in case of FRP, slip as well as elastic stretching both are important. At a give crack opening, force in the flexural reinforcement depends on unbounded length of reinforcement, stiffness of the reinforcement, and bond characteristics of the reinforcement.

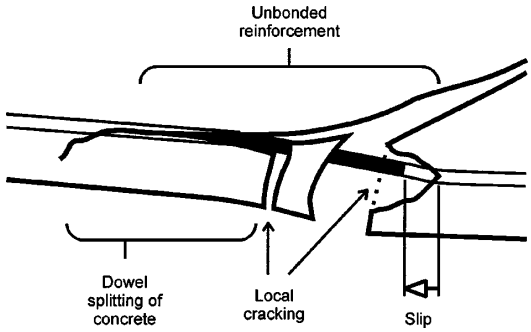

FIGURE 2.22 Compatibility of flexural reinforcement with crack opening[74]

2.4.4 Reinforcement-Concrete Bond

Different types of surfaces like straight-plane, spiral, deformed, sanded-straight and sanded-braided would have different bond characteristics. The bond between these FRP reinforcement and concrete may be either same or even better than the bond of steel reinforcement. Reinforcement can pull out from concrete in weaker beam, which destroys the beam action necessary for load transfer[69]. Reinforcement-concrete bond is key factor in shear failure[68,72].

2.4.5 Unbonded Length of Reinforcement

The unbounded length of reinforcement may be larger than the width of the crack. It increases with the development of local crack because of load transfer across the reinforcement-concrete interface[71]. Increase in unbonded length of reinforcement results in reduction of strain in the reinforcement at the given crack width; hence, the load carried by reinforcement will reduce. This will lead to re-establishment of equilibrium at the beam section because of which crack shall further enter into the compression-zone. Sometimes, re-establishment of equilibrium may not be possible, which results in any of the shear failure either shear-compression or diagonal-tension in the compression-zone of concrete, hence the failure of the beam.

2.4.6 Dowel-Splitting

The shear contribution by dowel action of the reinforcement across the shear crack is negligible compare to other contributions in case of steel reinforcement; where, because of low transverse stiffness in case of FRP reinforcement, it is even lower. Longitudinal cracks in the concrete along the flexural reinforcement will develop because of dowel action even at the smaller load[69]. Dowel splitting results in increase of unbonded length of flexural reinforcement, which may lead to unstable crack propagation into the compression-zone and resulting in failure of beam[73].

2.4.7 Dowel Rupture

Generally, dowel rupture does not occur in case of steel reinforcement; whereas, lower transverse strength of FRPs make them rupture. The dowel rupture occurs in FRP reinforcement before its pure tensile strength is achieved. This kind of failure is the

combined effect of shear and tensile actions across the reinforcement because of dowel action.

2.5 Predicting the Shear Contribution

Ideally, prediction of shear capacity of a beam shall be done through the detailed examination of all shear transfer mechanisms, crack propagation, and failure of the beam components to quantify the shear contribution of each element to the overall capacity of beam in shear. Typically, the shear capacity of the beam (V_n) is generally the sum of the shear contribution from concrete (V_c) and shear reinforcement (V_s) in reinforced concrete members.

$$V_n = V_c + V_s \tag{2.2}$$

2.5.1 Concrete Contribution

The "concrete contribution" in shear design of FRP reinforced element is modified by the ratio of the stiffness of FRP to steel in the proposed recommendations. Certainly, the stiffness of the reinforcement affects the shear capacity of the beam; however, it is one of the influencing parameters when steel is substituted by FRP reinforcement. Furthermore, the suggested design proposals of "concrete contribution" with FRP reinforcement have been validated with the beams without shear reinforcement experimentally. The load carried by the concrete at failure is governed by compatibility of the cracked concrete with the shear reinforcement in a shear reinforced beam. It is convenient to split the shear capacity of a beam conceptually into a "concrete contribution" and "stirrup contribution"; however, two mechanisms cannot be treated in isolation with brittle reinforcement; they must be compatible. The code proposals do not recognize this[74].

2.5.2 Stirrup Contribution

Shear reinforcement must not fail at a large crack opening; however, it must be effective at small crack openings, to restrain crack propagation. The "stirrup contribution" is the shear carried by stirrups across the crack just before the failure of first stirrup. The lower-bound plasticity theory allows us to assume that all the reinforcement yields along a crack with steel reinforcement. In contrast, the strain in FRP shear reinforcement varies along a crack[74]. Compatibility condition determines the distribution of stirrup strain along a

crack; however, compatibility of the shear reinforcement depends upon the bond characteristics of the reinforcement with surrounding concrete. Different FRP bars are manufactured with different surface finishes, and have different bond characteristics. Hence, the load carried by stirrups in the beams with the shear reinforcement of same ultimate strain-capacity but different bond characteristics will differ. The code proposals for FRP reinforcement assumes an artificial stirrup yield strain the "allowable strain" for use in the truss analogy[75].

2.6 Theories for Evaluation of Shear Resistance of Reinforced Concrete Members

Cambridge astrophysicist Sir Arthur Eddington has quoted that "No experiment is worthy of credence unless supported by an adequate theory." The researcher has to see the applicability of the finding after extensive research. Real job of the researcher is that to understand the experimental behavior of the complex phenomena influenced by various variables and present the findings with justification of adequate theory. Such as in determining the flexural strength of reinforced concrete elements, Hooke's observation in 1678 that plane sections remain plane is used universally.

Understanding shear in concrete has always challenged researchers. Various theories have been developed to understand the shear behavior in concrete along with extensive experimental programs, however, is not sufficient to predict the shear-capacity of beam effectively. The responsible are the poor quality design provisions. There are about 20 variables that influence the shear behavior as stated by Professor Frits Leonhardt[76].

Theories based on equilibrium considerations like strut-and-tie models and stress field can be applied when shear reinforcement is provided for safe designs. Theories also considering compatibility conditions and the tensile strength of concrete like compression field-based theories and fixed-angle softened-truss model have also been developed allowing accurate predictions of the shear response of transversely reinforced members.

Shear in members without shear reinforcement has traditionally been estimated by means of purely empirical or semi-empirical expressions like compressive force path method. Modified compression field theory (MCFT) has been applied successfully to the members without shear reinforcement. Above mentioned theories useful for the prediction of shear capacity are briefly discussed in following sections.

2.6.1 Truss Analogies

The truss analogy proposed by RITTER-MÖRSCH (1899) for the calculation of shear reinforcement in reinforced concrete members is the oldest and well known example of reasoning by means of "strut-and-tie models". Total shear capacity of a reinforced concrete beam is assumed to be the superposition of the "concrete contribution" (V_c) and "stirrup contribution" (V_s) predicted using the 45° truss analogy as shown in Fig. 2.23. The assumed internal equilibrium-state comprises inclined compressive struts of concrete and tensile shear reinforcement. A 45° strut angle is used to predict failure load when the shear reinforcement yields in original truss analogy[77]. While varying compressive strut angle is used to give reinforcement yield and web concrete failure simultaneously in modified truss analogy using explicit plasticity theory[78]. Both the truss analogies rely on stress-redistribution from the postulated fully developed plastic truss, to the actual equilibrium-state[68]. The truss mechanism is not observed experimentally: The assumed compressive struts would have to cross curved cracks in the shear-span, even though the crack surfaces are completely separate. Furthermore, the truss analogies are sectional design methods. The shear capacity is calculated on a critical vertical section, whereas in reality failure occurs along a single crack[69].

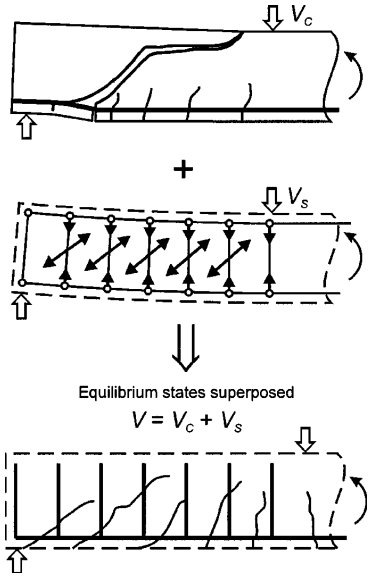

FIGURE 2.23 Superposition of concrete and stirrup contributions using 45° truss analogy[74]

2.6.2 Compressive-Force-Path Method

The Compressive Force Path Concept is based on realistic assessment of shear capacity of a beam without stirrups that assumes shear failure by excessive tensile stresses perpendicular to the compressive path but remains empirical. This happens due to change in the direction of the force path requiring a tensile resultant, dilation in the vertical direction due to varying intensity of the compressive stress field, and high tensile stresses at the tip of cracks. It should be noted that in this concept the entire shear is carried above the neutral axis through assumed stress conditions in the compression zone and shear reinforcement is placed to restrict critical shear crack which is assumed to yield. Finally the net shear capacity is found by superposition of concrete and shear reinforcement contribution.

2.6.3 Compression-Field Theory

The shear capacity is related to the compression in diagonally cracked concrete through equilibrium. Compression-field theory is based on the biaxial response of square elements of steel-reinforced concrete. The original constitutive relationships were derived analytically calculating the actual angle θ, and the crushing strength of the concrete struts. The crushing strength is a function of the tensile strain perpendicular to the strut, but these have been replaced by more realistic empirical equations[79]. If an isolated element is considered, the internal equilibrium state is avoided by the use of empirical constitutive relationships. If the element is part of a beam, simplifications must be made that to rely on stress-redistribution. Moreover, compression-field theory is based on sectional design method similar to truss analogy; however, shear is not a sectional failure.

2.6.4 Modified Compression Field Theory (MCFT)

The MCFT provides more realistic assessment of shear capacity of wide range of beam with shear reinforcement and also for the cases for without shear reinforcement. The compression field theory gives conservative estimate of shear strength because of neglecting tensile stress contribution in cracked concrete. While, MCFT accounts the contribution of tensile stresses in the concrete between cracks. The most authoritative assumption in the MCFT model is to treat the cracked concrete as a new material with empirically defined stress-strain behavior in reinforced concrete which can be traditionally different from the stress-strain curve of uncracked concrete.

2.6.5 Simplified Compression Field Theory (SCFT)

The shear strength of a section is a function of the two parameters inclination θ of the diagonal compressive stresses in the web, and the factor for tensile stresses in the cracked concrete, β, both depend on the longitudinal straining of the web, ε_x. For members without transverse reinforcement, β and θ values calculated from the MCFT are given as functions of ε_x and the crack spacing s_{xe} in a table, however, many engineers prefer simple equations to tables because they give a continuous range of values and are more convenient for spread sheet calculations[80], introduced the concept of simplified compression field theory for the shear design of concrete beams. The method provides a simplified version of MCFT, which provides simple equations for β and θ to be determined from the basic expressions of the MCFT, where the calculation of full load deformation analysis is not needed.

2.6.6 Strut and Tie Model (STM)

The STM is most rational and simple design approach which is widely used for the members like deep beams and/or non flexural members. The term truss is an assemblage of pin joined, uni-axially stressed tension or compression member where term D is used for Disturbed or D-region and term B is used for Beam or B-region, where in B-region beam action and in D-region arch action is expected. This design approach is not unique due to specific geometry of the structures, significant re-distribution of the stresses after cracking and is based on lower bond theory of plasticity and efficiency factors are applied to uni-axial strength of concrete to account for concrete softening. Sufficient reinforcement needs to be provided in all the direction of RC structure for the ductile failure. Application of Strut and Tie Model for more slender beams without transverse reinforcement may lead to unsafe solution. Diagonal crushing strength of concrete is required to be reduced in case of slender beams without transverse reinforcement[81]. In an equilibrium model, the designer specifies at least one load path which ensures that no part of this path is overstressed.

2.7 Review of the Shear Design Recommendations

Traditionally, shear capacity of the reinforced concrete elements is evaluated as the addition of concrete and stirrups contributions with steel reinforcement; similarly it is followed for FRP reinforcement also. Majority of the design recommendations produced for FRP applications, conceptually replaces the steel reinforcement by FRPs with due

modifications considering fundamental differences of the properties between them. Permissible stain approach in FRP stirrups is advisable to maintain the harmony and to control the shear crack width. This also helps to avoid failure of the FRP stirrups in the bent portion due to limited stress development (ACI 2006). The shear strength contribution for concrete (V_c) and FRP reinforcement (V_{FRP}) as specified by the ISIS Canada (2007), JSCE (1997) and ACI (2006) reviewed are as follows:

$$V_r = V_c + V_{FRP} \tag{2.3}$$

2.7.1 ISIS Canada Design Manual (2007)

$$V_c = 0.2\lambda\Phi_c\sqrt{f'_c}b_w d\sqrt{\frac{E_f}{E_s}} \text{ where, } \sqrt{\frac{E_f}{E_s}} \leq 1 \tag{2.4}$$

For the sections with an effective depth greater than 300 mm and not containing at least minimum transverse reinforcement the concrete resistance, Vc, is taken as,

$$V_c = \left(\frac{260}{1000+d}\right)\lambda\varphi_c\sqrt{f'_c}b_w d\sqrt{\frac{E_f}{E_s}} \text{ where, } \sqrt{\frac{E_f}{E_s}} \leq 1 \tag{2.5}$$

$$V_{FRP} = \varphi_{frp}\frac{A_{fv}\,\sigma_v d_v \cot\theta}{s} \tag{2.6}$$

$$\sigma_v = \frac{\left(0.05\frac{r_b}{d_b} + 0.3\right)f_{frpv}}{1.5} \tag{2.7}$$

$$\sigma_v = E_{fv}\varepsilon_{fv} \tag{2.8}$$

$$\varepsilon_{fv} = 0.0001\sqrt{f'_c\frac{\rho_{frp}E_f}{\rho_{frpv}E_{fv}}}\left[1 + 2\left(\frac{\sigma_N}{f'_c}\right)\right] \leq \mathbf{0.0025} \tag{2.9}$$

2.7.2 JSCE (1997) Recommendations

The shear contribution of concrete as recommended is obtained as

$$V_c = \beta_d\beta_p\beta_n f_{vcd}\, bd / \gamma_b \tag{2.10}$$

$$f_{cvd} = 0.2(f'c)^{1/3} \leq 0.72\ N/mm^2 \quad (2.11)$$

$$\beta_d = (1000 / d)^{1/4} \leq 1.5 \quad (2.12)$$

$$\beta_p = (100\ \rho_{fl} E_{fl} / E_s)^{1/3} \leq 1.5 \quad (2.13)$$

$$\beta_n = 1 + \frac{M_o}{M_d},\ \text{if}\ \beta_n > 2\ \text{or}\ N_f \geq 0 \quad (2.14)$$

$$\beta_n = 1 + \frac{2\,M_o}{M_d},\ \ \text{if}\beta_n < 0\ \text{or}\ N_f < 0 \quad (2.15)$$

The shear contribution by FRP stirrups is calculated as

$$V_{FRP} = [A_{fv}\, E_{fv}\, \varepsilon_{fv}\, (\sin\alpha s + \cos\alpha s) / s]\, z / \gamma_b \quad (2.16)$$

$$\varepsilon_{fv} = 0.0001\sqrt{f'_{mcd}\frac{\rho_{fl}E_{fl}}{\rho_{fv}E_{fv}}}\left[1 + 2\left(\frac{\sigma_N}{f'_{mcd}}\right)\right] \leq \mathbf{f_{FRPbend} / E_{fv}} \quad (2.17)$$

$$f_{FRPbend} = \left(0.05\frac{r_b}{d_b} + 0.3\right) f_{fuv} / \gamma_{mfb} \quad (2.18)$$

$$f'_{mcd} = \left(\frac{h}{300}\right)^{-1/10} f'_{cd} \quad (2.19)$$

$$\sigma_N = N_f / A_g \leq 0.4\, f'_{mcd} \quad (2.20)$$

2.7.3 ACI 440.1R-06 (ACI 2006)

The shear resistance of concrete V_c in FRP-RC element specified by the ACI 440.1R-06 (ACI 2006) is as follows

$$V_c = \frac{2}{5}\sqrt{f'_c}\, b_w c \quad (2.21)$$

$$c = kd \quad (2.22)$$

$$k = \sqrt{2\,\sigma_f n_f + (\sigma_f n_f)^2} - \sigma_f n_f \quad (2.23)$$

The shear resistance of FRP stirrups V_{FRP} of the member is calculated as

$$V_{FRP} = \frac{A_{fv}\sigma_{fv}d}{s} \quad (2.24)$$

$$\sigma_{fv} = \mathbf{0.004}E_{fv} \leq f_{FRPbend} \quad (2.25)$$

$$f_{FRPbend} = \left(0.05\frac{r_b}{d_b} + 0.3\right) f_{FRPu} / 1.5 \leq f_{FRPu} \quad (2.26)$$

2.8 Experimentation Using FRP Reinforcement

Ehab A. Ahmed et al.[46] have tested 3 CFRP reinforced and one steel reinforced large scale concrete beams of span 7,000 mm and a T-shaped cross section by keeping variation in stirrup material and shear reinforcement ratio. The comparison of and predications provided by various design guideline were produced. ACI 440.1R-06 design method predicts shear capacity conservatively; however, guidelines provided by Canadian (CAN/CSA S6-06) and Japanese (JSCE 1997) underestimate the FRP stirrup contribution due to low strain limits. It was observed that concrete contribution enhances after first shear crack also closer spacing of CFRP stirrups enhances the shear resistance due to confinement and controls the shear crack. Additionally it is observed that adequate level of conservatism can be achieved by adopting FRP stirrup strain of 4,000 microstrain in FRP-RC beams.

Muttoni and Ruiz[67] have studied the shear-carrying mechanisms after the development of critical shear crack. To estimate the shear strength of the members without shear reinforcement, a model is proposed based on an estimate of the crack width in the critical shear region, taking also into account the roughness of the crack and the compressive strength of concrete. In the study important observation is made that the plasticity-based solutions with an inclined compression strut overestimate the shear strength when a critical shear crack develops inside the theoretical strut and they defined the mechanism of shear resistance after development of critical shear crack. Developed analytical expression shown good agreement with 285 test results.

Robert Machial et al.[82] have calculated the shear strength contribution of FRP transverse reinforcement of 112 beams without shear reinforcement and 54 beams with FRP shear reinforcement from the published literature and compared the prediction of results of ACI 440.1R-06 and JSCE 1997. The JSCE 1997 guideline had better performance for calculating the concrete shear strength than the ACI guideline with an average calculated over experimental shear strength of 1.41 compared to 1.92. However, the ACI guideline

outperformed the JSCE 1997 guideline for calculating the transverse shear strength with an average calculated shear over experimental shear of 1.69 compared to 2.26.

A.K. El-Sayed et al.[83] have proposed the modification in shear design equation proposed by ACI Committee 440. Test results of the beam reinforced with different types and ratios of FRP bars indicates that the proposed a design approach for evaluating the concrete contribution to the shear resistance of FRP-reinforced concrete beams that accounts for the axial stiffness of FRP longitudinal reinforcement underestimates the concrete shear strength. The proposed equation was verified against experimental shear strengths of 98 specimens tested to date, and the calculated values are shown to compare well. In addition, the proposed equation was compared to the major design provisions using the available test results. Better and consistent predictions were obtained using the proposed equation.

Mohsen Kobraei et al.[84] have investigated the effects of CFRP bars as shear reinforcement instead of steel stirrups in RC beams. All beams were cast using a high strength concrete (HSC) and self-compacting concrete (SCC). In this approach, results of seven laboratory specimens show that using carbon fibre reinforced polymer (CFRP) shear reinforcement can be an acceptable alternative for normal stirrups in RC beams. It is observed that the CFRP shear reinforcement bars can be considered as an attractive alternative instead of normal stirrups where their ρ are 50 to 85% ρ_b. The beams with FRP reinforcement have greater capacity with less deflection compared to the concrete beams with steel reinforcement. Even, the ultimate capacity of both observed without significant difference with high strength concrete. The crack development with CFRP has good extension throughout the beam; however, the width of cracks is larger than the beams with steel reinforcement. In case of larger spacing of the replacement CFRP shear reinforcement bars, the number of cracks increase but the width of the crack is narrower.

Jongsung SIM et al.[85] have tested a set of 12 beams with steel and GFRP reinforcement. It is observed that with increase in shear span to depth ratio (a/d) failure load and shear failure angles decreased and even dominant failure mode change from shear failure mode to flexural and shear failure mode. Shear strengthening efficiency of the GFRP stirrups observed is similar to the steel stirrups, however, this very fundamental study for characterization of the shear failure, the authors are encouraged to extend it to further

research on the failure characterization of beams reinforced with the newly developed GFRP stirrups.

Emile Shehata et al.[86] have tested and analyzed fifty two designed panel specimens and ten large scale T-section along with 118 beams tested by others. Important evaluations are proposed in form of design guidelines for the use of FRP as shear reinforcement in concrete structures. It is observed that the bend effect on the strength capacity of FRP stirrups is more critical than the kink effect which is responsible for the development of beam action and contribution of FRP stirrup in shear contribution. Shear deformations are affected by elastic modulus and bond characteristics of stirrups material. Wider shear cracks, smaller depth of the compression zone and poor dowel action associated with the use of FRP as longitudinal reinforcement leads the less concrete contribution of the beams reinforced with CFRP strand in flexure. A minimum shear reinforcement ratio is recommended to ensure that the shear strength exceeds that shear cracking load for concrete beams with FRP reinforcement. To achieve the at least 50% guaranteed strength of FRP stirrups bend radius, r_b, should not be less than larger of four times the effective bar diameter or 50 mm and tail length, l_d, six times the effective bar diameter or 70 mm. Limiting strain of 0.002 is recommended for both CFRP and GFRP stirrups to control the shear crack width in concrete beams.

Mohsen A. Issa et al.[87] have tested total twelve beams having basalt fiber reinforcements. There were six beams of size 200 x 300 mm and six of size 300 x 200 mm in with and without shear reinforcement's category. Whole set was designed by varying flexural reinforcement ratio and span to depth (a/d) ratio. Crack patterns, failure modes, load-deflection, load-strain behavior, and shear capacity were observed from the test. It was observed that the shear capacity increases with the FRP reinforcement ratio for the same *a/d*, whereas the shear capacity decreases with the increase in *a/d*. It was observed that capacity prediction from standard provisions were both conservative and nonconservative. The predictions based on the modified compression field theory for the nonshear reinforced beams were the closest to the experimental.

2.9 Concluding Remarks of Literature Review

In this chapter different types of fibers, resins, and FRP reinforcement have been presented along with their properties. Advantages and disadvantages of FRP reinforcement along with their manufacturing process, thermal, bond, fatigue, creep and durability characteristics have been discussed. Uses of FRPs as primary reinforcement in various civil engineering applications are also presented.

Shear transfer mechanism, types of shear failure, theories for evaluation of shear capacity in RC beams specifically concrete and stirrup contributions have been presented.

Design approached for FRP-RC beams from three international design guidelines have been presented. Various experimentations done using different FRP reinforcement like CFRP, GFRP and BFRP have been presented.

From the literature review, it is observed that modulus of elasticity of the reinforcement plays a crucial role in overall load transfer mechanism and its capacity. Various types of FRP reinforcement have been developed, where they have different mechanical properties. Design recommendations are common for different types of FRP reinforcement. It was felt that lower modulus of elasticity GFRP reinforcement would give different behavior compare the higher modulus of elasticity of CFRP reinforcement, which may be the controlling parameter to have the marginal difference in experimental results and theoretical evaluations reported in the literature. Hence, it was concluded to go for experimentation using GFRP reinforcement.

CHAPTER : 3

Experimental Program

3.1 Introduction

The research program is performed to explore the scope for improving efficiency of the design recommendations related to the shear strength of the RC beam having FRP reinforcement. Hence the most influencing parameters that effect on the shear strength are determined by analytical study considering ACI standards. In the present study GFRP is used as longitudinal and transverse reinforcement. With reference to the parametric study as made in section 2.9, span to depth ratio, spacing of stirrups and modulus of elasticity are the major variables which makes effect on the total shear capacity.

As span/depth ratio and spacing of stirrups are most influencing parameters, they are taken as variable parameters in the testing. In the experimental program thirteen, full-scale, RC beams with GFRP reinforcement bars are taken, out of which one beam is reinforced with steel. The beams reinforced with GFRP reinforcement are grouped into three main series designated A, B, and C with the variation in shear span/depth ratio of 1.95, 2.54, and 2.93 respectively.

The variation in spacing ranging from 250 mm to 350 mm is considered to govern the shear failure due to combined effect of shear span to depth ratio, amount of flexural reinforcement, and spacing of stirrups.

Here, it is important to mention that the modulus of elasticity of shear reinforcement is also one of the major factors that would affect the shear contribution of FRP –RC beams; however, the variation in the modulus of elasticity is not included as manufacturer of FRP bars was supply with single grade of reinforcement only.

3.2 Beam Test Specimens

All beams are designed in such a manner that shear failure governs. GFRP bars are used as a replacement of steel reinforcement; hence, to match the performance of beam reinforced with GFRP bars, beams with steel reinforcement are also taken. The numbers of samples have been decided to cover the whole range of shear failure. Thus considering effect of

influencing parameters thirteen beams are taken for experimentation; where, one beam is reinforced with steel reinforcement and other twelve beams are fully reinforced with GFRP reinforcement. Details of design of beams and sample size are discussed in subsequent sections.

3.2.1 Influential Parameters on Shear Capacity

It is required to finalize the overall sample size and to decide the variation in parameter. It is found from the literature that the shear span to depth ratio is one of the most influencing parameter that affect on the shear capacity of a reinforced concrete beam. Hence, a statistical survey is made to determine the most influential parameters on shear capacity of the FRP-RC beam. It is observed from the literature survey that ACI recommendations are the more efficient as compared to ISIS Canada and JSCE recommendations; therefore, ACI recommendations were followed for designing of beams. The effect of variation in tensile strength of FRP reinforcement, stirrup diameter, bend radius, flexural reinforcement ratio and FRP tensile modulus on the shear capacity of FRP-RC beam is determined as per ACI 440.1R-06.

In first case, FRP tensile strength is varied as shown in Table D.1. It is observed that it affects the strength of the bent portion of FRP bars and spacing of stirrups required.

In second case, stirrup diameter is varied as shown in Table D.2. It is observed that it affects the nominal shear strength provided by concrete and spacing of stirrups required.

In third case, bend radius is varied as shown Table D.3. It is observed that it affects the strength of bend portion of FRP bar and spacing of stirrups required.

In fourth case, flexural reinforcement ratio is varied as shown Table D.4. It is observed that it affects the nominal shear strength provided by concrete and spacing of stirrups required.

In fifth and last case, modulus of elasticity is varied as shown in Table D.5. It is observed that it affects the nominal shear strength provided by concrete, design stress of FRP bars and spacing of stirrups required.

From the above analysis, it is observed that modulus of elasticity and tensile strength of the FRP bars affects the shear capacity in majority; however, manufacture was able to supply single grade of reinforcement. Hence, it is decided to go for variation in span to depth ratio and spacing of stirrup to cover whole range of shear failure. The variation of all the above mentioned parameter from first to fifth case is represented graphically in Fig. D.1 to Fig. D.5 respectively.

3.2.2 Design of Beams

Dimensional parameters of the beam are taken with width as 230 mm, depth as 300 mm, and length as 2000 mm. The RC beam with steel reinforcement is designed for two point load system as shown in Fig. 3.1 for the load W = 35 kN and shear span 'a' = 650 mm as per IS 456:2000.

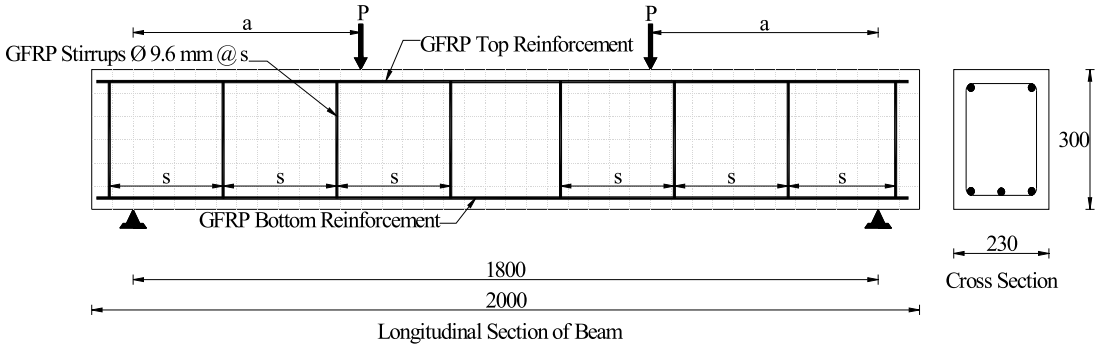

FIGURE 3.1 Cross sectional details of the beam

All the GFRP-RC beams are designed as per ACI 440.1R-06 for the loading arrangement as shown in Fig. 3.1. All three groups A, B, and C are designed for the load "W' equals to 35 kN, 30 kN, and 29 kN respectively. The design sheet containing all the three groups is attached as Appendix A.

Two different diameters of GFRP bars are used as flexural reinforcement particularly 15.25 mm and 18.71 mm in combination as per the design requirement. 9.5 mm GFRP reinforcement are used as top reinforcement in all the beams; whereas, 9.5 mm diameters stirrups are used in all the beams with different spacing. The spacing of the shear reinforcement is decided based on criteria that beam should fail in shear first before achieving flexural capacity.

3.2.3 Sample Size

Total six categories are taken for the final experimentation. These combinations are developed by combining three variations of shear span (500 mm, 650 mm, and 750 mm) and five variations in spacing of stirrups (250 mm, 275 mm, 300 mm, 325 mm, and 350 mm) in the case of beams reinforced with GFRP bars. Seventh category is of the beam reinforced with steel bars for the comparison purpose.

The objective of the study is to find the shear capacity of RC Beam with GFRP reinforcement, it is very important that the conclusions derived from the experimental study would cover all the possible type of failures. Hence, variations are taken in such a way that it covers all the possible type of shear failure like diagonal tension failure, shear compression failure, and shear tension failure occurs.

RC beam with steel reinforcement is taken for reference with same dimensional parameters and the shear span “a” as 650 mm. Design provisions of the beam are tabulated in Table 3.1.

Group A: comprised of four beams with shear span “a” as 500 mm with two variations in stirrups spacing as 250 mm and 275 mm each having 02 sets.

Group B: comprised of four beams was provided with shear span “a” as 650 mm with two variations in stirrups spacing as 275 mm and 300 mm each having 02 sets.

Group C: comprised of four beams was provided with shear span “a” as 750 mm with two variations in stirrups spacing as 325 mm and 350 mm each having 02 sets.

Details of all the twelve beams reinforced with GFRP reinforcement in flexure as well as shear are given in Table 3.1. Special notations were used to designate each beam.

TABLE 3.1 Details of the flexural and shear reinforcement

Beam[a]	a (mm)	a/d	Top Bars	Bottom Bars	Stirrups Dia. (mm)	S (mm)
SB.2.1	650	2.33	2-#10	3-#16	#8	275
GA.1.1	500	1.79	2-Φ9.5	2-Φ18.71 + 1-Φ15.25	Φ9.5	250
GA.1.2						
GA.2.1	500	1.79	2-Φ9.5	2-Φ18.71 + 1-Φ15.25	Φ9.5	275
GA.2.2						
GB.2.1	650	2.33	2-Φ9.5	2-Φ18.71 + 1-Φ15.25	Φ9.5	275
GB.2.2						
GB.3.1	650	2.33	2-Φ9.5	2-Φ18.71 + 1-Φ15.25	Φ9.5	300
GB.3.2						
GC.4.1	750	2.69	2-Φ9.5	3-Φ18.71	Φ9.5	325
GC.4.2						
GC.5.1	750	2.69	2-Φ9.5	3-Φ18.71	Φ9.5	350
GC.5.2						

[a]G$.%.N: G Type of Longitudinal and shear reinforcement (S : Steel and G : GFRP); $ denotes distance "a", the location of two point load as per Fig. 1 (A = 500mm, B = 650mm, and C = 750mm); % denotes spacing of shear reinforcement (1 = 250mm, 2 = 275mm, 3 = 300mm, 4 = 325mm and 5 = 350mm), N denotes serial number of the beam of that type. # denotes tor steel reinforcement and Φ denotes GFRP reinforcement.

3.3 Materials

3.3.1 Concrete

All the specimens were casted in the Material Testing Laboratory of Marwadi Education Foundation's Group of Institutions, Gujarat, India using ready mixed concrete with a target compressive strength of 30 MPa at 28-days supplied by the Lafarge India Pvt. Ltd. Properties of raw materials like cement and aggregates (coarse and fine) are listed in Table 3.2 and 3.3 respectively. Mix proportion used and supplied by the manufacture for the grade M30 is given in Table 3.4. All the beams and cubes were casted from the same batch and the actual properties of the concrete used were determined. Measurements on fresh concrete were carried out such as slump and density. The samples were kept in moulds for 24 hours; thereafter they were removed from the moulds and kept in curing tank until testing. The compressive strength was tested after 1, 7 and 28 days Measurements on hardened concrete by testing of standard cubes 150 x 150 x 150 mm included the

compressive strength according to IS 456:2000 as well as the elastic modulus according to IS 456:2000. The properties of the fresh and hardened concrete are displayed in Table 3.5.

TABLE 3.2. Physical properties of cement

Type of Property	Experimental Value	Value specified by IS 8112:1989
Standard Consistency (%)	30.6	N/A
Fineness (m^2/kg)	314	225 (Min.)
Specific Gravity	3.12	3.15
Setting Time (Minutes)		
Initial	90	30 (Min.)
Final	175	600 (Max.)
Compressive strength (MPa)		
3 days	28.5	23 (Min.)
7 days	41.44	33 (Min.)
28 days	49.86	43 (Min.)

TABLE 3.3. Physical properties of coarse and fine aggregates

Property	Value obtained experimentally as per IS: 383-1970	
	Coarse Aggregate	Fine Aggregate
Type	Crushed	Natural
Maximum Size (mm)	20	4.74
Specific Gravity	2.72	2.61
Water Absorption (%)	0.78	0.71
Surface Moisture (%)	Nil	0.9
Fineness Modulus	5.12	2.78

TABLE 3.4. Mix design for M-25 grade concrete.

Materials required as per the mix design (IS 10262:2009)				
Water-Cement Ratio	**Cement (kg)**	**Water (kg)**	**Fine Aggregate (kg)**	**Coarse Aggregate (kg)**
0.5	394.32	197.16	669.53	1121.8

TABLE 3.5. Properties of fresh and hardened concrete.

Slump (mm)	**Average Compressive Strength (f'c) (MPa)**			**Modulus of Elasticity (E_c) (GPa)**
	3 Days	**7 Days**	**28 Days**	
81	15.35	24.86	34.65	22.04

3.3.2 Steel

As mentioned in Table 3.1, 16 mm diameter tor steel reinforcement are used as flexural reinforcement, 10 mm bars as top reinforcement and 8 mm bars as stirrups. Strength and dimensional properties of the average of three bars are listed in Table 3.6 and 3.7 respectively.

TABLE 3.6. Mechanical properties of tor steel bars.

Sr. No.	**Kind of Specimen**	**Nominal Diameter (mm)**	**Gauge Length (mm)**	**Yield Stress (N/mm^2)**	**Ultimate Tensile Stress (N/mm^2)**	**Percentage Elongation (%)**	**Percentage Reduction in Area (%)**
1	Tor Steel	8	40	461.59	575.82	19.63	44.83
2		10	50	449.35	583.48	19.32	46.32
3		16	80	451.45	578.9	20.08	43.55

TABLE 3.7. Weight & dimensional properties of tor steel bars.

Sr. No.	Kind of Specimen	Nominal Diameter (mm)	Actual Diameter (mm)	Cross Sectional Area (mm^2)	Weight (kg/m)
1	Tor Steel	8	8.04	50.83	0.399
2		10	9.61	72.48	0.569
3		16	11.65	106.62	0.837

3.3.3 GFRP Reinforcement

- **GFRP Straight Bars :** Three types of diameters 9.5 mm, 15.25 mm, and 18.71 mm supplied by Dextra India Private Limited are used in longitudinal direction. The manufacturer was supplying single grade of modulus of elasticity of GFRP bars. GFRP reinforcement made of continuous longitudinal glass fibers impregnated in a thermosetting vinyl ester resin using infusion process with a average fiber content of 81.87% (by weight), are used as flexural and shear reinforcement. The bond performance with surrounding concrete of the supplied GFRP reinforcement is improved by providing sand-coated surface. Photographs of the supplied GFRP rebar are shown as Fig. 3.2 & 3.3.

FIGURE3.2 GFRP bars

FIGURE3.3 GFRP bars close view

Few of the properties like ultimate stress, modulus of elasticity and ultimate strain etc. are tested in the laboratory. Tensile test is done as per ASTM D7205; where, the shear test is done as per ASTM D4475 to cross check all the properties which are very much crucial for the study. Sample for tension test, loaded sample in universal testing machine and failed samples are shown in Fig. 3.4, 3.5, and 3.6 respectively. Snap shots of the tensile test and shear test are shown in Fig. 3.3 and 3.4 respectively. These properties found very close to the data supplied by the manufacturer. A comparison between experimental and supplied properties is shown in Table 3.8. Detail properties of the GFRP bars are given in Appendix B. Stress Vs Strain relationship of GFRP bars of 9.5mm, 15.25 mm and 18.71 mm derived experimentally are plotted in Fig. 3.10.

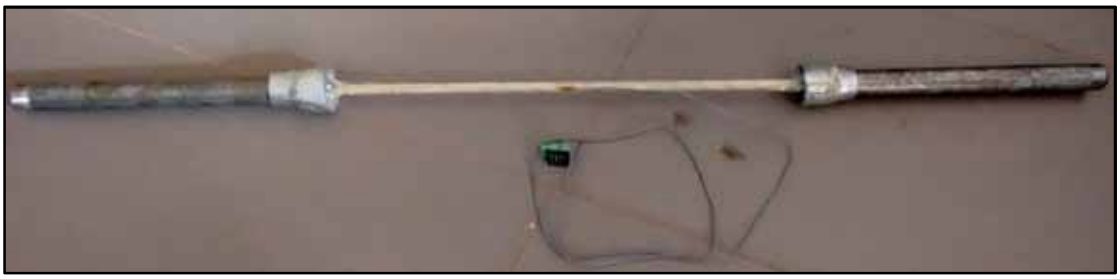

FIGURE3.4 Sample for tension test of GFRP bar

FIGURE3.5 Loaded sample in UTM for tension test of GFRP bar

FIGURE3.6 Failed sample of GFRP bar in tension

FIGURE3.7 Sample for shear test on GFRP bar

FIGURE3.8 Assembly with failed sample of GFRP bar in shear

FIGURE3.9 Sample of GFRP bar failed in shear test

TABLE 3.8. Comparison of experimental and supplied properties of GFRP reinforcement

d_b (mm)	f'_{frpu} (Mpa)	E_{frp} (Gpa)	Ultimate Strain	Transverse Strength (MPa)	f'_{frpu} (Mpa)	E_{frp} (Gpa)	Ultimate Strain	Transverse Strength (MPa)
	Manufacturer Data				Experimental Results			
9.5	871	48.3	1.93	--	891	48.4	1.841	--
15.25	904	48.2	2.05	159.22	911	48.2	1.89	160.43
18.71	955	47.3	2.16	--	963	47.4	2.03	--

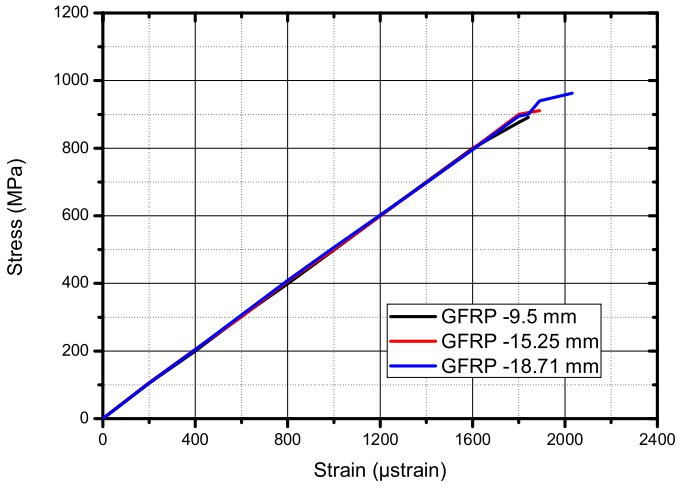

FIGURE3.10 Stress Vs Strain relationship GFRP bars

- **GFRP Stirrups :** The GFRP bars are brittle material and they cannot be bent onsite; whereas, as per the structural requirement GFRP bars shall be ordered cut to size and shape. Hence, in this study considering clear cover 25 mm, factory made prefabricated stirrups procured of width 180 mm, overall depth 250 mm, and bend radius r_b 38 mm (4 times d_b) as GFRP reinforcement cannot be bent on site due to its brittle nature. Schematic diagram and photograph of GFRP stirrup are shown as Fig. 3.11 and 3.12 respectively. Detail properties of the GFRP stirrup are given in Appendix C.

3.3.4 Modulus of Elasticity of Steel and GFRP reinforcement

It is worth mentioning that modulus of elasticity of steel is around 200 GPa whereas of GFRP is 48 GPa. This relatively low modulus of elasticity of FRP bars influences the two components of shear strength V_c and V_{frp} significantly.

Lower modulus of elasticity of FRP composite materials develops wider and deeper cracks in the beam. Deeper crack decreases the contribution to shear strength from uncracked concrete due to the lower depth of concrete in compression, whereas, wider cracks decreases the contribution from aggregate interlock and residual tensile stresses. Additionally, due to small transverse strength of FRP bars and wider cracks, the contribution of dowel action would be very small. Hence, shear capacity of concrete members reinforced with FRP reinforcement is lower than that of members reinforced with steel.

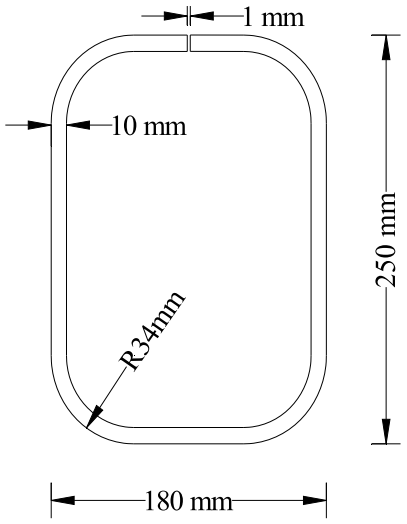

FIGURE 3.11 Schematic diagram of stirrup

FIGURE 3.12 Photograph of stirrup

3.4 Instrumentation

In this experimental study, it is required to find out the strain developed at various locations like stirrups in the shear zone, flexural reinforcement and concrete surface in the shear zone. In parallel, to observe overall behavior, it is required to measure the central deflection. Hence, the development of strain, deflection and crack along with the increase in load are recorded.

TML – Tokyo Sokki Kenkyujo Co. Ltd., Japan is one of the leading companies for the manufacturing of such state-of-the-art advanced instrumentation. Measurement of strain depends on the type of material; hence, different types of strain gauges for different applications like strain on concrete, composite or steel, displacement transducers and data logger are derived from TML, Japan. These strain gauges and displacement transducers and connected with data logger and one can observe and record the time dependant variation in these parameters.

3.4.1 Strain Gauges

To determine a degree of deformation in the material/element due to mechanical strain to determine forces such as load or stress; or indirectly, degree of safety of material/structural element using that material, strain is measured.

The electrical resistance changes due to deformation produced in an element due to application of external force in metallic material. These changes in electrical resistance are measured by strain gauges when sticked to the material through electrical insulation. The variation in strain of material is proportional to the changes in electrical resistance. The strain generated in the test specimen is relayed via electrical insulation to the resistance wire or the foil in the gauge while the deformation is produced. As a result, the fine wire or foil experiences a variation in electrical resistance. This variation is exactly proportional to the strain.

Strain gauge features,

- Simple construction with a small mass and volume so as not to interfere with the stresses on the specimen.
- Short distance between measuring points for localized evaluation.
- Good frequency response for tracking rapid fluctuations in stresses.
- Simultaneous measurement of multiple points and remote measurement.
- Electrical output for easy data processing.

Strain gauges are provided with various convenient features as well as default limitations. These limitations may be in terms of fatigue, temperature, measurement environment or amount of strain. Relevant limitation must be examined before the selection of the strain gauge.

To observe strain on the reinforcement and concrete, strain gauges manufactured by Tokyo Sokki Kenkyujo Co. Ltd. (TML), Japan are used. Specific strain gauges like PL-90-11-3L for concrete (surface), BFLA-5-5-3L for composite reinforcement (GFRP) and FLA – 3-11- 1L for steel are used to observe the strain.

- **Strain Gauge PL-90-11-3L for Concrete (Surface) :** This is a foil strain gauge having polyester resin backing. It is mainly used for measurement on concrete, mortar, or rock. It is available in different gauge length like 60 mm, 90 mm, and 120 mm which can be used as per the size of the aggregate present in the mix. The gauge length of this strain gauge is 90 mm, whereas gauge factor and resistance are 2.10 ± 1 % and 119.90 ± 0.5 Ω respectively. CN-E/RP-2 type adhesive shall be used while applying strain gauge on the material/element. PL type strain gauge and its application on the concrete surface are shown in Fig. 3.13 and 3.14

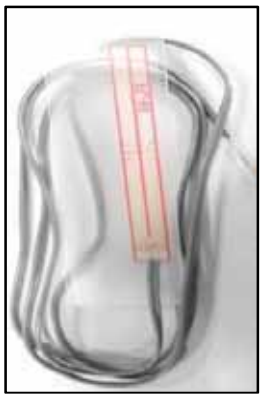

FIGURE 3.13 Strain gauge PL-90-11-3L

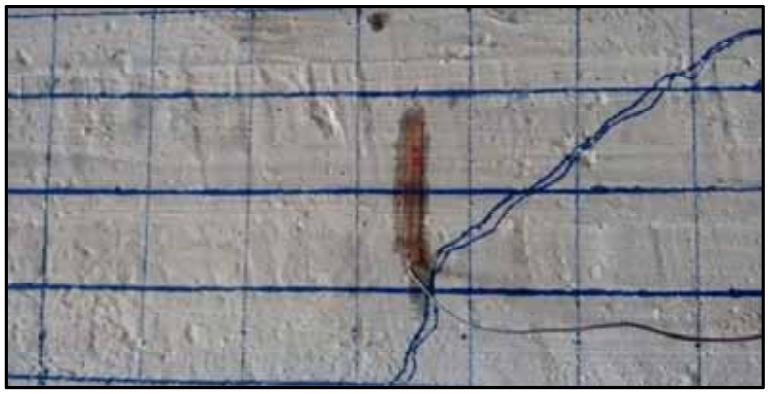

FIGURE 3.14 PL-90-11-3L applied on concrete surface

- **Strain Gauge BFLA-5-5-3L for Composite Reinforcement :** BFLA-5-5-3L is specifically design for measurement on composite materials. A grid configuration is specifically designed to reduce the tightening effect of the gauge to the specimen. The temperature compensation is available for this material with thermal expansion coefficient of 3, 5, or 8 ppm/°C, this series of strain gauge is applicable to composites, ceramic, and carbon materials. The gauge length of this strain gauge is 5 mm, whereas gauge factor and resistance are 2.09 ± 1 % and 120.40 ± 0.5 Ω respectively. CN/EB-2 type adhesive shall be used while applying strain gauge on the material/element.

BFLA-5-5-3L type strain gauge and its application on GFRP reinforcement are shown in Fig. 3.15 and 3.16 respectively.

FIGURE 3.15 Strain gauge BFLA-5-5-3L

FIGURE 3.16 BFLA-5-5-3L applied on composite reinforcement

- **Strain Gauge FLA-3-11-1L for Steel Reinforcement :** FLA-3-11-1L is an ordinary strain gauge integrated with T-type thermocouple. The T-type thermocouple is composed of the Cu and the Cu-Ni wire which are used as a lead wire of the strain gauge. The strain measurement with quarter bridge 3-wire method and temperature measurement both are possible when combined with TML data loggers. The gauge length of this strain gauge is 3 mm, whereas gauge factor and resistance are 2.10 ± 1 % and 120.40 ± 0.5 Ω respectively. CN/P-2 type adhesive shall be used while applying strain gauge on the material/element. FLA-3-11-1L type strain gauge and its application on GFRP reinforcement are shown in Fig. 3.17 and 3.18 respectively.

FIGURE 3.17 Strain gauge FLA-3-11-1L

FIGURE 3.18 FLA-3-11-1L applied on concrete surface

3.4.2 Displacement Transducer

CDP-100 displacement transducer manufactured by TML is a compact and easy to operate strain transducer. Highly accurate measurements can be made; because, it is designed to produce a large output and to deliver stable performance. It is suitable for both static and dynamic measurements. Its input/output resistance is 350 Ω and rated output is 5 mV/V±0.1% (10000 x 10^{-6} strain ± 0.1%). It works with the frequency response of 3 Hz and spring force of 4.9 N. CDR-100 was used to measure mid-span deflection in the beam as shown in Fig. 3.19.

FIGURE 3.19 Displacement transducer CDR-100.

3.4.3 Data Recorder

TMR-200 MULTI RECORDER is a Small Multi-Channel Data Acquisition System enabling combination of various measuring units according to experimental purposes. The testing objects are analog input such as stress, load, pressure, acceleration, etc. using strain gauges and strain gauge based transducers and digital input/output such as CAN etc. on vehicle onboard measurement. The recorder TMR-200 can be easily installed on any kind of stationary structure such as buildings, bridges or machines as well as moving elements like ships, aircraft or automobiles. Technological advancement has improved various testing themes for safety and convenience using computer controlled products. Sensors are also improved day by day. In compatibility with such versatile sensors, expanded units such as CAN/VOICE/GPS unit and telemeter unit are added to ordinary strain, voltage and temperature measuring units.

TMR-200 features,

- Combination of a plentiful and various sensor input/output units for strain, temperature, voltage, CAN, etc.
- The maximum measurement of 80 channels
- 100kHz high speed sampling
- Vibration tolerance and small size suitable for vehicle onboard
- Battery operation
- Data recovery at power interruption and measurement restart at power recovery
- Various settings, monitoring and measurement result display with the display unit
- Compatible with large capacity CF card
- USB and LAN interfaces
- Histogram analysis in real time

FIGURE 3.20 TMR-200 multi recorder

As this reorder TMR-200 as shown in Fig. 3.20 is having 8 channel for the data recording; data are recorded from four strain gauges on shear reinforcement in the shear zone on either side, one on flexural reinforcement at mid-span, two on the concrete surface in the shear crack zone on either side and mid-span deflection through displacement transducer.

3.5 Specimen Preparation

There are total thirteen beams to cast one with steel reinforcement and other twelve with GFRP reinforcement. All the beams were cast on the same day and from the same ready mix concrete supplied Lafarge India Private Limited, Rajkot at Advanced Material Testing Laboratory of Marwadi Education Foundation.

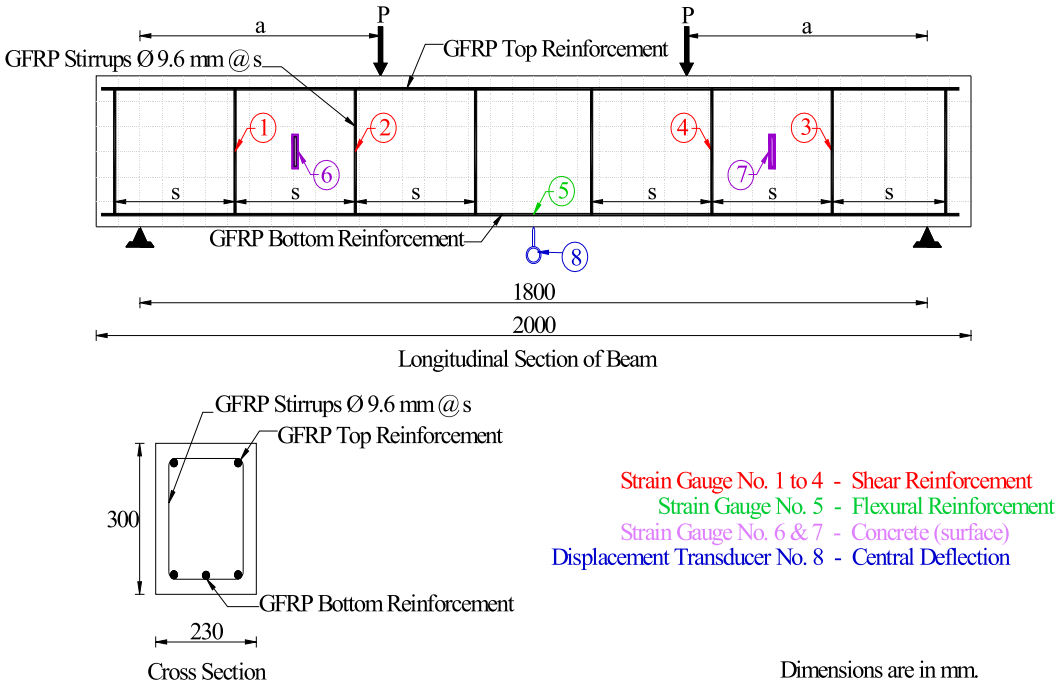

FIGURE 3.21 Strain gauge and deflection locations for the data observation and recording

As mentioned in section 3.4.3, data recording during the test was taken from eight locations like strain observations at seven locations and one central deflection as shown in Fig. 3.21. At initial stage, reinforcement cages as shown in Fig. 3.22 were prepared as per the longitudinal reinforcement as well as spacing of stirrups as per the details given in Table 3.1. Subsequently, strain gauges were applied on the reinforcement as per the locations decided. Standard procedure specified by manufacturer was followed at the time of application of strain gauges like smoothening of surface and fine polishing of the portion where strain gauge is to be pasted. Consequently, specified adhesive was applied on the reinforcement as well as on the back of the strain gauge. By placing the strain gauge at specified location, it was pressed for minimum three minutes with non-adhesive polythene sheet supplied by the manufacturer for this purpose.

Then, these reinforcement cages were placed in plywood formwork prepared at the laboratory only. Bundled extension wires were arranged such a way that strain gauge and wire would not get damaged at the time of concreting. Snap shot of the strain gauge applied, bird view of all the beams collectively with reinforcement cages, and beam after concreting are shown as Fig. 3.23 3.24, and 3.25 respectively.

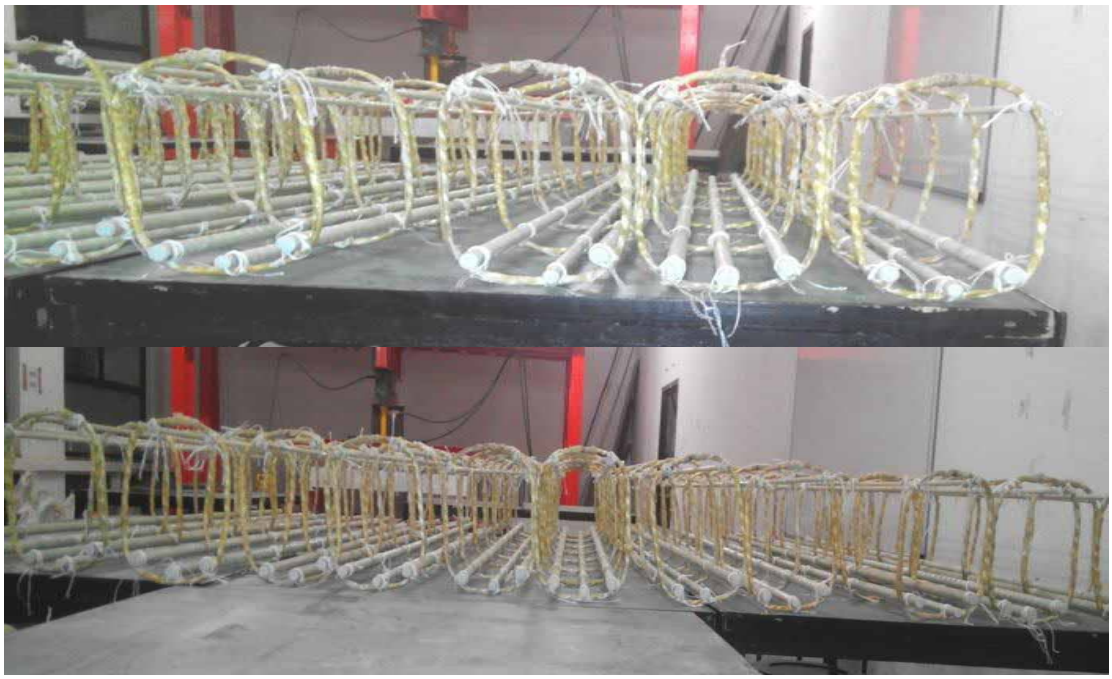

FIGURE 3.22 Reinforcement cages of GFRP reinforcement

FIGURE 3.23 Application of strain gauge on longitudinal and shear reinforcement

FIGURE 3.24 Bird view of the reinforcement cages placed in the plywood formwork

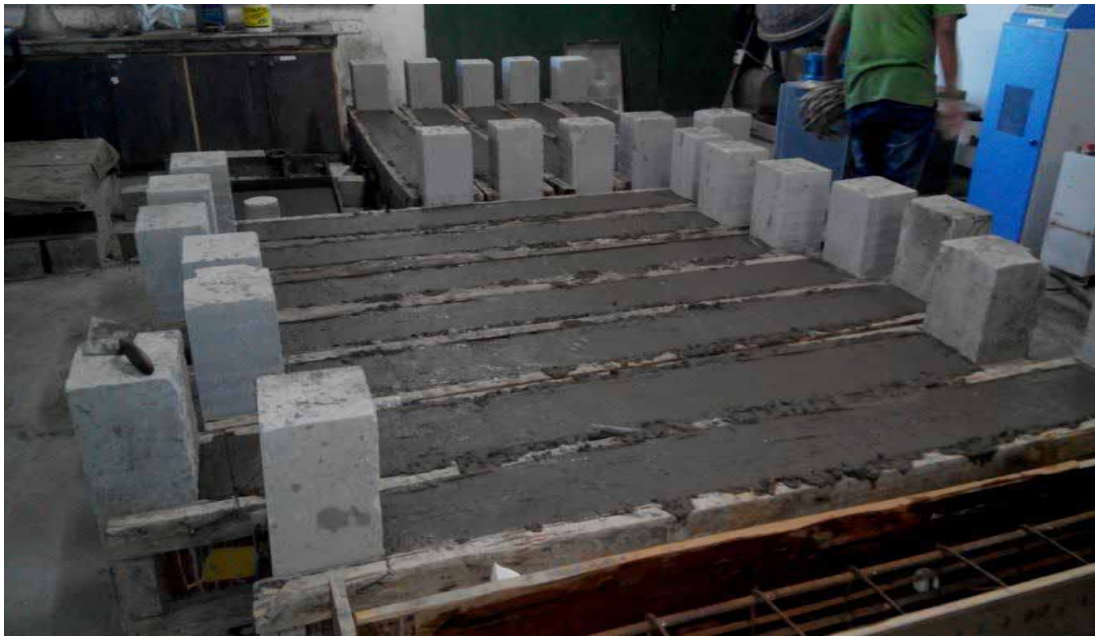

FIGURE 3.25 Beams after completion of concreting

3.6 Test Setup

A versatile loading frame of capacity 550 kN was designed and erected at Advanced Material Testing Laboratory of Marwadi Education foundation. The frame can test the real size beam or slab up to 3.5 m span. Schematic diagram and front view of the frame is shown as Fig. 3.26 and 3.27 respectively.

The frame is equipped with the double acting loading jack of 550 kN capacity manufactured by ENERPAC. The specimens were tested as simply supported beams by four point load system with different load positions in term of shear span "a" as mentioned in Table 3.1. To distribute the load from the jack as two concentrated load a steel beam was used as per in Fig. 3.27 and 3.28. Spacers were used to fill the gap between jack and the steel beam transferring the load to the specimen.

Data observation and recording were to be made from eight locations particularly from four locations on GFRP stirrups, one on GFRP flexural reinforcement, two on concrete surface and one displacement transducer to for central deflection were connected to the TMR-200 multi recorder as per Fig. 3.21 and close view of the same is shown as Fig. 3.28. Even this multi recorder was connected to laptop to observe the strain development, central deflection and store the data in the hard disk directly. Multi recorder had the facility to observe and store the data and then same could be transferred to laptop, however, due to bigger screen laptop was found convenient for the process.

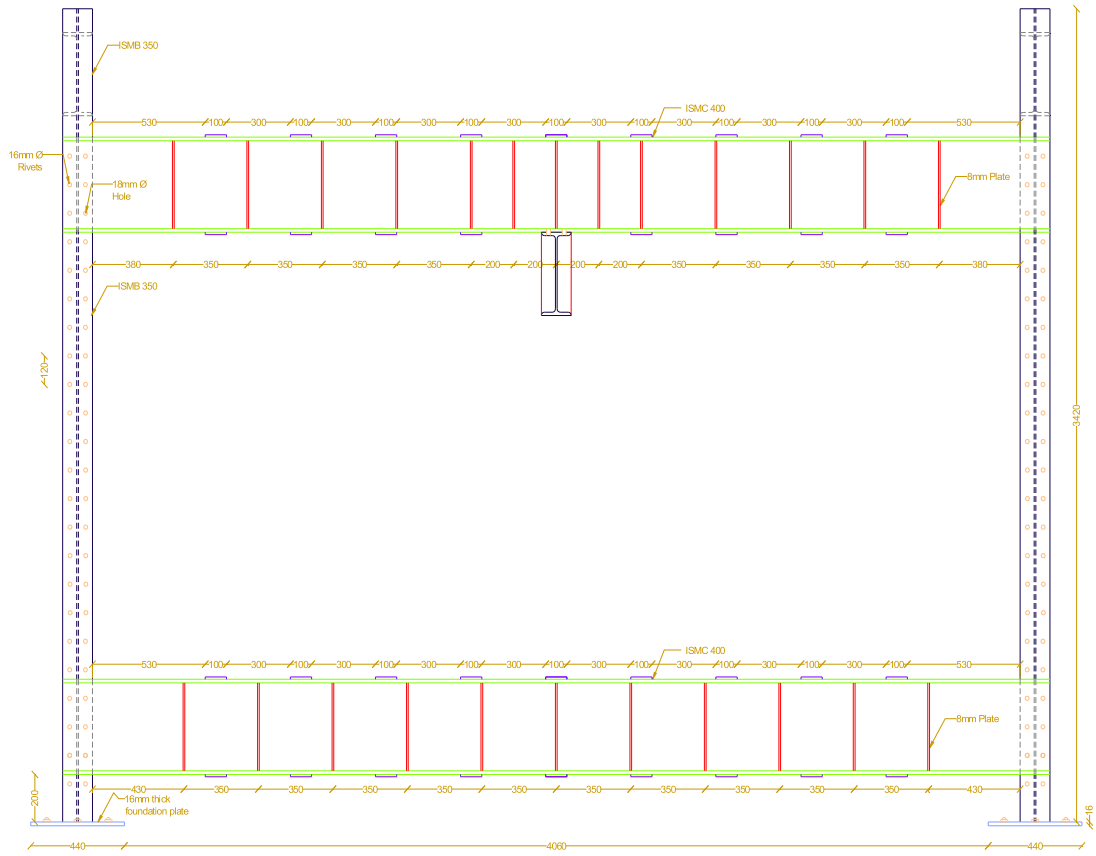

FIGURE 3.26 Schematic diagram of 550 kN loading frame

FIGURE 3.27 Front view of 550 kN loading frame

FIGURE 3.28 Gauges & displacement transducer connected to multi recorder TMR-200

3.7 Loading Procedure

After the marking are made on the beams at 50 mm interval vertically and horizontally to observe the crack location, beams were transferred on the loading frame using lifting chain block of capacity 2 tonne. Where positions of supports were kept 1800 mm apart and beams were of 2000 mm long. Hence, projection of 100 mm shall be observed on each side. Then the cylindrical loading keys were place as per the shear span "a" for the particular beam. Beam with steel rebars was used to transfer the load from jack to the beam through loading keys to create four point load system; two supports and two loads. Depending on the gap between beam and jack, spacers were placed to reduce the travel distance of the loading jack.

Displacement transducer CDR-100 was placed in the position at the bottom of the beam at mid-span with initial displacement as zero before loading. All the seven strain gauges and displacement transducer were connected to the multi recorder TMR-200 and TMR-200 was connected to the laptop. All the activities are controlled through the software provided by TML for the data observation and recording. Once the constants, unit of different observations like strain or displacement and interval of data capturing are input in the software, specimen would be ready for the test. When the loading is started on the specimen, recording also shall be started in the recorder/software in parallel. One can

observe variations in parameter (strain or displacement) with time with the progress of test. Relation of parameter vs time would automatically be stored as data file in the device/laptop when the test is over. Details of the location of channels and their data observation are given in Table 3.9.

TABLE 3.9 Details of data observation and their locations.

Channel No.	Location	Parameter	Unit
CH1	Left Side Stirrup - 1	μStrain	(mm/mm)
CH2	Left Side Stirrup - 2	μStrain	(mm/mm)
CH3	Right Side Stirrup - 1	μStrain	(mm/mm)
CH4	Right Side Stirrup - 2	μStrain	(mm/mm)
CH5	Flexural Reinforcement at Mid-Span	μStrain	(mm/mm)
CH6	Concrete Surface - Left	μStrain	(mm/mm)
CH7	Concrete Surface - Right	μStrain	(mm/mm)
CH8	Central Deflection	Deflection	mm

The load was monotonically applied approximately up to 90% of the expected failure load using hydraulic jack connected to the frame with a controlled rate of 5 kN/min. Thereafter, to reduce the accidental chances because of brittle shear failure, the load applied was displacement-controlled at a rate of 0.6 mm. Close observation was kept during the test and various stages like load at the first flexural crack, first shear crack and second shear crack were recorded. Even development of load with time was also recorded so that load vs parameters like strain and deflection can be matched finally.

Maximum crack width of 0.5 mm is permissible in the GFRP reinforced elements; hence, beam shall be considered failed after the crack width of 0.5 mm. Even after that, the test was continued up to ultimate failure. Detailed discussion on data observation, load at cracks, type of failure and final results is done in the subsequent chapter.

CHAPTER : 4

Experimental Results and Discussion

4.1 General

Results obtained from the testing of thirteen full-scale GFRP reinforced concrete beams of this experimental program are presented. The results of each test including measurements of stirrup strains, flexural strain, concrete surface strain and central deflection, etc. at various load stages are recorded. The first crack load in shear or flexure, crack pattern and mode of failure at ultimate are reported in this section. The strain values are recorded at eight locations as shown in Fig. 3.20 on both sides of the beam. However, data observed are useful from the locations from where the failure has occurred. Hence, the charts of the subsequent sections showing relationship between various strains against the applied shear force are of the failure locations only.

The beams with GFRP reinforcement are grouped into three main categories designated as GA, GB, and GC for the shear span of 500 mm, 650 mm, and 750 mm respectively. Each main category is further divided in to two subcategories according to three varying spacing of stirrups. In such a way, there are six subcategories and in each sase duplicate beams are cast. All the beams are tested as simply supported with two point loading system.

4.2 Test Results of Category SB

The beam specimen prepared with the conventional steel reinforcement is considered as the reference beam for comparison of test results obtained from the beams containing GFRP bars, as main reinforcement. The code SB.2.1 represents “S” means steel reinforcement, “B” stands for shear span “a = 650 mm”, 2 is for spacing of stirrups as 275 mm and 1 is the serial number of this category.

4.2.1 Specimen SB.2.1

Beam SB.2.1 is designed to carry 35 kN load with reinforcement configuration shown in Table 2.1. First flexural crack is developed at 32.41 kN shear force. Subsequently, first shear crack is observed at 40.08 kN force on the left side of the beam. The second shear crack developed at 42.48 kN force on the right side of the beam. The failure shear forces at first and second shear crack are observed as 44.88kN and 48.56 kN respectively at 0.5 mm shear crack width. The strain values for stirrups, flexural reinforcement and concrete surface are 823, 2289 and 755 μstrain respectively at 0.5mm shear crack width. The central deflection is 11.45 mm. The crack pattern showed the propagation of crack from the point of load application towards the support. Sudden failure of the beam in shear is observed on left side with a crack angle of 45°. At the final failure of beam, the crack is extended along with longitudinal reinforcement and shear tension failure is occurred in the beam as shown in Fig. 4.1. Relationships namely shear force - strain values and shear force - mid-span deflection are shown in Fig. 4.2 and 4.3 respectively. The test results are tabulated in Table E.1.

FIGURE 4.1 The crack patterns and ultimate failure of SB.2.1.

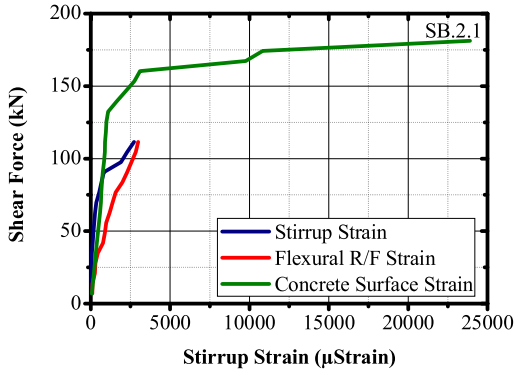

FIGURE 4.2 Relationship of shear force and strain variation for SB.2.1.

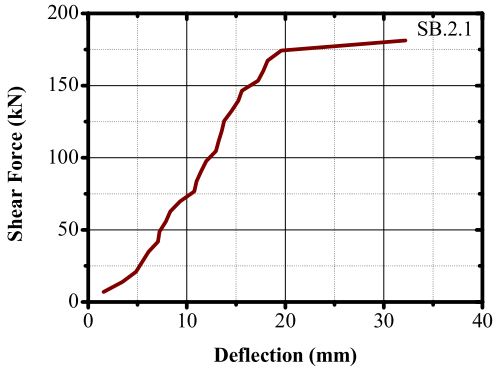

FIGURE 4.3 Relationship of shear force and mid-span deflection for SB.2.1.

4.3 Test Results of Category GA

In this category, four beams specimens of rectangular section having same shear span "a = 500 mm" were tested as simply supported beams with two point loading system. The set is divided into two subcategories with spacing of stirrups 250 mm and 275 mm with duplicate casting in each case designated as GA.1.1, GA.1.2, GA.2.1 and GA.2.2. The code GA.1.1 represents "G" means GFRP reinforcement, "A" stands for shear span "a = 500 mm", 1 is for spacing of stirrups as 250 mm and 1 is the serial number of that category.

4.3.1 Specimen GA.1.1

Beam GA.1.1 is designed to carry 35 kN load with reinforcement configuration shown in Table 2.1. First flexural crack is developed at 31.37 kN shear force. Subsequently, first shear crack is observed at 54.02 kN on the right side of beam. The second shear crack is developed at 59.25 kN shear force on left side. The failure shear forces at first and second shear crack are observed as 72.94 kN and 67.61 kN respectively at 0.5 mm shear crack width. The strain values for stirrups, flexural reinforcement and concrete surface are 3689, 5638 and 6350 µstrain respectively at 0.5mm shear crack width. The central deflection is 31.00 mm. The crack pattern showed the propagation of crack from the point of load application towards the support. Sudden failure of the beam in shear is observed on right side with a crack angle of 49°. At the final failure of beam, the crack is divided into two parts from middle of the crack and diagonal tension failure is occurred in the beam as

shown in Fig. 4.4. Relationships namely shear force - strain values and shear force - mid-span deflection are shown in Fig. 4.5 and 4.6 respectively. The test results are tabulated in Table E.2.

FIGURE 4.4 The crack patterns and ultimate failure of GA.1.1.

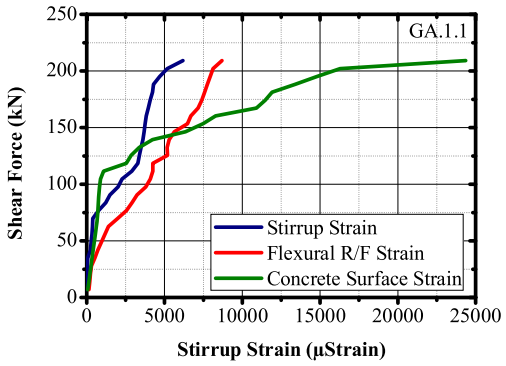

FIGURE 4.5 Relationship of shear force and strain variation for GA.1.1

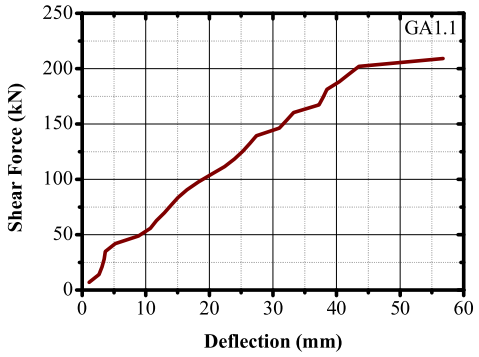

FIGURE 4.6 Relationship of shear force and mid-span deflection for GA.1.1.

4.3.2 Specimen GA.1.2

Beam GA.1.2 is the duplicate casting with same configuration as GA.1.1. First flexural crack is developed at 22.65 kN shear force. Subsequently, first shear crack is observed on right side of the beam at 59.25 kN. The second shear crack is developed on left side at 62.73 kN shear force. The failure shear forces at first and second shear crack are observed

as 68.88 kN and 66.22 kN respectively at 0.5 mm shear crack width. The strain values for stirrups, flexural reinforcement and concrete surface are 2846, 3698 and 7728 μstrain respectively at 0.5mm shear crack width. The central deflection is 24.92 mm. The crack pattern showed the propagation of crack from the point of load application towards the support. Sudden failure of the beam in shear is observed on right side with a crack angle of 49°. At the final failure of beam, the crack is divided into two parts from middle of the crack and diagonal tension failure is occurred in the beam as shown in Fig. 4.7. Relationships namely shear force - strain values and shear force - mid-span deflection are shown in Fig. 4.8 and 4.9 respectively. The test results are tabulated in Table E.3.

FIGURE 4.7 The crack patterns and ultimate failure of GA.1.2.

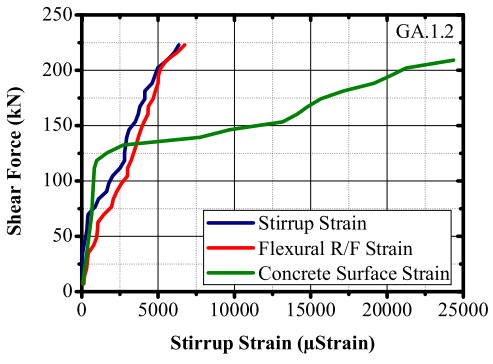

FIGURE 4.8 Relationship of shear force and strain variation for GA.1.2.

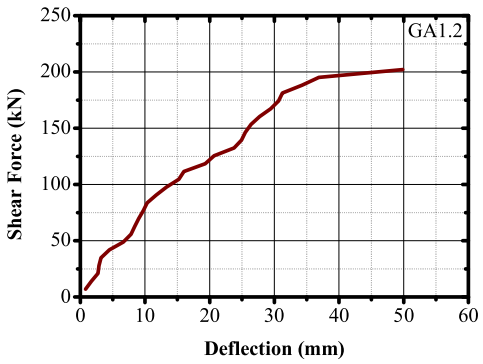

FIGURE 4.9 Relationship of shear force and mid-span deflection for GA.1.2.

4.3.3 Specimen GA.2.1

Beam GA.2.1 is designed for W = 35 kN load with reinforcement configuration shown in Table 2.1. First flexural crack is developed at 27.88 kN shear force. Subsequently, first shear crack is observed on right side of the beam at 54.02 kN. The second shear crack is developed on left side at 57.50 kN shear force. The failure shear forces at first and second shear crack are observed as 74.47 kN and 63.07 kN respectively at 0.5 mm shear crack width. The strain values for stirrups, flexural reinforcement and concrete surface are 5506, 5606 and 3390 μstrain respectively at 0.5mm shear crack width. The central deflection is 25.24 mm. The crack pattern showed the propagation of crack from the point of load application towards the support. Sudden failure of the beam in shear is observed from lower crack on right side with a crack angle of 46°. Diagonal tension failure with stirrup rupture is occurred in the beam as shown in Fig. 4.10. Relationships namely shear force - strain values and shear force - mid-span deflection are shown in Fig. 4.11 and 4.12 respectively. The test results are tabulated in Table E.4.

FIGURE 4.10 The crack patterns and ultimate failure of GA.2.1.

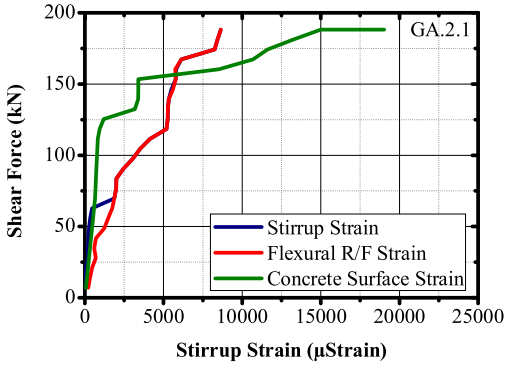

FIGURE 4.11 Relationship of shear force and strain variation for GA.2.1.

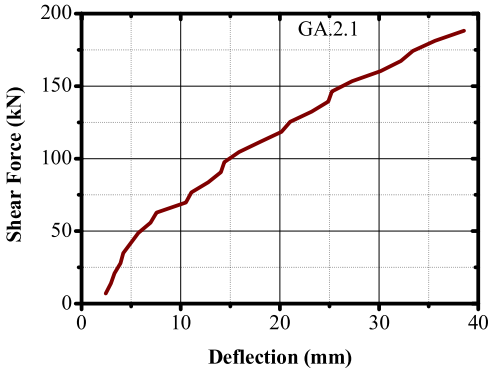

FIGURE 4.12 Relationship of shear force and mid-span deflection for GA.2.1.

4.3.4 Specimen GA.2.2

Beam GA.2.2 is the duplicate casting with same configuration as GA.2.1. First flexural crack is developed at 29.62 kN shear force. Subsequently, first shear crack is observed on left side of the beam at 55.76 kN. The second shear crack is developed on right side at 71.44 kN shear force. The failure shear forces at first and second shear crack are observed as 74.65 kN and 73.15 kN respectively at 0.5 mm shear crack width. The strain values for stirrups, flexural reinforcement and concrete surface are 5890, 4383 and 6246 µstrain respectively at 0.5mm shear crack width. The central deflection is 26.40 mm. The crack pattern showed the propagation of crack from the point of load application towards the support. Sudden failure of the beam in shear is observed on right side with a crack angle of 47°. At the final failure of beam, the crack is divided into two parts from middle of the crack and diagonal tension failure is occurred in the beam as shown in Fig. 4.13. Relationships namely shear force - strain values and shear force - mid-span deflection are shown in Fig. 4.14 and 4.15 respectively. The test results are tabulated in Table E.5.

FIGURE 4.13 The crack patterns and ultimate failure of GA.2.2.

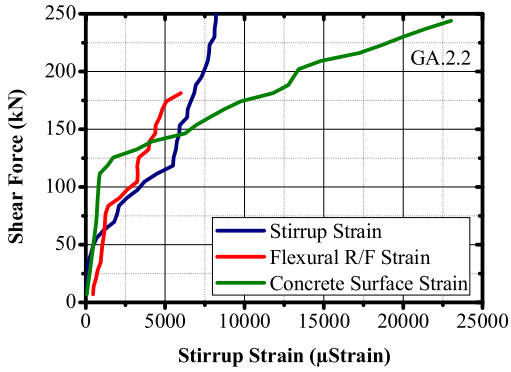

FIGURE 4.14 Relationship of shear force and strain variation for GA.2.2.

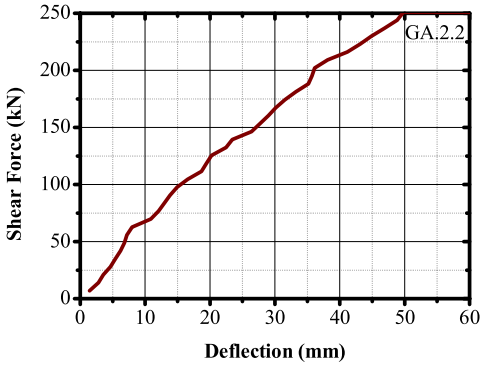

FIGURE 4.15 Experimental Shear Force vs Mid-Span Deflection Relationship of Specimen GA.2.2.

4.4 Test Results of Category GB

In this category, four beams specimens of rectangular section having same shear span "a = 650 mm" are tested as simply supported beams. The set is divided into two subcategories with spacing of stirrups 275 mm and 300 mm with duplicate casting in each case designated as GB.2.1, GB.2.2, GB.3.1 and GB.3.2. The code GB.2.1 represents "G" means

GFRP reinforcement, “B” stands for shear span “a = 650 mm”, 2 is for spacing of stirrups as 275 mm and 1 is the serial number of that category.

4.4.1 Specimen GB.2.1

Beam GB.2.1 is designed for W = 30 kN load with reinforcement configuration shown in Table 2.1. First flexural crack is developed at 24.40 kN shear force. Subsequently, first shear crack is observed on right side of the beam at 38.84 kN. The second shear crack is developed on left side at 43.56 kN shear force. The failure shear forces at first and second shear crack are observed as 51.30 kN and 45.27 kN respectively at 0.5 mm shear crack width. The strain values for stirrups, flexural reinforcement and concrete surface are 5184, 4370 and 5532 μstrain respectively at 0.5mm shear crack width. The central deflection is 22.12 mm. The crack pattern showed the propagation of crack from the point of load application towards the support. Sudden failure of the beam in shear is observed on right side with a crack angle of 46°. Shear compression failure with crushing at top of the shear crack is occurred in the beam as shown in Fig. 4.16. Relationships namely shear force - strain values and shear force - mid-span deflection are shown in Fig. 4.17 and 4.18 respectively. The test results are tabulated in Table E.6.

FIGURE 4.16 The crack patterns and ultimate failure of GB.2.1.

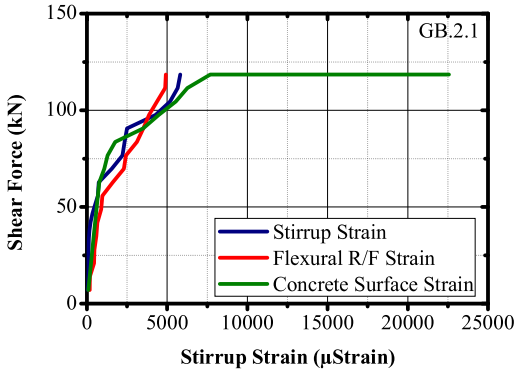

FIGURE 4.17 Relationship of shear force and strain variation for GB.2.1.

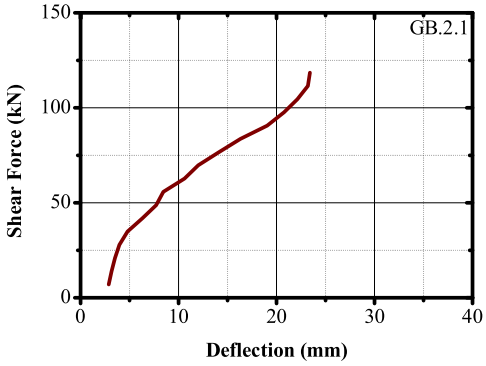

FIGURE 4.18 Relationship of shear force and mid-span deflection for GB.2.1.

4.4.2 Specimen GB.2.2

Beam GB.2.2 is the duplicate casting with same configuration as GB.2.1. First flexural crack is developed at 31.37 kN shear force. Subsequently, first shear crack is observed on left side of the beam at 38.84 kN. The second shear crack is developed on right side at 48.79 kN shear force. The failure shear forces at first and second shear crack are observed as 57.01kN and 52.76 kN respectively at 0.5 mm shear crack width. The strain values for stirrups, flexural reinforcement and concrete surface are 3980, 4430 and 4358 µstrain respectively at 0.5mm shear crack width. The central deflection is 23.80 mm. The crack pattern showed the propagation of crack from the point of load application towards the support. Sudden failure of the beam in shear is observed on right side with a crack angle of 50°. Shear compression failure with crushing at top of the shear crack is occurred in the beam as shown in Fig. 4.19. Relationships namely shear force - strain values and shear force - mid-span deflection are shown in Fig. 4.20 and 4.21 respectively. The test results are tabulated in Table E.7.

FIGURE 4.19 The crack patterns and ultimate failure of GB.2.2.

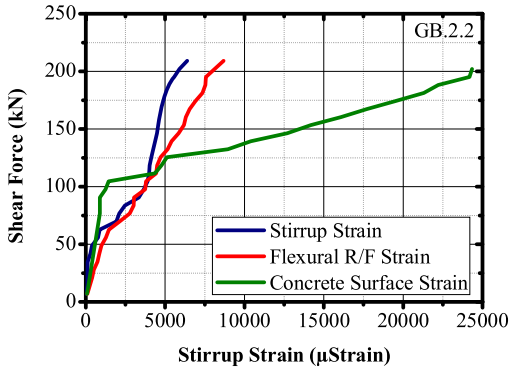

FIGURE 4.20 Relationship of shear force and strain variation for GB.2.2.

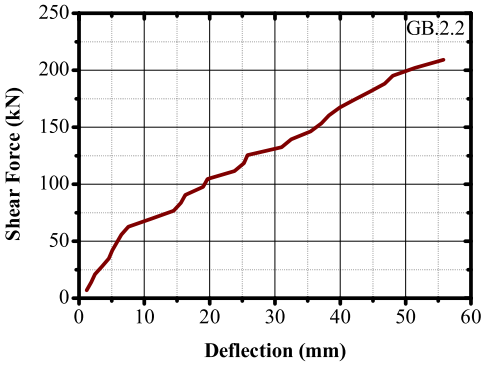

FIGURE 4.21 Relationship of shear force and mid-span deflection for GB.2.2.

4.4.3 Specimen GB.3.1

Beam GB.3.1 is designed for W = 30 kN load with reinforcement configuration shown in Table 2.1. First flexural crack is developed at 22.65 kN shear force. Subsequently, first shear crack is observed on right side of the beam at 38.84 kN. The second shear crack is developed on left side at 57.50 kN shear force. The failure shear forces at first and second shear crack are observed as 51.44 kN and 58.71 kN respectively at 0.5 mm shear crack width. The strain values for stirrups, flexural reinforcement and concrete surface are 3578, 4680 and 7234 µstrain respectively at 0.5mm shear crack width. The central deflection is 24.88 mm. The crack pattern showed the propagation of crack from the point of load

application towards the support. Sudden failure of the beam in shear is observed on both sides; however, primary failure is from left side with a crack angle of 46°. Shear compression failure with crushing at top of the shear crack is occurred in the beam as shown in Fig. 4.22. Relationships namely shear force - strain values and shear force - mid-span deflection are shown in Fig. 4.23 and 4.24 respectively. The test results are tabulated in Table E.8.

FIGURE 4.22 The crack patterns and ultimate failure of GB.3.1.

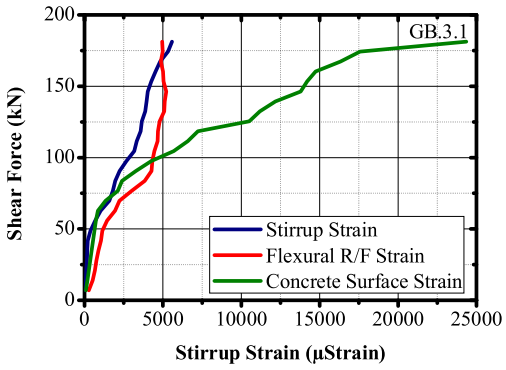

FIGURE 4.23 Relationship of shear force and strain variation for GB.3.1.

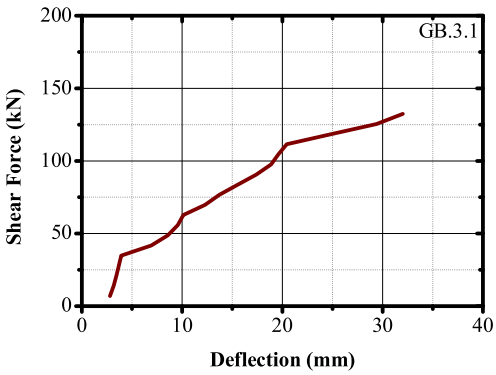

FIGURE 4.24 Relationship of shear force and mid-span deflection for GB.3.1.

4.4.4 Specimen GB.3.2

Beam GB.3.2 is the duplicate casting with same configuration as GB.3.1. First flexural crack is developed at 26.14 kN shear force. Subsequently, both the shear crack on either side of the beam are observed at 45.31 kN. The failure shear forces at first and second shear crack are observed as 49.59 kN and 50.79 kN respectively at 0.5 mm shear crack width. The strain values for stirrups, flexural reinforcement and concrete surface are 4522, 4468 and 5815 μstrain respectively at 0.5mm shear crack width. The central deflection is 21.96 mm. The crack pattern showed the propagation of crack from the point of load application towards the support. Sudden failure of the beam in shear is observed on both sides; however, primary failure is from left side with a crack angle of 45°. Shear compression failure with crushing at top of the shear crack with stirrup rupture is occurred in the beam as shown in Fig. 4.25. Relationships namely shear force - strain values and shear force - mid-span deflection are shown in Fig. 4.26 and 4.27 respectively. The test results are tabulated in Table E.9.

FIGURE 4.25 The crack patterns and ultimate failure of GB.3.2.

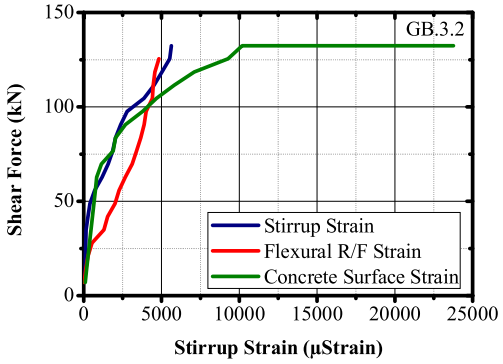

FIGURE 4.26 Relationship of shear force and strain variation for GB.3.2.

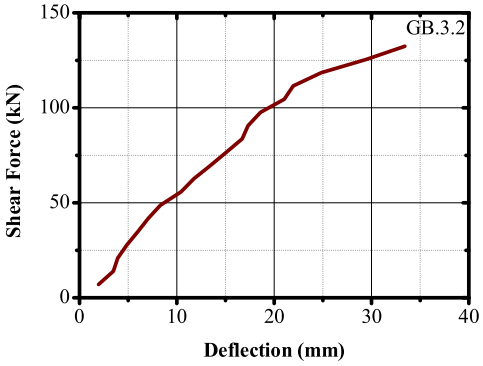

FIGURE 4.27 Relationship of shear force and mid-span deflection for GB.3.2.

4.5 Test Results of Category GC

In this category, four beams specimens of rectangular section having same shear span "a = 750 mm" are tested as simply supported beams. The set is divided into two subcategories with spacing of stirrups 325 mm and 350 mm with duplicate casting in each case designated as GC.4.1, GC.4.2, GC.5.1 and GC.5.2. The code GC.3.1 represents "G" means GFRP reinforcement, "C" stands for shear span "a = 750 mm", 4 is for spacing of stirrups as 325 mm and 1 is the serial number of that category.

4.5.1 Specimen GC.4.1

Beam GC.4.1 is designed for W = 29 kN load with reinforcement configuration shown in Table 2.1. First flexural crack is developed at 34.85 kN shear force. Subsequently, both the shear crack on either sides of the beam are observed at 45.31 kN. The failure shear forces at first and second shear crack are observed as 48.03 kN and 48.23 kN respectively at 0.5 mm shear crack width. The strain values for stirrups, flexural reinforcement and concrete surface are 4639, 4186 and 1351 μstrain respectively at 0.5mm shear crack width. The central deflection is 17.88 mm. The crack pattern showed the propagation of crack from the point of load application towards the support. Sudden failure of the beam in shear is observed on right side with a crack angle of 39°. Shear tension failure with propagation of shear crack along the reinforcement is observed in the beam as shown in Fig. 4.28. Relationships namely shear force - strain values and shear force - mid-span deflection are shown in Fig. 4.29 and 4.30 respectively. The test results are tabulated in Table E.10.

FIGURE 4.28 The crack patterns and ultimate failure of GC.4.1.

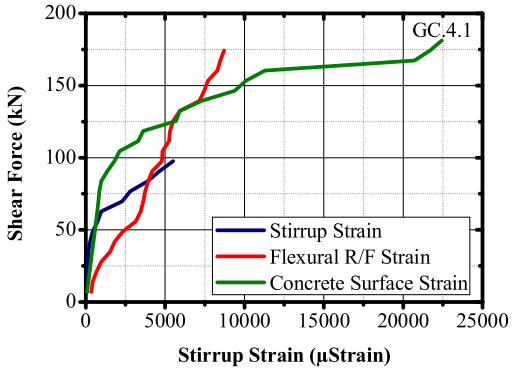

FIGURE 4.29 Relationship of shear force and strain variation for GC.4.1.

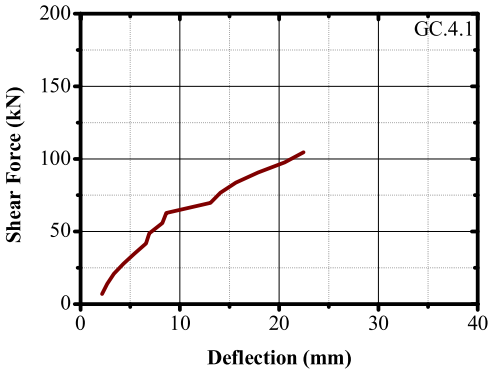

FIGURE 4.30 Relationship of shear force and mid-span deflection for GC.4.1.

4.5.2 Specimen GC.4.2

Beam GC.4.2 is the duplicate casting with same configuration as GC.4.1. First flexural crack is developed at 20.91 kN shear force. Subsequently, first shear crack is observed on right side of the beam at 38.34 kN. The second shear crack is developed on left side at 40.08 kN shear force. The failure shear forces at first and second shear crack are observed as 54.78kN and 48.58 kN respectively at 0.5 mm shear crack width. The strain values for

stirrups, flexural reinforcement and concrete surface are 4246, 5980 and 3208 µstrain respectively at 0.5mm shear crack width. The central deflection is 23.36 mm. The crack pattern showed the propagation of crack from the point of load application towards the support. Sudden failure of the beam in shear is observed on right side with a crack angle of 42°. Shear tension failure with propagation of shear crack along the reinforcement is observed in the beam as shown in Fig. 4.31. Relationships namely shear force - strain values and shear force - mid-span deflection are shown in Fig. 4.32 and 4.33 respectively. The test results are tabulated in Table E.11.

FIGURE 4.31 The crack patterns and ultimate failure of GC.4.2.

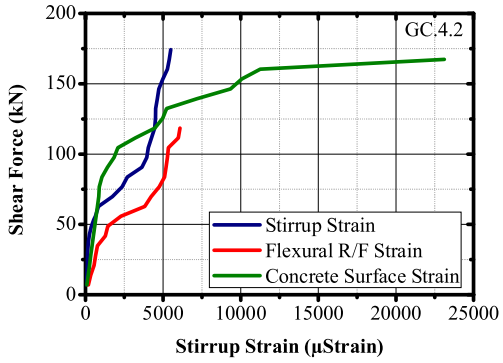

FIGURE 4.32 Relationship of shear force and strain variation for GC.4.2.

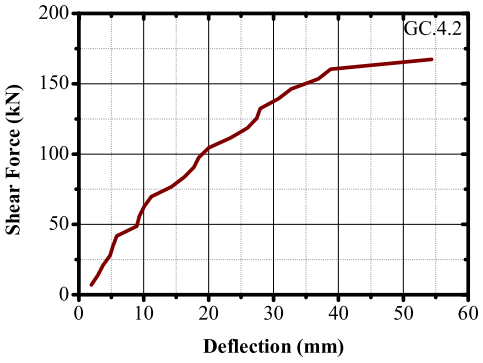

FIGURE 4.33 Relationship of shear force and mid-span deflection for GC.4.2.

4.5.3 Specimen GC.5.1

Beam GC.5.1 is designed for W = 29 kN load with reinforcement configuration shown in Table 2.1. First flexural crack is developed at 17.43 kN shear force. Subsequently, first shear crack is observed on right side of the beam at 34.85 kN. The second shear crack is developed on left side at 50.53 kN shear force. The failure shear forces at first and second shear crack are observed as 54.51 kN and 54.78 kN respectively at 0.5 mm shear crack width. The strain values for stirrups, flexural reinforcement and concrete surface are 5820, 4790 and 2893 μstrain respectively at 0.5mm shear crack width. The central deflection is 21.04 mm. The crack pattern showed the propagation of crack from the point of load application towards the support. Failure of the beam occurred in shear from both the crack simultaneously with a crack angle of 45°. Shear tension failure with propagation of shear crack along the reinforcement is observed in the beam as shown in Fig. 4.34. Relationships namely shear force - strain values and shear force - mid-span deflection are shown in Fig. 4.35 and 4.36 respectively. The test results are tabulated in Table E.12.

FIGURE 4.34 The crack patterns and ultimate failure of GC.5.1.

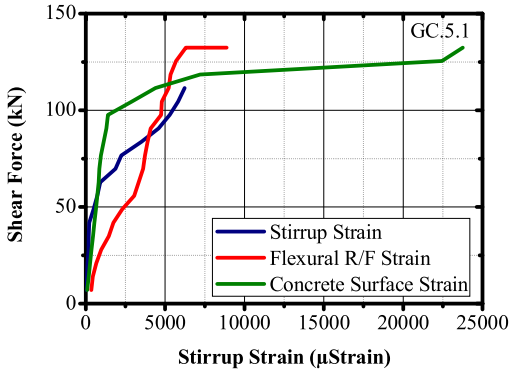

FIGURE 4.35 Relationship of shear force and strain variation for GC.5.1.

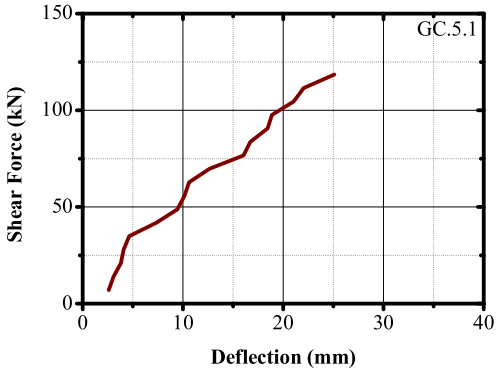

FIGURE 4.36 Relationship of shear force and mid-span deflection for GC.5.1.

4.5.4 Specimen GC.5.2

Beam GC.5.2 is the duplicate casting with same configuration as GC.5.1. First flexural crack is developed at 22.65 kN shear force. Subsequently, first shear crack is observed on right side of the beam at 48.79 kN. The second shear crack is developed on left side at 50.53 kN shear force. The failure shear forces at first and second shear crack are observed as 54.96 kN and 59.25 kN respectively at 0.5 mm shear crack width. The strain values for stirrups, flexural reinforcement and concrete surface are 6534, 6104 and 7288 µstrain respectively at 0.5mm shear crack width. The central deflection is 22.36 mm. The crack pattern showed the propagation of crack from the point of load application towards the support. Sudden failure of the beam occurred in shear from left side with a crack angle of 45°. Shear tension failure with propagation of shear crack along the reinforcement is observed in the beam as shown in Fig. 4.37. Relationships namely shear force - strain values and shear force - mid-span deflection are shown in Fig. 4.38 and 4.39 respectively. The test results are tabulated in Table E.13.

FIGURE 4.37 The crack patterns and ultimate failure of GC.5.2.

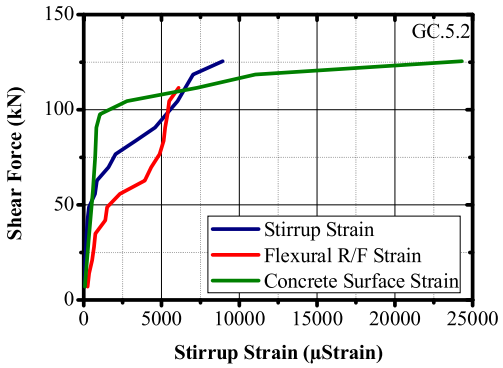

FIGURE 4.38 Relationship of shear force and strain variation for GC.5.2.

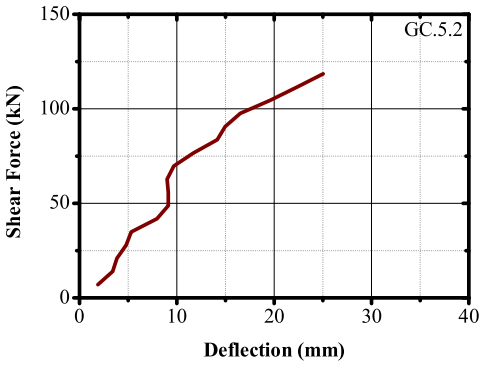

FIGURE 4.39 Relationship of shear force and mid-span deflection for GC.5.2.

4.6 Summary of Results

As per the sample size mentioned in Table 2.1, total thirteen beams are cast for the experimentation and their results in the form of shear force at first flexural crack, shear force at first and second shear crack, shear force at 0.5 mm crack width in the cases of first and second shear cracks, ultimate shear force, their crack angles, type of shear failure and overall behavior during the test are discussed in preceding sections. The test results are summarized in Table 4.1.

It is observed during the test that initially flexural cracks were developing and subsequently shear cracks developed. Beyond the shear crack development the progress of flexural crack is completely vanished. The strain values are recorded at various locations like on stirrups, flexural reinforcement and concrete surface and similar behavior for the stain response is observed as in case of the crack mechanism. At the initial stage of the test, the flexural strain is developed and it remained constant beyond the stage of the shear crack development and the shear strain continued to increase until the final failure of the beam.

The development of strain in the beams reinforced with GFRP is very high compared to steel reinforced beam at 0.5 mm crack width. The average strain in stirrup remained 4712 μstrain in GFRP reinforced beams as compared to 823 μstrain in steel reinforced. As more strain developed at every stage of loading, deflection observed is also very high in GFRP reinforced beams compared to the reference beams before ultimate failure. Summary of strain developed on stirrups, flexural reinforcement, concrete surface and deflection at 0.5 mm crack width is complied in Table 4.2.

It can be observed from the Table 4.1 that each category of shear span like 500 mm, 650 mm and 750 mm have failed in specific type of failure like diagonal tension, shear compression and shear tension respectively. In first case a = 500 mm, the shear span is dominated by shear force compare the amount of bending moment in overall sectional capacity. Hence, diagonal tension failure occurred due to dominated shear force. In second case a = 650 mm, the shear span is subjected to shear force and bending moment proportionately in overall sectional capacity. Hence, shear compression failure has occurred in majority. While in third case a = 750 mm, shear tension failure occurred as this zone was dominated by bending moment compare to shear force.

TABLE 4.1 Experimental results of all beam specimens

Beam	Shear Force at First Flexural Crack (kN)	Shear Force at Crack Developed (kN)		Shear Force at 0.5 mm Crack Width (kN)		Ultimate Shear Force (kN)	Crack Angle (Degree)	Type of Shear Failure[a]
		First Crack	Second Crack	First Crack	Second Crack			
SB.2.1	32.41	40.08	42.46	44.88	48.56	56.81	45	ST
GA.1.1	31.37	54.02	59.25	72.94	67.61	102.81	49	DT
GA.1.2	22.65	59.25	62.73	68.88	66.22	111.52	49	DT
GA.2.1	27.88	54.02	57.50	74.47	63.07	94.10	46	SR
GA.2.2	29.62	55.76	71.44	74.65	73.15	130.69	47	DT
GB.2.1	24.40	38.34	43.56	51.30	45.27	59.25	46	SC
GB.2.2	31.37	38.34	48.79	57.01	52.76	97.58	50	SC
GB.3.1	22.65	38.34	57.50	51.44	58.71	90.61	47	SC
GB.3.2	26.14	45.31	45.31	49.59	50.79	66.22	45	SR
GC.4.1	34.85	45.31	45.31	48.03	48.23	49.49	39	ST
GC.4.2	20.91	38.34	40.08	54.78	48.58	66.22	42	ST
GC.5.1	17.43	34.85	50.53	54.51	54.78	55.76	45	ST
GC.5.2	22.65	48.79	50.53	54.96	52.00	59.25	45	ST

[a]ST = Shear Tension, DT = Diagonal Tension, SR = Stirrups Rupture and SC = Shear Compression.

TABLE 4.2 Experimental strain and deflection values at 0.5 mm crack width of all specimens

Beam	Shear Force	Stirrup Strain	Flexural Strain	Concrete Strain	Deflection
	(kN)	(μStrain)	(μStrain)	(μStrain)	(mm)
SB.2.1	90.61	823	2289	755	11.45
GA.1.1	146.37	3689	5638	6350	31.00
GA.1.2	139.4	2946	3698	7728	24.92
GA.2.1	146.37	5506	5606	3390	25.24
GA.2.2	146.37	5890	4383	6246	26.40
GB.2.1	104.55	5184	4370	5532	22.12
GB.2.2	111.52	3987	4430	4358	23.80
GB.3.1	118.49	3578	4684	7234	24.88
GB.3.2	111.52	4522	4468	5815	21.96
GC.4.1	90.61	4639	4186	1351	17.88
GC.4.2	111.52	4246	5980	3208	23.36
GC.5.1	104.55	5820	4790	2893	21.04
GC.5.2	111.52	6534	6104	7288	22.36

4.7 Discussion on Test Results

Following subsections are presenting the discussion on behavior of various observatory parameters like deflection, crack width, flexural strain, concrete surface strain and stirrup strain with the increase of load during the test of all the beams collectively.

4.7.1 Shear Force vs Deflection Relationship

The average deflection of all the beams observed is 17.68 mm at the average load of 130.88 kN. The relationships of applied shear force-central deflection for all beams are shown in Fig. 4.40. Thought the beams reinforced with GFRP are of varying stirrup

spacing and span to depth ratio, the overall behaviour of all beams in deflection is nearly similar. However, the reference beam showed less deflection compare to GFRP. Thus, the variation in spacing or the span to depth ratio does not have any significant effect on the central deflection of all test specimens.

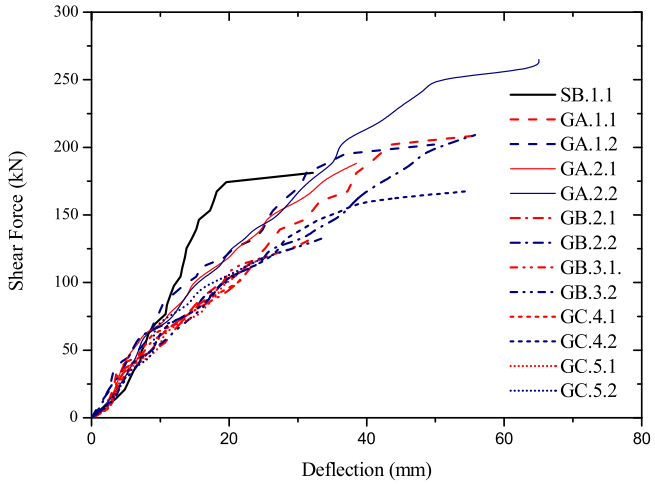

FIGURE 4.40 Shear force – midspan deflection relationship of all beam specimens.

4.7.2 Shear Force vs Crack Width Relationship

As the FRP is noncorrosive material by nature, the corrosion of reinforcement may not be primary serviceability criteria for members, reinforced with GFRP bars compared to the conventionally reinforced members. The minimum specified limit for shear crack width is 0.5 mm as per JSCE standard compared to 0.7 mm in ISIS Canada and ACI. Minimum specified limit of 0.5 mm is followed as the test conditions in the present study. PL-90-11-3L type of concrete surface strain gauges are applied in the perpendicular direction of the shear crack in each shear zone of the beam as specified in Fig. 3.21. Diagonal tension along the crack would act as an axial tension in the concrete strain gauge; hence, strain developed will provide the crack width over the surface indirectly. Fig. 4.41 shows the measured crack width formed diagonally in the shear zone of all the test specimens.

Beams containing GFRP stirrups with smaller spacing, exhibited cracks at large load compared to beams containing larger spacing of stirrups. The average strain observed in the stirrups at 0.5 mm crack width is 4712 μstrain which higher than the limits specified in any of three referred standards.

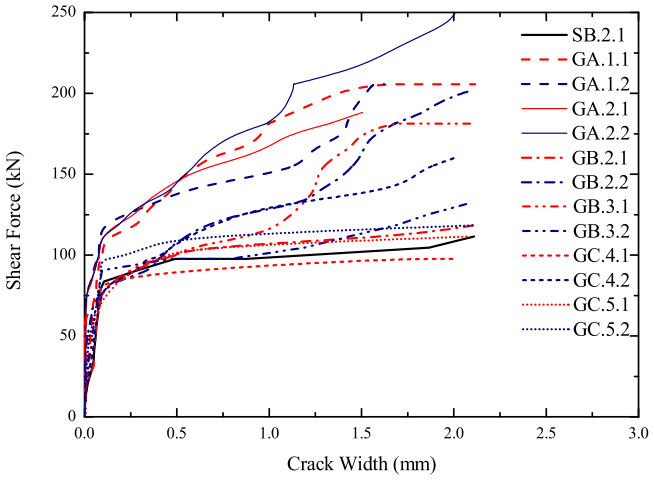

FIGURE 4.41 Shear force – crack width relationship of all beam specimens.

4.7.3 Shear Force vs Flexural Strains on GFRP Longitudinal Reinforcement

FLA type strain gauge is used to observe flexural strains on longitudinal reinforcement at location no.5 as shown in Fig. 3.21. The average flexural strains developed in longitudinal reinforcement at design load are 1343, 1920 and 3633 μstrain observed at the average shear force of 197.77 kN, 158.56 kN and 142.88 kN respective to load positions of shear span "a" equals to 500 mm, 650 mm and 750 mm. The variation in strain development at design load as well as at ultimate load is observed as the effective depth of corner and central longitudinal reinforcement due to bend radius r_b provided in stirrups are different. The average ultimate strains developed are 8137 and 5781 in central and corner longitudinal reinforcement respectively. The relationships of shear force and flexural strain in longitudinal reinforcement at mid-span of all beams are shown in Fig. 4.42.

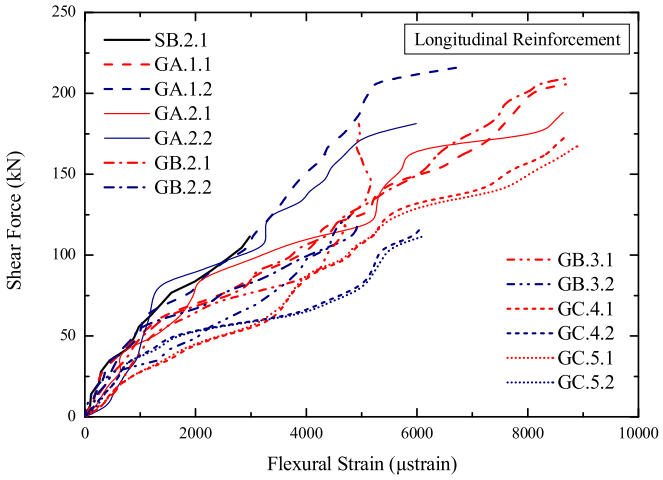

FIGURE 4.42 Shear force – flexural strain on longitudinal reinforcement relationship at midspan.

4.7.4 Shear Force vs Concrete Surface Strains

The passive use of concrete strain gauge is to observe crack width over the concrete surface. All the beams are designed as the shear deficit. Therefore, the expected failure of beams is in shear. PL type strain gauge is applied on the concrete surface in the shear zone area where the shear crack is expected at location no. 6 and 7 as per Fig. 3.21. Maximum strain observed through concrete strain gauge is 23516 µstrain after that the strain gauges failed. The relationship of shear force and concrete strain for all the beams are shown in Fig. 4.43.

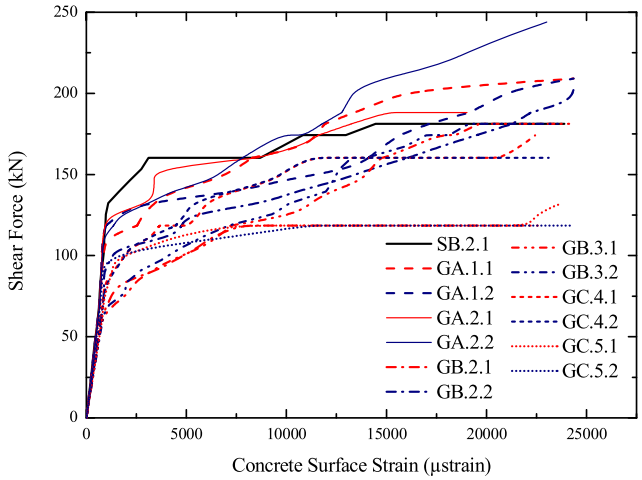

FIGURE 4.43 Shear force – concrete surface strain relationship of all beam specimens.

4.7.5 Shear Force vs Stirrup Strains

Total four FLA type strain gauges on the straight portion of the GFRP stirrups symmetrically two in each of the shear zone area of the beam are applied as shown in Fig. 3.21. The relationships of applied shear-stirrup strain of all the beams are shown in Fig. 4.44. In the first group of shear span namely A=500 mm, strain observed on stirrups at 0.5 mm crack width in the beams GA.1.1, GA.1.2, GA.2.1 and GA.2.2 are 3689, 2946, 5506 and 5890 µstrain at 146.37 kN, 139.4 kN, 146.37 kN and 146.37 kN, In second group of shear span B=650 mm, stirrups strain in the beams GB.2.1, GB.2.2, GB.3.1and GB.3.2 are 5184. 3987, 3578 and 4522 µstrain at 104.55 kN, 111.52 kN, 118.49 kN and 111.52 kN respectively. Whereas, in third group of shear span C=750 mm, beams GC.4.1, GC.4.2, GC.5.1and GC.5.2 have observed 4639, 4246, 5820 and 6534 µstrain at 90.61 kN, 111.52 kN, 104.55 kN and 111.52 kN respectively. The average maximum strain in GFRP stirrup observed is 6705 µstrain with a maximum strain of 8936 µstrain in the cases where stirrups failure occurred.

Small strain value for steel beam of 2726 µstrain at 111.52 kN is attributed to the fact that the strain in steel remains lower than the GFRP. It can also be seen that the stirrup strain increases with the spacing of stirrups and thereby the contribution of GFRP stirrups in shear resistance in a beam increases. It is worth mentioning that testing is done with controlled rate of loading and the produced results are of location where shear failure is occurred. In general, the stirrups strains remained very small until diagonal cracks are developed; then, rapid increase in the strain of GFRP stirrups is observed until the final failure.

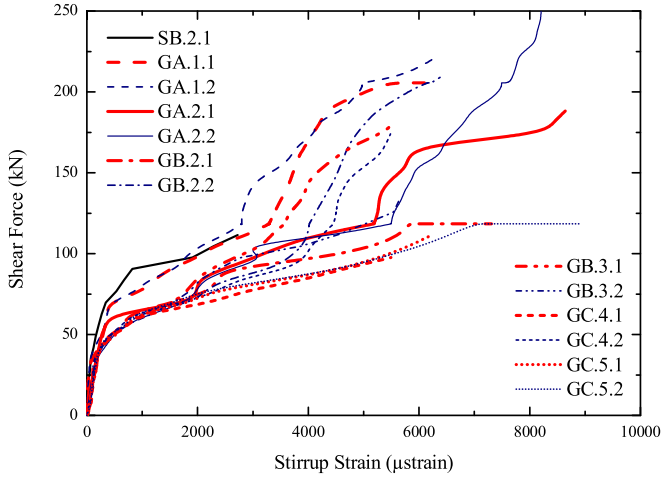

FIGURE 4.44 Shear force – stirrup strain relationship of all beam specimens.

CHAPTER : 5

Design Approach

5.1 General

The proposed design modification for predicting shear capacity of FRP-RC beams is provided in this section. The design recommendations are available in ACI, Canadian and Japanese design code formats. All the codes have different approaches to predict the shear capacity and majority of them provides conservative results. The experimentation is planned to investigate the actual strain development in stirrup and to compare them with the permissible strain as suggested in the above mentioned standards. It is fair to consider the actual value of the strain obtained from the experiments in the analytical models suggested by the codes in the capacity evaluation of FRP-RC beams. Therefore the proposed modification in permissible shear values helps to reduce the gap between experimental and predicted shear capacity in all the codes.

5.2 General Factors Affecting the Shear Contribution in FRP–RC Beams

As mentioned in the literature review and results of the experimental program that the shear capacity of the FRP reinforced beam is influenced by the following parameters:

- ✓ Type of FRP, and its Unidirectional Rigidity
- ✓ Modulus of Elasticity of FRP
- ✓ Concrete Strength
- ✓ Amount of Flexural Reinforcement
- ✓ Amount of Shear Reinforcement (Spacing)
- ✓ Shear Span-to-Depth Ratio
- ✓ Bend Radius of Stirrups
- ✓ Type of Surface of FRP Reinforcement

By keeping variation in span-to-depth ratio and spacing of FRP stirrup in the experimentation, modification in the guideline is proposed.

5.3 Experimental and Predicted Shear Strength as per Current Design Recommendations

All the beams are designed as shear deficit as per ACI guidelines. The flexural reinforcement provided is as per the design need and the shear reinforcement provided is less then the design requirements. This is obtained by varying the spacing of stirrups.

As per the final reinforcement provided in flexure as well as shear, reverse calculation of the capacity of the beam specimen in shear is made as per current design recommondations by ISIS Canada, Japanese and ACI codes. Calculation sheet of all the codes are attached in Appendix F.

The current shear design approach adopted by Canadian, Japanese and ACI codes and their comparison of experimental with predicted shear capacity are discussed in present sections.

5.3.1 Intelligent Sensing for Innovative Structures, Canada (ISIS Canada 2007)

As per the (2.6) to (2.9) shown in section 2.7.1, various parameters like permissible stress, modulus of elasticity, diameter of shear reinforcement, permissible strain, reinforcement ratio, bend radius of FRP reinforcement, stress in concrete due to axial loads and characteristic strength of concrete affect the total shear contribution as per ISIS Canada 2007. Here, permissible stress in shear reinforcement are calculated by two different approaches. One that is governed by the bend radius (2.7) and another (2.8) is governed by various parameters like reinforcement ratio, characterictic strength of concrete, stress in flexural & shear reinforcement, and modulus of elasticity of flexural & shear reinforcement. İn later case the final strain is governed by permissble upper limit as 0.0025 (2500 μstrain).

From the design sheet it is observed that predicted shear capacity of the beam is governed by (2.8) which is controlled by upper permissible strain as 2500 μstrain. The average stirrup strain as per calculation shown in Table F.1 (Appendix F), is 1270 μstrain; whereas, the experimentally obtained average strain at 0.5 mm crack width has remained 4712 μstrain.

As per Table 5.1 the average ratio of experimental to predicted shear capacity has remained 2.28 with standard deviation (SD) of 0.36. This clearly justifies that the permissible strain in design recommendation is substantially lower than the actual strain developed in the stirrups. If design recommendations are developed such a way that it reflects the strain value nearer to the strain developing in actual, it will reduce the gap between experimental and predicted shear capacity.

TABLE 5.1 Experimental results and shear prediction as per ISIS Canada 2007.

Beam	Shear Force (kN)				Stirrup Strain (µstrain)		ISIS (2007)	
	At First Flexural Crack	At First Shear Crack	At 0.5 mm Shear Crack Width (V_{Exp})	At Ultimate Failure	At 0.5 mm Crack Width	Ultimate Stirrup Strain	Predicted Load (V_{Pred})	V_{Exp}/V_{Pred}
SB.2.1	32.41	40.08	44.88	56.81	1809	2726	--	--
GA.1.1	31.37	54.02	72.94	102.81	3989	6189	26.82	2.72
GA.1.2	22.65	59.25	68.88	111.52	3946	6363	26.82	2.57
GA.2.1	27.88	54.02	74.47	94.10	5106	8642	26.23	2.84
GA.2.2	29.62	55.76	74.65	130.69	5890	8204	26.23	2.85
GB.2.1	24.40	38.34	51.30	59.25	5184	6386	26.23	1.96
GB.2.2	31.37	38.34	57.01	97.58	3987	7312	26.23	2.17
GB.3.1	22.65	38.34	51.44	90.61	3978	5578	25.75	2.00
GB.3.2	26.14	45.31	49.59	66.22	4522	5634	25.75	1.93
GC.4.1	34.85	45.31	48.03	49.49	4639	5499	25.64	1.87
GC.4.2	20.91	38.34	54.78	66.22	4246	5488	25.64	2.14
GC.5.1	17.43	34.85	54.51	55.76	5520	6228	25.23	2.16
GC.5.2	22.65	48.79	54.96	59.25	5534	8936	25.23	2.18
							Average	**2.28**
							SD	**0.36**

5.3.2 Japan Society of Civil Engineering standard (JSCE 1997)

As per the (2.16) to (2.20) shown in section 2.7.2, various parameters like permissible stress, modulus of elasticity, diameter of shear reinforcement, permissible strain, reinforcement ratio, bend radius of FRP reinforcement, stress in concrete due to axial loads orientation of the stirrup and design compressive strength of concrete allowing for size effect affect the total shear contribution as per JSCE 1997. Here, strain in stirrup (2.17) depends on various parameters like permissible stress, modulus of elasticity, diameter of shear reinforcement, reinforcement ratio, stress in concrete due to axial loads orientation of the stirrup and design compressive strength of concrete allowing for size effect which is controlled by bend strength (2.18) of the FRP reinforcement as upper limit.

From the design sheet it is observed that predicted shear capacity of the beam is governed by (2.17) which is controlled by the ratio $\mathbf{f_{FRPbend} / E_{fv}}$ as upper limit. The average stirrup strain as per calculation shown in Table F.2 (Appendix F), is 1336 µstrain and average upper limit considering bend strength is 3827 µstrain; whereas, the experimentally obtained average strain at 0.5 mm crack width has remained 4712 µstrain.

As per Table 5.2 the average ratio of experimental to predicted shear capacity has remained 1.82 with standard deviation (SD) of 0.32. It can be observed that the strain considered in the design calculated is substantially lower than the actual strain developed in the stirrups. Hence, this also motivates to modify the design recommendations to reduce the gap of experimental to predicted results.

TABLE 5.2 Experimental results and shear prediction as per JSCE 1997.

Beam	Shear Force (kN)				Stirrup Strain (μstrain)		JSCE (1997)	
	At First Flexural Crack	At First Shear Crack	At 0.5 mm Shear Crack Width	At Ultimate Failure	At 0.5 mm Crack Width	Ultimate Stirrup Strain	Predicted Load (V_{Pred})	V_{Exp}/V_{Pred}
SB.2.1	32.41	40.08	44.88	56.81	1809	2726	--	--
GA.1.1	31.37	54.02	72.94	102.81	3989	6189	32.71	2.23
GA.1.2	22.65	59.25	68.88	111.52	3946	6363	32.71	2.11
GA.2.1	27.88	54.02	74.47	94.10	5106	8642	32.42	2.30
GA.2.2	29.62	55.76	74.65	130.69	5890	8204	32.42	2.30
GB.2.1	24.40	38.34	51.30	59.25	5184	6386	32.42	1.58
GB.2.2	31.37	38.34	57.01	97.58	3987	7312	32.42	1.76
GB.3.1	22.65	38.34	51.44	90.61	3978	5578	32.16	1.60
GB.3.2	26.14	45.31	49.59	66.22	4522	5634	32.16	1.54
GC.4.1	34.85	45.31	48.03	49.49	4639	5499	33.33	1.44
GC.4.2	20.91	38.34	54.78	66.22	4246	5488	33.33	1.64
GC.5.1	17.43	34.85	54.51	55.76	5520	6228	33.12	1.65
GC.5.2	22.65	48.79	54.96	59.25	5534	8936	33.12	1.66
							Average	**1.82**
							SD	**0.32**

5.3.3 American Concrete Institute (ACI 440.1R-06)

As per the (2.24) to (2.26) shown in section 2.7.3, various parameters like permissible stress, modulus of elasticity, diameter of shear reinforcement, permissible strain, bend radius of FRP reinforcement, and depth of beam affect the total shear contribution as per ACI 2006. Here, stress in stirrup (2.25) depends on permissible strain and modulus of elasticity of FRP shear reinforcement which is controlled by bend strength (2.26) of the FRP reinforcement as upper limit.

From the design sheet it is observed that predicted shear capacity of the beam is governed by Eq, (2.25) which is controlled by permissible strain and modulus of easticity with bend strenth as upper limit. The average stress considered in stirrup as per calculation shown in Table F.3 (Appendix F), is 236.5 Mpa at permissible strain of 4000 μstrain and average upper limit of bend strength is 325.8 MPa; whereas, the experimentally obtained average strain at 0.5 mm crack width has remained 4712 μstrain.

As per Table 5.3 the average ratio of experimental to predicted shear capacity has remained 1.62 with standard deviation (SD) of 0.23. Here also, it can be observed that the stress considered in the design calculation is substantially lower than the actual stress that would develop in the stirrups at 4712 μstrain as compared to stress considered at 4000 μstrain. Even, the upper limit set for permissible stress is also higher than the considered value. Hence, this also motivates to modify the design recommendations to reduce the gap of experimental to predicted results.

TABLE 5.3 Experimental results and shear prediction as per ACI 2006.

Beam	Shear Force (kN)				Stirrup Strain (μstrain)		ACI (2006)	
	At First Flexural Crack	At First Shear Crack	At 0.5 mm Shear Crack Width	At Ultimate Failure	At 0.5 mm Crack Width	Ultimate Stirrup Strain	Predicted Load (V_{Pred})	V_{Exp}/V_{Pred}
SB.2.1	32.41	40.08	44.88	56.81	1809	2726	--	--
GA.1.1	31.37	54.02	72.94	102.81	3989	6189	39.12	1.86
GA.1.2	22.65	59.25	68.88	111.52	3946	6363	39.12	1.76
GA.2.1	27.88	54.02	74.47	94.10	5106	8642	37.25	2.00
GA.2.2	29.62	55.76	74.65	130.69	5890	8204	37.25	2.00
GB.2.1	24.40	38.34	51.30	59.25	5184	6386	37.25	1.38
GB.2.2	31.37	38.34	57.01	97.58	3987	7312	37.25	1.53
GB.3.1	22.65	38.34	51.44	90.61	3978	5578	35.69	1.44
GB.3.2	26.14	45.31	49.59	66.22	4522	5634	35.69	1.39
GC.4.1	34.85	45.31	48.03	49.49	4639	5499	35.37	1.36
GC.4.2	20.91	38.34	54.78	66.22	4246	5488	35.37	1.55
GC.5.1	17.43	34.85	54.51	55.76	5520	6228	34.24	1.59
GC.5.2	22.65	48.79	54.96	59.25	5534	8936	34.24	1.61
							Average	**1.62**
							SD	**0.23**

5.4 Error Analysis

All the experimental work would be subjected to some error. The following equations are used for calculating standard error of experimental data.

$$\text{Standard Deviation (S.D.)} = \sqrt{\frac{\sum(x-\bar{x})^2}{n-1}} \quad (5.1)$$

$$\text{Standard Error (S.E.)} = \frac{\text{S.D.}}{\sqrt{n}} \quad (5.2)$$

$$\text{Range of Error Bar} = \bar{x} \pm \text{S.E.} \quad (5.3)$$

Where, $\bar{x}$ = Mean of Observations

n = Number of Observations

Standard deviation and standard error calculated from Eq. (5.1) and (5.2) respectively for the various strains like stirrup strain at 0.5 mm crack width, ultimate stirrup strain, flexural strain and concrete surface strain are presented in Table 5.4. It can be observed from the Table 5.4 that the standard error for the stirrup strain is 205 µstrain and average strain at 0.5 mm crack width and maximum strain are 4712 and 5890 µstrain respectively. Hence, reduced values of average and maximum strain are 4507 and 5685 µstrain respectively. Therefore, 4500 (round off) µstrain may be permissible up to which strain is really developing in the stirrup and that value shall be permissible limit for the strain development in the FRP stirrup. A column chart with standard error is shown in Fig. 5.1. The error bars shown in each column is the standard error of that particular group. For example, 205 is the standard error of stirrup strain at 0.5 mm crack width as per Table 5.4, this range of error of ±205 is shown in column of stirrup strain at 0.5 mm crack width of each beam.

TABLE 5.4 Various strain with standard error.

Beam Specimen	Stirrup Strain at 0.5mm Crack Width (µstrain)	Ultimate Stirrups Strain (µstrain)	Flexural Strain (µstrain)	Concrete Surface Strain (µstrain)
GA.1.1	3989	6189	8694	24364
GA.2.1	5106	6363	8642	19032
GA.2.2	5890	8204	5986	23016
GB.2.1	5184	6386	8678	22568
GB.2.2	3987	7312	4922	24342
GB.3.1	3978	5578	5208	24352
GB.3.2	4522	5634	4838	23772
GC.4.1	4639	5499	8716	22440
GC.4.2	4246	5488	6090	23120
GC.5.1	5520	6228	8883	23761
GC.5.2	5534	8936	6104	24306
S.D.	**709**	**1258**	**1645**	**1523**
S.E.	**205**	**363**	**672**	**440**

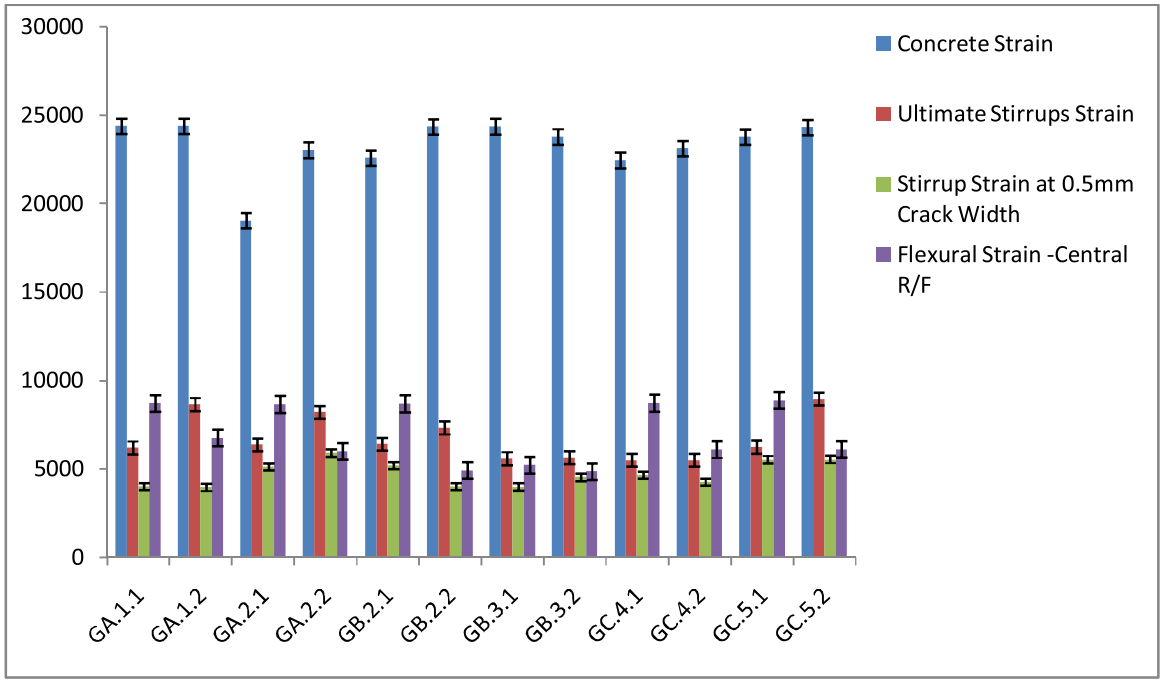

FIGURE 5.1 Various strains with error bar.

5.5 Comparison of Experimental Results with Proposed Modified Permissible Strain Values of Standard Design Recommendation

The least stirrups strength derived from bend strength from (2.7) and the value from (2.8) are used by ISIS Canada (2007). Here, Equation (2.8) governs the design which remains well below compared to actual stress in the stirrups. The calculated average ratio of shear capacities namely experimental to the predicted (V_{Exp}/V_{Pred}) is 2.29 with standard deviation (SD) 0.36. Where, JSCE (1997) has kept the bend strength as the upper limit; however, the value used in design given by (2.17) governs the stirrups capacity which also remains very low compare to actual one. Here, the same average ratio V_{Exp}/V_{Pred} is 1.82 with SD 0.31, which is quite less than the provisions by ISIS Canada. In case of ACI (2006) the average ratio V_{Exp}/V_{Pred} is 1.63 with SD 0.23. ACI (2006) uses constant strain value as an upper limit to predict the shear capacity, which is reasonable in comparison and conservative by values.

ISIS Canada and JSCE recommends strain values depending on other parameters where it requires investigating individual parameter affecting overall shear contribution which may reduce the gap between experimental and predicted values. Whereas, ACI uses the permissible strain value directly without any dependency with upper limit of FRP bend

strength. Hence, if this permissible strain value is increased to 4500 μstrain from 4000 μstrain, the gap between experimental to predicted value will decrease.

TABLE 5.5 Comparison of experimental and predicted load after proposed modification.

Beam	Shear Force (kN)	Current Permissible Stirrup Strain 4000 μstrain		Proposed Permissible Stirrup Strain 4500 μstrain	
	At 0.5 mm Shear Crack Width	Predicted Load ($V_{Pred.}$)	V_{Exp}/V_{Pred}	Predicted Load (V_{Pred})	V_{Exp}/V_{Pred}
GA.1.1	72.94	39.12	1.86	41.70	1.75
GA.1.2	68.88	39.12	1.76	41.70	1.65
GA.2.1	74.47	37.25	2.00	39.59	1.88
GA.2.2	74.65	37.25	2.00	39.59	1.89
GB.2.1	51.30	37.25	1.38	39.59	1.30
GB.2.2	57.01	37.25	1.53	39.59	1.44
GB.3.1	51.44	35.69	1.44	37.83	1.36
GB.3.2	49.59	35.69	1.39	37.83	1.31
GC.4.1	48.03	35.37	1.36	37.35	1.29
GC.4.2	54.78	35.37	1.55	37.35	1.47
GC.5.1	54.51	34.24	1.59	36.08	1.51
GC.5.2	54.96	34.24	1.61	36.08	1.52
		Average	**1.62**		**1.53**
		SD	**0.23**		**0.22**

It can be seen from the Table 5.5 that, if permissible strain is increased from 4000 μstrain to 4500 μstrain, the ratio of experimental to predicted load reduces from 1.62 to 1.53 with standard deviation from 0.23 to 0.22.

CHAPTER : 6

Conclusion & Recommendations

6.1 Conclusions

The experimental behaviour and shear strength obtained through the advanced testing of the beams reinforced with GFRP longitudinal and lateral reinforcement are presented and discussed. The main variables are shear span to depth ratio and spacing of the shear reinforcement (stirrup). Sand-coated GFRP stirrups of 9.5 mm diameter are used as shear reinforcement with different spacing. The experimental test results are compared to the shear design provisions provided by ISIS Canada (2007), JSCE (1997) and ACI (2006). The findings of the research work are summarized as follows:

- In the FRP-RC beams, GFRP stirrups as shear reinforcement did not affect the failure mechanism as a beam action in all the beams. Initial hair crack in flexure and consequently shear failure happened in all the beams.
- Strain development started at the initial stage of loading at higher stirrup spacing of 350 mm compare to lower stirrup spacing of 250 mm. However, spacing did not affect the ultimate strain developed in the stirrups.
- Due to collective effect of shear span to depth ratio, cross section of beam, amount of shear and anchorage reinforcement, groups with shear span to depth ratio 1.79, 2.33 and 2.69 failed in diagonal tension, shear compression and shear tension in majority respectively.
- The average maximum strain in GFRP stirrup observed was 6705 microstrains with a maximum strain of 8936 microstrains in the cases where stirrups failure occurred. The average strain observed in the stirrups at 0.5 mm crack width is 4712 microstrain which higher than the limits specified in any of the standard.
- Crack angle of the failed specimens varied from 39° to 49° with an average of around 45°, which shows good agreement with traditional truss model.

- Shear capacity predicted by ISIS Canada (2007) is the most conservative with the ratio V_{Exp}/V_{Pred} as 2.29 out of three. Contributions concrete and shear both are underestimated by this standard. There is no point in calculating concrete contribution by considering steel as the reference material to define permissible strain value as steel and FRP have different characteristics fundamentally. Permissible strain value 0.0025 is also very low compared to actual values as well as 0.004 as used by ACI (2006).
- JSCE (1997) also gives the conservative prediction with the ratio V_{Exp}/V_{Pred} as 1.82. Keeping the bend strength as upper limit is reasonable but (2.15) underestimates the strain value to be considered.
- ACI (2006) have shown good agreement with the ratio V_{Exp}/V_{Pred} as 1.63 which is yet conservative. Initially ACI-440.1R-03 had proposed permissible strain value as 0.002 similar to the steel reinforcement. This has been revised in ACI-440.1R-06 as 0.004 considering the linear elastic behavior and ultimate strain value of FRPs. There is room to increase the strain limit to improve the efficiency of the recommendations.
- As average strain on stirrups is 4712 and maximum strain is 5890 at 0.5 mm crack width, if permissible strain is increased to 0.0045, the average ratio V_{Exp}/V_{pred} reduces from 1.63 to 1.53 and SD reduces from 0.23 to 0.22.

6.2 Recommendations for Future Work

On the basis of observations and conclusions from the current study, following recommendations are suggested for the future research for the beams having FRP reinforcement.

- This study have been done using GFRP reinforcement, similar study shall be done using CFRP or AFRP reinforcement to have generalized conclusion for FRP.
- Research is needed to characterize bond strength with the type of surface of FRP reinforcement combining with the concrete strength.
- The long-term performance and durability of GFRP is also another area for future research.
- To make FRP as primary reinforcement, options to improve fire resistance is the prime need of investigation, research is required.
- More experimentation is required on effect of bend parameters of stirrups.
- Behavior of GFRP reinforcement under cyclic loading shall be investigated.

References

1. Chen M. and Das S. (2009), "Experimental study on repair of corroded steel beam using CFRP", Steel and Composite Structures, 9(2), 103-118, ISSN: 1229-9367.

2. Michaluk, C. R., Rizkalla, S. H., Tadros, G., and Benmokrane, B. (1998). "Flexural behavior of one-way slabs reinforced by fiber reinforced plastic reinforcement." ACI Struct. J., 95(3), 353–364, ISSN : 0889-3241.

3. Deitz, D. H., Harik, I. E., and Gesund, H. (1999). "One-way slabs reinforced with glass fiber reinforced polymer reinforcing bars." ACI Proc., 4th Int. Symp., ACI special publication, SP188-25, Detroit, 279–286.

4. Yost, J. R., Gross, S. P., and Dinehart, D. W. (2001), "Shear strength of normal strength concrete beams reinforced with deformed GFRP bars", Journal of Composites for Construction, 5(4), 268–275, ISSN: 1090-0268.

5. Alam, M. S., and Hussein, A. (2013), "Size effect on shear strength of FRP reinforced concrete beams without stirrups", Journal of Composites for Construction, 10.1061/(ASCE)CC.1943-5614.0000346, 507–516, ISSN: 1090-0268.

6. Alam, M. S., and Hussein, A. (2013), "Unified shear design equation for concrete members reinforced with fiber–reinforced polymer without stirrups", Journal of Composites for Construction, 10.1061/(ASCE)CC.1943 -5614.0000342, 575–583, ISSN: 1090-0268.

7. Refai A. El. and Farid Abed, M.ASCE (2015), "Concrete Contribution to Shear Strength of Beams Reinforced with Basalt Fiber-Reinforced Bars", Journal of Composites for Construction, 10.1061/(ASCE)CC.1943-5614.0000648, 04015082-1-04015082-13, ISSN: 1090-0268.

8. Noel M. and Fam A. (2016), "Design Equations for Concrete Bridge Decks with FRP Stay-in-Place Structural Forms", Journal of Composites for Construction, 20(5), 04016024.

9. Djeddi F., Ghernouti Y., Abdelaziz Y. and Alex L. (2016), "Strengthening in flexure–shear of RC beams with hybrid FRP systems: Experiments and numerical modeling", Journal of Composites for Construction, 20(5), 04016024.

10. Grace N.F. and Rout S.K. (2014), "Performance of innovative durable CFCC prestressed and reinforced beams under shear", Indian Concrete Journal 88(3), 8-18.

11. Panda, K. C., Bhattacharyya, S. K. and Barai, S. V. (2013), "Shear strengthening effect by bonded GFRP strips and transverse steel on RC T-beams", Structural Engineering and Mechanics, 47(1), 75-98, ISSN: 1225-4568.

12. Panda, K. C., Bhattacharyya, S. K. and Barai, S. V. (2013), "Effect of transverse steel on the performance of RC T-beams strengthened in shear zone with GFRP sheet", Construction and Building Materials, 41, 79-90, ISSN : 0950-0618.

13. Mohamed H. M., Afifi M. Z. and Benmokrane B. (2014), "Performance Evaluation of Concrete Columns Reinforced Longitudinally with FRP Bars and Confined with FRP Hoops and Spirals under Axial Load", Journal of Composites for Construction, 10.1061/(ASCE)BE.1943-5592.0000590, 04014020-1 - 04014020-12.

14. Al-Tamimi A., Abed, F. H. and Al-Rahmani A. (2014), "Effects of harsh environmental exposures on the bond capacity between concrete and GFRP reinforcing bars", Advances in Concrete Construction, 2(1), 1-11, ISSN:2287-5301.

15. Intelligent Sensing for Innovative Structures (ISIS) (2007), Reinforcing concrete structures with fiber reinforced polymers, ISIS Canada, Univ. of Winnipeg, Winnipeg, MB, Canada.

16. Japan Society of Civil Engineering (JSCE) (1997), "Recommendation for design and construction of concrete structures using continuous fiber reinforcing materials." Tokyo.

17. International Federation for Structural Concrete (fib) (2007), "FRP reinforcement in RC structures, Bulletin No. 40." CEB-FIP, Lausanne, Switzerland.

18. Canadian Standards Association (CSA) (2006), "Canadian highway bridge design code." CSA S6-06, Toronto.

19. Canadian Standards Association (CSA) (2012), "Design and Construction of Buildings Components with Fiber-Reinforced Polymers." CSA S806-12, Toronto.

20. American Concrete Institute (ACI) (2006), "Guide for the design and construction of concrete reinforced with FRP bars." ACI 440.1R-06, Farmington Hills, MI.

21. Altin S., Anil O., and Kara M. E. (2011), "Retrofitting of shear damaged RC beams using CFRP strips", Steel & Composite Structures, 11(3), 207-223, ISSN: 1229-9367.

22. Panda, K. C., Bhattacharyya, S. K. and Barai, S. V. (2012), "Shear behaviour of RC T-beams strengthened with U-wrapped GFRP sheet", Steel & Composite Structures, 12(2), 149-166, ISSN: 1229-9367.

23. ASCE-ACI Committee 445 on Shear and Torsion. (1998), "Recent approaches to shear design of structures." Journal of Structural Engineering, 10.1061/(ASCE)0733-9445(1998)124:12(1375), 1375–1417, ISSN: 0733-9445.

24. Guadagnini, M., Pilakoutas, K., and Waldron, P. (2003), "Shear performance of FRP reinforced concrete beams." Journal of Reinforced Plastics and Composites, 22(15), 1389–1407, ISSN: 0731-6844.

25. Guadagnini, M., Pilakoutas, K., and Waldron, P. (2006), "Shear resistance of FRP RC beams: Experimental study." Journal of Composites for Construction, 10.1061/(ASCE)1090-0268(2006)10:6(464), 464–473, ISSN: 1090-0268.

26. Tureyen, A. K., and Frosch, R. J. (2003), "Concrete shear strength: Another perspective." ACI Structural Journal, 100(5), 609–615, ISSN : 0889-3241.

27. El-Sayed, A., El-Salakawy, E., and Benmokrane, B. (2005), "Shear strength of one-way concrete slabs reinforced with fiber-reinforced polymer composite bars." Journal of Composites for Construction, 10.1061/(ASCE)1090 - 0268(2005)9:2(147), 147–157, ISSN: 1090-0268.

28. El-Sayed, A. K., El-Salakawy, E. F., and Benmokrane, B. (2006), "Shear strength of FRP-reinforced concrete beams without transverse reinforcement." ACI Structural Journal, 103(2), 235–243, ISSN : 0889-3241.

29. El-Sayed, A. K., El-Salakawy, E. F., and Benmokrane, B. (2006), "Shear capacity of high-strength concrete beams reinforced with FRP bars." ACI Structural Journal, 103(3), 383–389, ISSN : 0889-3241.

30. El-Sayed, A. K., Soudki, K., and Kling, E. (2009), "Flexural behavior of self-consolidating concrete slabs reinforced with GFRP bars." FRPRCS-9, Sidney, Australia.

31. Kilpatrick, A. E., and Dawborn, R. (2006), "Flexural shear capacity of high strength concrete slabs reinforced with longitudinal GFRP bars", FIB, Naples, Italy, 1–10.

32. Razaqpur, A. G., and Isgor, O. B. (2006), "Proposed shear design method for FRP-reinforced concrete members without stirrups." ACI Structural Journal, 103(6), 93–102, ISSN : 0889-3241.

33. Matta, F., Nanni, A., Hernandez, T. M., and Benmokrane, B. (2008), "Scaling of strength of FRP reinforced concrete beams without shear reinforcement." CICE2008, Zurich, Switzerland.

34. Steiner, S., El-Sayed, A. K., Benmokrane, B., Matta, F., and Nanni, A. (2008), "Shear behaviour of large-size beams reinforced with glass FRP bars." Advanced Composite Materials in Bridges and Structures: 5th International Conference, ACMBS-II, 1397–1406.

35. Hoult, N. A., Sherwood, E. G., Bentz, E. C., and Collins, M. P. (2008), "Does the use of FRP reinforcement change the one-way shear behavior of reinforced concrete slabs?" Journal of Composites for Construction, 10.1061/(ASCE) 1090-0268(2008)12:2(125), 125–133, ISSN: 1090-0268.

36. Alam, M. S., Hussein, A., and Ebrahim, E. A. A. (2009), "Shear strength of concrete beams reinforced with glass fibre reinforced polymer (GFRP) bars." Proc., CSCE 2009 Annual General Conference, Vol. 2, 874–882.

37. Jang, H., Kim, M., Cho, J., and Kim, C. (2009), "Concrete shear strength of beams reinforced with FRP bars according to flexural ratio and shear span to depth ratio." FRPRCS-9, Sidney, Australia.

38. Alam, M. S., and Hussein, A. (2011), "Experimental investigation on the effect of longitudinal reinforcement on shear strength of fibre reinforced polymer reinforced concrete beams." Canadian Journal of Civil Engineering, 38(3), 243–251, ISSN : 0315-1468.

39. Alam, M. S., and Hussein, A. (2012), "Effect of member depth on shear strength of high-strength fiber-reinforced polymer-reinforced concrete beams." Journal of Composites for Construction, 10.1061/(ASCE)CC.1943-5614.0000248, 119–126, ISSN: 1090-0268.

40. Alam, M. S., and Hussein, A. (2013), "Size effect on shear strength of FRP reinforced concrete beams without stirrups" Journal of Composites for Construction, 10.1061/(ASCE)CC.1943-5614.0000346, 507–516, ISSN: 1090-0268.

41. Alam, M. S., and Hussein, A. (2013), "Unified shear design equation for concrete members reinforced with fiber–reinforced polymer without stirrups." Journal of Composites for Construction, 10.1061/(ASCE)CC.1943 -5614.0000342, 575–583, ISSN: 1090-0268.

42. Razaqpur, A.G. and Saverio Spadea (2014), "Shear Strength of FRP Reinforced Concrete Members with Stirrups", Journal of Composites for Construction, 10.1061/(ASCE)CC.1943-5614.0000483, 04014025-(1-15) , ISSN: 1090-0268.

43. Maruyama, T., Honama, M., and Okmura, H. (1993), "Experimental study on tensile strength of bent portion of FRP rods." ACI special publications: Fiber reinforced plastic reinforcement for concrete structures, ACI-SP-138, A. Nanni and C. W. Dolan, eds., American Concrete Institute, Farmington Hills, Mich., 163–176.

44. Shehata, E. F. G. (1999), "Fiber reinforced polymer (FRP) for shear reinforcement in concrete structures." Ph.D. thesis, Department of Civil and Geological Engineering, Univ. of Manitoba, Manitoba, Canada.

45. El-Sayed, A. K., El-Salakawy, E., and Benmokrane, B. (2007), "Mechanical and structural characterization of new carbon FRP stirrups for concrete members." Journal of Composites for Construction, 11(4), 352–362 , ISSN: 1090-0268.

46. Ehab A. Ahmed; Ehab F. El-Salakawy; and Brahim Benmokrane (2010), "Shear Performance of RC Bridge Girders Reinforced with Carbon FRP Stirrups." Journal of Bridge Engineering, 10.1061/(ASCE)BE.1943-5592.0000035, 44-54, ISSN: 1084-0702.

47. Erki, M. A., and Rizkalla, S. (1993), "FRP Reinforcements for Concrete Structures: A Sample of International Production." Concrete International, 15(6), 48-53.

48. Nayera Ahmed Abdel-Raheem Mohamed (2013), "Strength And Drift Capacity Of GFRP Reinforced Concrete Shear Walls", PhD Thesis, University of Sherbrooke, Sherbrooke(Québec), Canada

49. Gangarao V. S., Taly Narendra, P.V. Vijay (2006), Reinforced Concrete Design with FRP Composites, CRC Press, Taylor & Francis Group.

50. American Concrete Institute (ACI) (Reapproved-2002), "State-of-the-Art Report on Fiber Reinforced Plastic (FRP) Reinforcement for Concrete Structures." ACI 440R-96, Farmington Hills, MI.

51. Momamed Elarbi Moh Mahroug (2013), "Experimental and computational investigations on the use of basalt and carbon fibre reinforced polymer bars in continuous concrete slabs", PhD Thesis, School of Engineering, Design and Technology (EDT), University of Bradford, UK.

52. ISIS Canada Research Network (2007), "Reinforcing Concrete Structures with Fibre Reinforced Polymers", Design Manual No. 3, Version 2, University of Manitoba, Canada.

53. Austin Beau Connor (2013), "Experimental investigation on the shear characteristics of GFRP reinforcement systems embedded in concrete", M.E. Thesis, Department of Civil and Environmental Engineering, University of Louisville, Kentucky, United States.

54. Sayed-Ahmed E.Y., and Shrive N.G. (1998), "CFRP Post-tensioned Masonry Diaphragm Walls," Proceedings of the Annual CSCE Conference, 2nd Structural Specialty Conference, Halifax, Nova Scotia, pp. 571-582.

55. Challal, O. and Benmokrane, B. (1993), "Physical and Mechanical Performance of an Innovative Glass-Fibre-Reinforced Plastic Rod," Canadian Journal of Civil Engineering, Vol.20, No.2, 254-268, ISSN : 0315-1468.

56. Nanni, A., Nenninger, J., Ash, K., and Liu, J. (1997), "Experimental BondBehaviour of Hybrid Rods for Concrete Reinforcement," Structural Engineering and Mechanics, V.5, No.4, 339-354, ISSN: 1225-4568.

57. Benmokrane, B., Chaallal O., and Masmoudi, R. (1996), "Flexural Response of Concrete Beams Reinforced with FRP Reinforcing Bars," ACI Structural Journal, V.93, No. 1 May-June 1996, 46-55, ISSN : 0889-3241.

58. Tanigaki, M., Okamoto, T., Tamura, T., Matsubara, S., and Nomura, S. (1989), "Study of Braided Aramid Fiber Rods for Reinforcing Concrete," Braided Aramid Rods for Reinforcing Concrete, FiBRA.

59. Yagi, K., Hoshijima, T., Ando, T., Tanaka, T. (1997), "The Durability Tests of Carbon Fiber Reinforced Plastics Rod Produced by Pultrusion Method," Proceedings, International Conference on Engineering Materials, Edited by Al-Manaseer, Nagataki and Joshi, CSCE/JSCE, Ottawa, Ontario, Volume 2, 327-340.

60. Coomarasamy, A. and Goodman, S. (1997), "Investigation of the Durability Characteristics of Fiber Reinforced Polymer (FRP) Materials in Concrete Environment", American Society for Composites-Twelfth Technical Conference, Dearborn, Michigan.

61. Porter, M.L., Mehus, J., Young, K.A., O'Neil, E.F., and Barnes, B.A. (1997), "Aging of Fiber Reinforcement in Concrete," Proceedings of the Third International Symposium on Non-Metallic (FRP) Reinforcement for Concrete Structures (FRPRCS-3), Japan Concrete Institute, Sapporo, Japan, V. 2, 59-66.

62. Porter, M.L., and Barnes, B.A., (1998), "Accelerated Durability of FRP Reinforcement for Concrete Structures." Proceedings of the First International Conference on Composites for Construction (CDCC 1998), Sherbrooke, Québec, 191-198.

63. Benmokrane, B., and Rahman, H.(Editors) (1998), "Durability of Fibre Reinforced Polymer (FRP) Composites for Construction," Proceedings of the First International Conference on Composites for Construction (CDCC'98), 5-7 August 1998, Sherbrooke, Québec, Canada.

64. Wegian, F., and Abdalla, H. (2005), "Shear capacity of concrete beams reinforced with fiber reinforced polymers". Composite Structures. 71, 130-138, ISSN : 0263-8223.

65. Keller, T. (2001), "Recent all-composite and hybrid fibre-reinforced polymer bridges and buildings." Progress in Structural Engineering and Materials. 3: 132-140.

66. Raffaello Fico (2008), "Limit state design of concrete structures reinforced with FRP bars", PhD Thesis, University of Naples Federico II, Italy.

67. Muttoni Aurelio and Ruiz Miguel Fernández (2008), "Shear Strength of Members without Transverse Reinforcement as Function of Critical Shear Crack Width", ACI Structural Journal, 163-172, ISSN : 0889-3241.

68. Kani, G. N. J. (1964), "The Riddle of Shear Failure and its Solution", ACI Structural Journal, 61-4, 441–467, ISSN : 0889-3241.

69. Kotsovos, M.D., and Pavlovic, M.N. (1999), "Ultimate Limit-State Design of Concrete Structures - A New Approach", Thomas Telford Ltd., London.

70. S. L. Sveinsdóttir (2012), "Experimental research on strengthening of concrete beams by the use of epoxy adhesive and cement-based bonding material", M. S. Thesis, Reykjavík University, Iceland.

71. Stratford T. J., and Burgoyne C. J. (2002), "Crack-Based Analysis of Shear in Concrete with Brittle Reinforcement", Mag. Concrete Res., 54(5), 321-332.

72. Bazant, Z. P., and Kazemi, M. T. (1991), "Size Effect on Diagonal Shear Failure of Beams Without Stirrups", ACI Struct. J., 88(3), 268–276, ISSN : 0889-3241.

73. Stratford T.J., "The Shear of Conc. with Ela., FRP Rein.", PhD thesis, Uni. of Camb., UK, 2000.

74. Stratford Tim and Burgoyne Chris (2001), “Shear Analysis of Concrete with Brittle Reinforcement”, Journal of Composite for Construction, ASCE, 323-330, ISSN: 1090-0268.

75. Guadagnini M., Pilakoutas K., & Waldron P. (1999), “Shear Design for Fibre Rein. Poly. Rein. Conc. Ele., Proc. of Fiber Rein. Polymer R/F for Reinf. Conc. Str.”, American Conc. Inst., 11–21.

76. M.P. Collins, E.C. Bentz, E.G. Sherwood, Liping X.J. (2007), “An Adequate Theory for the Shear Strength of Rein. Conc. Str.”, Morley Symp. on Conc. Plast. & its App., Uni. of Camb.

77. Regan, P.E. (1993), “Research on Shear: A Benefit to Humanity or a Waste of Time?”, Struct. Eng., 71-19 337–347.

78. Nielsen, M.P., Braestrup, M.W., and Bach, F. (1978), “Rational Analysis of Shear in Reinforced Concrete Beams”, IABSE Proceedings, Zurich, Switzerland, 15/78.

79. Vecchio, F. J., and Collins, M. P. (1986), “The Modified Compression Field Theory for Reinforced Concrete Elements Subjected to Shear”, ACI Structural Journal, 83(2), 219–231, ISSN : 0889-3241.

80. Evan C. Bentz, Frank J. Vecchio, and Michael P. Collins (2006), “Simplified Modified Comp. Field Theory for Calculating Shear Strength of Rein. Conc. Ele.”, ACI Structural Journal, 614-625, ISSN : 0889-3241.

81. Collins, M. P., Mitchell, D., Adebar, P., and Vecchio, F. J. (1996), “A General Shear Design Method”, ACI Structural Journal, 93(1), 36-45, ISSN : 0889-3241.

82. Machial Robert, Shahria A. M., and Rteil A. (2010), “Shear strength contribution of transverse FRP reinforcement in bridge girders”, IABSE-JSCE Joint Conference on Advances in Bridge Engineering-II.

83. El-Sayed A.K., El-Salakawy E.F., and Benmokrane B. (2007); “Shear Strength of Concrete Beams Reinforced with FRP Bars: Design Method”, Non-Metallic (FRP) Reinforcement for Concrete Structures, 955-974.

84. Mohsen Kobraei, Jumaat Mohd Zamin and Shafigh Payam (2011), “An experimental study on shear reinforcement in RC beams using CFRP-bars”, Scientific Research and Essays, 3447-3460.

85. Jongsung Sim, Park C. and Park S. (2007), “Experimental Verification on the Shear Contribution of GFRP Stirrups Embeded in Reinforced Concrete Beams”, FRPRCS-8 University of Patras, Greece.

86. Emile Shehata, Ryan Morphy, and Sami Rizkalla (2000), "Fibre reinforced polymer shear reinforcement for concrete members: behaviour and design Guidelines", Canadian Journal of Civil Engineering, Vol. 27, NRC Canada, pp 859-872.

87. Issa M.A., Ovitigala T. and Ibrahim M. (2016), "Shear behavior of basalt fiber reinforced concrete beams with and without basalt frp stirrups", Journal of Composites for Construction, 20(4), 4015083.

Publications

1. Tarak P. Vora and Dr. Bharat J. Shah, A State of the Art Use of FRP in Prestressed Concrete Structures, 2011, International Conference on Current Trends in Technology - NUiCONE – 2011, Nirma University, Ahmedabad, pp 1-6.

2. Tarak P. Vora and Dr. Bharat J. Shah, A Comprehensive Review on Shear Capacity of FRP Reinforcement in RC and PC Structures, 2012, Structural Engineering Convention, SEC-12, S.V.N.I.T., pp 431-437, ISBN : 978-93-82062-72-1.

3. Tarak P. Vora and Dr. Bharat J. Shah, A Comparative Study of Deflection and Crack Patterns of RC Beams Strengthen in Flexure With GFRP Laminates, Structural Engineering Convention, SEC-14, IIT Delhi, pp 4323-4337, ISBN : 978-93-84898-71-7.

1. Tarak P. Vora and Dr. Bharat J. Shah, Theories and Recommendations for Shear Analysis of Concrete with FRP Reinforcement, International Journal of Advance Research in Engineering, Science & Technology, Vol. 3(4), pp 195-202, ISSN : 2394-2444.

2. Tarak P. Vora and Dr. Bharat J. Shah, Experimental investigation on shear capacity of RC beams with GFRP rebar & stirrups, Steel & Composite Structures (SCI Indexed : Impact Factor – 1.795(2015)), Vol. 21(6) – 2016, pp 1265-1285, ISSN: 1229-9367.

Paper in Communication

1. Tarak P. Vora and Dr. Bharat J. Shah, Parametric Study for Shear Capacity of Reinforced Concrete Beam Having GFRP Reinforcement, International Journal of Civil & Structural Engineering.

Appendix A : Design of FRP-RC Beam by ACI 440.1R-06

Design Data					
l	Span (m)	1.8	1.8	1.8	
LL	LL (kN/m)	35	30	29	
	Sustained load (kN/m)	0	0	0	
f'_c	Specified compressive strength of concrete (MPa)	30	30	30	
ε_{cu}	Ultimate strain in concrete	0.003	0.003	0.003	
f^*_{fu}	Tensile Strength (Mpa)	905	905	905	
ε^*_{fu}	Rupture Strain	0.0152	0.0152	0.0152	
E_f	Modulus of Elasticity (Mpa)	47300	47300	47300	
C_E	Reduction Factor Table 7.1 (ACI-440.1R-06)	0.8	0.8	0.8	
β_1	Factor	0.85	0.85	0.85	
a	Distance of loading	0.5	0.65	0.75	
h	Overall Height of Member	300	300	300	
Assumptions					
b	Width of beam (mm)	112.84	112.84	150.26	
	Width of beam provided (mm)	230	230	230	
D	Depth of beam (mm)	300	300	300	
	Cover (mm)	25	25	25	
	Longi. Bar Dia. (mm)-1	18.71	18.71	18.71	
	Longi. Bar Dia. (mm)-2	15.25	15.25		
	No of Longi. Bar-1	2	2	3	
	No of Longi. Bar-2	1	1		
	Stirrups Dia. (mm)	9.5	9.5	9.5	
	Density of Concrete (kN/m^3)	24	24	24	
	Load Factor (DL)	1	1	1	
	Load Factor (LL)	1	1	1	
k_b	For Deformed FRP Bars	1.4	1.4	1.4	
A_f	Area of FRP Reinforcement (mm^2)	733	733	825	
A_{fv}	Area of FRP Stirrups Reinforcement (mm^2)	71	71	71	
d	Effective Depth	256	256	256	
r_b		40	40	40	
Load Calculation					
	Self Wt. of Beam (kN/m)	1.66	1.66	1.66	

W_{DL}	Dead Load (kN/m)	1.66	1.66	1.66	
M_U	Total Moment	18.25	20.25	22.50	
Design Rupture Stress of FRP Bars					
f_{fu}	Design Rupture Stress	724.00	724.00	724.00	f^*_{fu} C_E
Determine the Area of FRP Bars Required for Flexural Strength					
ρ_{fb}	FRP reinforcement ratio producing balanced strain conditions	0.0049	0.0049	0.0049	$\rho_{fb} = 0.85\frac{f'_c}{f_{fu}}\beta_1\frac{E_f\varepsilon_{cu}}{E_f\varepsilon_{cu}+f_{fu}}$
ρ_f	FRP reinforcement ratio	0.0124	0.0124	0.0140	$\rho_f = \frac{A_f}{bd}$
f_f	Stress in FRP reinforcement in tension (MPa)	431.44	431.44	403.09	$f_f = \left[\sqrt{\frac{(E_f\varepsilon_{cu})^2}{4}+\frac{0.85\beta_1 f'_c}{\rho_f}E_f\varepsilon_{cu}}-0.5E_f\varepsilon_{cu}\right]$
M_n	Nominal moment capacity (kNm)	72.41	72.41	75.71	$M_n = \rho_f f_f\left(1-0.59\frac{\rho_f f_f}{f'_c}\right)bd^2$
ϕ	Strength reduction factor	0.93	0.93	1.01	$\phi = 0.30+\frac{\rho_f}{4\rho_{fb}}$ for $\rho_{fb} < \rho_f \le 1.4\rho_{fb}$
	ϕM_n	67.60	67.60	76.73	
	Check $\phi M_n \ge M_u$	OK	OK	OK	
Check for Crack Width					
M_{DL}	Moment Due to Dead Load (kNm)	0.747	0.747	0.747	$M_{DL} = \frac{\omega_{DL}\ell^2}{8}$
M_{LL}	Moment Due to Live Load (kNm)	17.5	19.5	21.75	$M_{LL} = \frac{\omega_{LL}\ell^2}{8}$
	$M_{DL} + M_{DL}$	18.25	20.25	22.50	
n_f	Ratio of modulus of elasticity of FRP bars to modulus of elasticity of concrete	1.82	1.82	1.82	$n_f = \frac{E_f}{E_c} = \frac{E_f}{4750\sqrt{f'_c}}$
k	Ratio of depth of neutral axis to reinforcement depth	0.191	0.191	0.202	$k = \sqrt{2\rho_f n_f + (\rho_f n_f)^2} - \rho_f n_f$
f_f	(Mpa)	104.33	115.71	114.57	$f_f = \frac{M_{DL+LL}}{A_f d(1-k/3)}$
β	Ratio of distance from neutral axis to extreme tension fiber to distance from neutral axis to center of tensile reinforcement	1.212	1.212	1.214	$\beta = \frac{h-kd}{d(1-k)}$
d_c	Thickness of concrete cover measured from extreme tension fiber to center of bar or wire location closest thereto (mm)	44	44	44	$d_c = h - d$
s	Distance	142.29	142.29	142.29	$s - b \quad 2d_c$

w	Maximum crack width (mm)	0.62	0.69	0.69	$w = 2\frac{f_f}{E_f}\beta k_b\sqrt{d_c^2+\left(\frac{s}{2}\right)^2}$
	Check (w < 0.7 mm)	OK	OK	OK	
Check for long term deflection of the beam					
I_e	Moment of Inertia	5.18E+08	5.18E+08	5.18E+08	$I_g = \frac{bh^3}{12}$
f_r	Stress	3.40	3.40	3.40	$f_r = 0.62\sqrt{f_c'}$
M_{cr}	Cracking Moment	11.71579	11.71579	11.71579	$M_{cr} = \frac{2f_r I_g}{h}$
I_{cr}	MI of transformed cracked section	66165424	66165424	73272898	$I_{cr} = \frac{bd^3}{3}k^3 + \eta_f A_f d^2(1-k)^2$
β_d	reduction coefficient used in calculating deflection	0.51	0.51	0.57	$\beta_d = \frac{1}{5}\left[\frac{\rho_f}{\rho_{fb}}\right]$
$(I_e)_{DL+LL}$	Moment of Inertia	1.18E+08	1.04E+08	1.05E+08	$(I_e)_{DL+LL} = \left(\frac{M_{cr}}{M_a}\right)^3\beta_d I_g + \left[1-\left(\frac{M_{cr}}{M_a}\right)^3\right]I_{cr}$
$(\Delta_i)_{DL+LL}$	Deflection due to DL+LL	2.23	2.81	3.12	$(\Delta_i)_{DL+LL} = \frac{5M_{DL+LL}\ell^2}{48E_c(I_e)_{DL+LL}}$
$(\Delta_i)_{DL}$	Deflection due to DL	0.1009	0.1469	0.1678	$(\Delta_i)_{DL} = \frac{w_{DL}}{w_{DL+LL}}(\Delta_i)_{DL+LL}$
$(\Delta_i)_{LL}$	Deflection due to LL	2.13	2.66	2.94	$(\Delta_i)_{LL} = \frac{w_{LL}}{w_{DL+LL}}(\Delta_i)_{DL+LL}$
λ	Constant	1.2	1.2	1.2	$\lambda = 0.60\xi$
Δ_{LT}	Long term deflection	2.77	3.48	3.85	$\Delta_{LT} = (\Delta_i)_{LL} + \lambda[(\Delta_i)_{DL} + 0.20(\Delta_i)_{LL}]$
	Check	OK	OK	OK	$\Delta_{LT} \le \frac{\ell}{240}$
Design for Shear					
V_u	Factored shear force at section	36.15	31.15	30.15	$V_u = \frac{w_u\ell}{2} - w_u d$
c	Constant	48.98	48.98	51.64	c = kd
V_c	Nominal shear strength provided by concrete	24.68	24.68	26.02	$V_c = \frac{2}{5}\sqrt{f_c'}\,b_w c$
f_{fb}	Strength of bent portion of FRP bar	325.8	674.4632	325.8	$f_{fb} = \left(0.05\frac{r_b}{d_b} + 0.3\right)f_{fu}$
f_{fv}	The design stress of FRP stirrup is limited to:	236.5	236.5	236.5	$f_{fv} = 0.004E_f \le f_{fb}$
	Check	OK	OK	OK	
s	Stirrups Spacing – 1(mm)	605.27	509.65	605.75	$s = \frac{\phi A_{fv} f_{fv} d}{(V_u - \phi V_c)}$
s	Stirrups Spacing – 2(mm)	128.0725	128.0725	128.0725	s < d/2

s	Stirrups Spacing - 3(mm)	416.4879	416.4879	416.4879	s < $A_{fv}f_{fv}/0.35b_w$
s	Spacing should be less than (mm)	128.0725	128.0725	128.0725	
	Spacing provided (mm)	250	275	325	
	Reverse Design Value (kN)	44.27	41.93	39.33	

Appendix B : GFRP Bars Data Sheet from Manufacturer

Dextra

CERTIFICATE OF ANALYSIS

PRODUCT IDENTIFICATION	COA: DBPG1502006
PRODUCT CODE	ASTEC-GR45P
PRODUCT NAME	**ASTEC GFRP REBAR, MoE 45 Gpa, IN DIAMETER 10mm**
PRODUCT TYPE	GFRP
PRODUCTION DATE	FEBRUARY 2, 2015
BAR DESIGNATION(mm)	10
QTY(pcs)	30
P.O.	10166
MANUFACTURER	DEXTRA BUILDING PRODUCTS (GUANGDONG) CO.,Ltd
LOT NUMBER	S100615001

TEST RESULTS:

NO.	ITEM	STANDARDS	RESULT	TEST METHOD
1	BARCOL HARDNESS (AVERAGE VALUE)	≥ 50	60	ASTM D2583
2	FIBRE CONTENT, % (AVERAGE VALUE)	≥ 70	82.72	ASTM D2584
3	ULTIMATE TENSILE LOAD, kN (GUARANTEED:AVG. - 3.0 SIGMA)	≥ 59	62	ASTM D7205
4	ULTIMATE TENSILE STRENGTH, MPa (GUARANTEED:AVG. - 3.0 SIGMA)	≥ 834	871	ASTM D7205
5	MODULUS OF ELASTICITY, GPa (AVERAGE VALUE)	≥ 45	48.3	ASTM D7205
6	ULTIMATE STRAIN (AVERAGE VALUE)	≥ 1.85	1.93	ASTM D7205
7	CROSS SECTIONAL AREA, mm² (AVERAGE VALUE)	57 - 85	70.9	ASTM D792
8	**DIAMETER, mm (AVERAGE VALUE)**	8.5 - 10.41	**9.5**	ASTM D792
9	DIAMENSION IN LENGTH, m	PER SPEC	PASS	RULER
10	TRACE MARKING	BLUE	BLUE	VISUAL

REMARK:	
1	THE TRACE MARKING BLUE CORRESPONDS TO LOT NUMBER S190615002
2	TENSILE STRENGTH, MOE AND ULTIMATE STRAIN IS BASED ON STANDARD CROSS SECTIONAL AREA.
3	ABOVE INSPECTION METHODS ARE SPECIFIED BY ACI 440.3R-12

CONCLUSION	WE HEREBY CERTIFY THAT THIS BATCH OF PRODUCT IS IN CONFORMITY WITH THE QUALITY CONTROL STANDARDS.

Dextra

CERTIFICATE OF ANALYSIS

PRODUCT IDENTIFICATION	COA: DBPG 1502005
PRODUCT CODE	ASTEC-GR45P
PRODUCT NAME	**ASTEC GFRP REBAR, MoE 45 Gpa, IN DIA. 16mm**
PRODUCT TYPE	GFRP
PRODUCTION DATE	FEBRUARY 2, 2015
BAR DESIGNATION(mm)	16
QTY(pcs)	12
P.O.	10166
MANUFACTURER	DEXTRA BUILDING PRODUCTS (GUANGDONG) CO.,Ltd
LOT NUMBER	S160615002

TEST RESULTS:

NO.	ITEM	STANDARDS	RESULT	TEST METHOD
1	BARCOL HARDNESS (AVERAGE VALUE)	≥ 50	62	ASTM D2583
2	FIBRE CONTENT, % (AVERAGE VALUE)	≥ 70	82.64	ASTM D2584
3	ULTIMATE TENSILE LOAD, kN (GUARANTEED:AVG. - 3.0 SIGMA)	≥ 144	180	ASTM D7205
4	ULTIMATE TENSILE STRENGTH, MPa (GUARANTEED:AVG. - 3.0 SIGMA)	≥ 725	904	ASTM D7205
5	MODULUS OF ELASTICITY, GPa (AVERAGE VALUE)	≥ 45	48.2	ASTM D7205
6	ULTIMATE STRAIN (AVERAGE VALUE)	≥ 1.61	2.05	ASTM D7205
7	TRANSVERSE SHEAR, MPa (GUARANTEED:AVERAGE)	≥ 124	159.22	ASTM D4475
8	DYE WICKING (AVERAGE)	NON-CONTINUE CRACK	PASS	ASTM D5117
9	CROSS SECTIONAL AREA, mm² (AVERAGE VALUE)	159 - 237	182.8	ASTM D792
10	**DIAMETER, mm (AVERAGE VALUE)**	14.22 - 17.45	**15.25**	ASTM D792
11	DIAMENSION IN LENGTH, m	PER SPEC	PASS	RULER
12	TRACE MARKING	BLUE	BLUE	VISUAL

REMARK:

1	THE TRACE MARKING BLUE CORRESPONDS TO LOT NUMBER S190615002
2	TENSILE STRENGTH, MOE AND ULTIMATE STRAIN IS BASED ON STANDARD CROSS SECTIONAL AREA.
3	ABOVE INSPECTION METHODS ARE SPECIFIED BY ACI 440.3R-12

CONCLUSION	WE HEREBY CERTIFY THAT THIS BATCH OF PRODUCT IS IN CONFORMITY WITH THE QUALITY CONTROL STANDARDS.

Dextra

CERTIFICATE OF ANALYSIS

PRODUCT IDENTIFICATION	COA: DBPG1502004
PRODUCT CODE	ASTEC-GR45P
PRODUCT NAME	**ASTEC GFRP REBAR, MoE 45 Gpa, IN DIAMETER 19mm**
PRODUCT TYPE	GFRP
PRODUCTION DATE	FEBRUARY 3, 2015
BAR DESIGNATION(mm)	19
QTY(pcs)	30
P.O.	10166
MANUFACTURER	DEXTRA BUILDING PRODUCTS (GUANGDONG) CO.,Ltd
LOT NUMBER	S190615002

TEST RESULTS:

NO.	ITEM	STANDARDS	RESULT	TEST METHOD
1	BARCOL HARDNESS (AVERAGE VALUE)	≥ 50	56	ASTM D2583
2	FIBRE CONTENT, % (AVERAGE VALUE)	≥ 70	80.26	ASTM D2584
3	ULTIMATE TENSILE LOAD, kN (GUARANTEED:AVG. - 3.0 SIGMA)	≥ 195	271	ASTM D7205
4	ULTIMATE TENSILE STRENGTH, MPa (GUARANTEED:AVG. - 3.0 SIGMA)	≥ 685	955	ASTM D7205
5	MODULUS OF ELASTICITY, GPa (AVERAGE VALUE)	≥ 45	47.3	ASTM D7205
6	ULTIMATE STRAIN (AVERAGE VALUE)	≥ 1.52	2.16	ASTM D7205
7	CROSS SECTIONAL AREA, mm^2 (AVERAGE VALUE)	230 - 341	274.9	ASTM D792
8	**DIAMETER, mm (AVERAGE VALUE)**	19.02 - 20.83	**18.71**	ASTM D792
9	DIAMENSION IN LENGTH, m	PER SPEC	PASS	RULER
10	TRACE MARKING	BLUE	BLUE	VISUAL

REMARK:

1	THE TRACE MARKING BLUE CORRESPONDS TO LOT NUMBER S190615002
2	TENSILE STRENGTH, MOE AND ULTIMATE STRAIN IS BASED ON STANDARD CROSS SECTIONAL AREA.
3	ABOVE INSPECTION METHODS ARE SPECIFIED BY ACI 440.3R-12

CONCLUSION	WE HEREBY CERTIFY THAT THIS BATCH OF PRODUCT IS IN CONFORMITY WITH THE QUALITY CONTROL STANDARDS.

Appendix C : GFRP Stirrup Data Sheet from Manufacturer

Dextra

CERTIFICATE OF ANALYSIS

PRODUCT IDENTIFICATION	COA: DBPG 1502007
PRODUCT CODE	ASTEC-GR45P
PRODUCT NAME	**ASTEC GFRP BENDBAR, IN DIAMETER 10mm**
PRODUCT TYPE	GFRP
PRODUCTION DATE	FEBRUARY 4, 2015
BAR DESIGNATION(mm)	10
QTY(pcs)	180
P.O.	10166
MANUFACTURER	DEXTRA BUILDING PRODUCTS (GUANGDONG) CO.,Ltd
LOT NUMBER	C100715001

TEST RESULTS:

NO.	ITEM	STANDARDS	RESULT	TEST METHOD
1	BARCOL HARDNESS (AVERAGE VALUE)	≥ 50	60	ASTM D2583
2	FIBRE CONTENT, % (AVERAGE VALUE)	≥ 70	85.95	ASTM D2584
3	ULTIMATE TENSILE LOAD, kN (MINIMA VALUE)	≥ 59	66	ASTM D7205
4	ULTIMATE TENSILE STRENGTH, MPa (MINIMA VALUE)	≥ 834	921	ASTM D7205
7	CROSS SECTIONAL AREA, mm^2 (AVERAGE VALUE)	57 - 85	71.9	ASTM D792
8	**DIAMETER, mm (AVERAGE VALUE)**	8.5 - 10.41	**9.56**	ASTM D792
9	DIAMENSION IN LENGTH, M	PER SPEC	PASS	RULER
10	TRACE MARKING	PURPLE	PURPLE	VISUAL

REMARK:

1	THE TRACE MARKING BLUE CORRESPONDS TO LOT NUMBER S190615002
2	TENSILE STRENGTH, MOE AND ULTIMATE STRAIN IS BASED ON STANDARD CROSS SECTIONAL AREA.
3	ABOVE INSPECTION METHODS ARE SPECIFIED BY ACI 440.3R-12

CONCLUSION	WE HEREBY CERTIFY THAT THIS BATCH OF PRODUCT IS IN CONFORMITY WITH THE QUALITY CONTROL STANDARDS.

Appendix D : Influential Parameters on Shear Capacity

TABLE D.1 Variation in tensile strength and its effect on shear design parameters.

Design Data					
	Span (m)	3.35	3.35	3.35	3.35
	LL (kN/m)	5.8	5.8	5.8	5.8
	Sustained load (kN/m)	3	3	3	3
f'_c	Specified compressive strength of concrete (MPa)	27.6	27.6	27.6	27.6
ε_{cu}	Ultimate strain in concrete	0.003	0.003	0.003	0.003
f^*_{fu}	**Tensile Strength (Mpa)**	**415**	**500**	**620.2**	**750**
ε^*_{fu}	Rupture Strain	0.014	0.014	0.014	0.014
E_f	Modulus of Elasticity (Mpa)	44800	44800	44800	44800
C_E	Reduction Factor Table 7.1 (ACI-440.1R-06)	0.8	0.8	0.8	0.8
β_1	Factor	0.85	0.85	0.85	0.85
Design for Shear					
V_u	Factored shear force at section	20.54	20.54	20.54	20.54
V_c	Nominal shear strength provided by concrete	17.90	17.90	17.90	17.90
f_{fb}	**Strength of bent portion of FRP bar**	**149.40**	**180.00**	**223.27**	**270.00**
f_{fv}	The design stress of FRP stirrup is limited to:	179.20	179.20	179.20	179.20
	Check	Check	OK	OK	OK
s	**Spacing of Stirrups**	**258.06**	**330.84**	**502.28**	**911.22**

TABLE D.2 Variation in stirrup diameter and its effect on shear design parameters.

Design Data					
	Span (m)	3.35	3.35	3.35	3.35
	LL (kN/m)	5.8	5.8	5.8	5.8
	Sustained load (kN/m)	3	3	3	3
f'_c	Specified compressive strength of concrete (MPa)	27.6	27.6	27.6	27.6
ε_{cu}	Ultimate strain in concrete	0.003	0.003	0.003	0.003
f^*_{fu}	Tensile Strength (Mpa)	415	500	620.2	750
ε^*_{fu}	Rupture Strain	0.014	0.014	0.014	0.014
E_f	Modulus of Elasticity (Mpa)	44800	44800	44800	44800
C_E	Reduction Factor Table 7.1 (ACI-440.1R-06)	0.8	0.8	0.8	0.8
β_1	Factor	0.85	0.85	0.85	0.85
	Stirrups Dia. (mm)	**6**	**8**	**9.5**	**12**
Design for Shear					
V_u	Factored shear force at section	20.49	20.52	20.54	20.58
V_c	**Nominal shear strength provided by concrete**	**18.04**	**17.96**	**17.90**	**17.80**
f_{fb}	Strength of bent portion of FRP bar	223.27	223.27	223.27	223.27
f_{fv}	The design stress of FRP stirrup is limited to:	179.20	179.20	179.20	179.20
	Check	OK	OK	OK	OK
s	**Spacing of Stirrups**	**202.82**	**358.06**	**502.28**	**794.49**

TABLE D.3 Variation in bend radius and its effect on shear design parameters.

Design Data					
	Span (m)	3.35	3.35	3.35	3.35
	LL (kN/m)	5.8	5.8	5.8	5.8
	Sustained load (kN/m)	3	3	3	3
f'_c	Specified compressive strength of concrete (MPa)	27.6	27.6	27.6	27.6
ε_{cu}	Ultimate strain in concrete	0.003	0.003	0.003	0.003
f^*_{fu}	Tensile Strength (Mpa)	415	500	620.2	750
ε^*_{fu}	Rupture Strain	0.014	0.014	0.014	0.014
E_f	Modulus of Elasticity (Mpa)	44800	44800	44800	44800
C_E	Reduction Factor Table 7.1 (ACI-440.1R-06)	0.8	0.8	0.8	0.8
β_1	Factor	0.85	0.85	0.85	0.85
	Bend Radius	**3**	**4**	**5**	**6**
Design for Shear					
V_u	Factored shear force at section	20.54	20.54	20.54	20.54
V_c	Nominal shear strength provided by concrete	17.90	17.90	17.90	17.90
f_{fb}	**Strength of bent portion of FRP bar**	**223.27**	**248.08**	**272.89**	**297.70**
f_{fv}	The design stress of FRP stirrup is limited to:	179.20	179.20	179.20	179.20
	Check	OK	OK	OK	OK
s	**Spacing of Stirrups**	**502.28**	**502.28**	**502.28**	**502.28**

TABLE D.4 Variation in FRP reinforcement ratio and its effect on shear design parameters.

Design Data					
	Span (m)	3.35	3.35	3.35	3.35
	LL (kN/m)	5.8	5.8	5.8	5.8
	Sustained load (kN/m)	3	3	3	3
f'_c	Specified compressive strength of concrete (MPa)	27.6	27.6	27.6	27.6
ε_{cu}	Ultimate strain in concrete	0.003	0.003	0.003	0.003
f^*_{fu}	Tensile Strength (Mpa)	415	500	620.2	750
ε^*_{fu}	Rupture Strain	0.014	0.014	0.014	0.014
E_f	Modulus of Elasticity (Mpa)	44800	44800	44800	44800
C_E	Reduction Factor Table 7.1 (ACI-440.1R-06)	0.8	0.8	0.8	0.8
β_1	Factor	0.85	0.85	0.85	0.85
ρf	**FRP reinforcement ratio**	**0.009**	**0.011**	**0.014**	**0.016**
Design for Shear					
V_u	Factored shear force at section	20.54	20.54	20.54	20.54
V_c	**Nominal shear strength provided by concrete**	**15.29**	**16.92**	**18.35**	**19.65**
f_{fb}	Strength of bent portion of FRP bar	223.27	223.27	223.27	223.27
f_{fv}	The design stress of FRP stirrup is limited to:	179.20	179.20	179.20	179.20
	Check	OK	OK	OK	OK
s	**Spacing of Stirrups**	**298.51**	**402.18**	**565.79**	**865.14**

TABLE D.5 Variation in modulus of elasticity and its effect on shear design parameters.

Design Data					
	Span (m)	3.35	3.35	3.35	3.35
	LL (kN/m)	5.8	5.8	5.8	5.8
	Sustained load (kN/m)	3	3	3	3
f'_c	Specified compressive strength of concrete (MPa)	27.6	27.6	27.6	27.6
ε_{cu}	Ultimate strain in concrete	0.003	0.003	0.003	0.003
f^*_{fu}	Tensile Strength (Mpa)	415	500	620.2	750
ε^*_{fu}	Rupture Strain	0.014	0.014	0.014	0.014
E_f	**Modulus of Elasticity (Mpa)**	**44800**	**45000**	**50000**	**60000**
C_E	Reduction Factor Table 7.1 (ACI-440.1R-06)	0.8	0.8	0.8	0.8
β_1	Factor	0.85	0.85	0.85	0.85
Design for Shear					
V_u	Factored shear force at section	20.54	20.54	20.54	20.54
V_c	**Nominal shear strength provided by concrete**	**17.90**	**18.79**	**19.60**	**20.37**
f_{fb}	Strength of bent portion of FRP bar	223.27	223.27	223.27	223.27
f_{fv}	**The design stress of FRP stirrup is limited to:**	**179.20**	**200.00**	**220.00**	**240.00**
	Check	OK	OK	OK	Check
s	**Spacing of Stirrups**	**502.28**	**536.91**	**571.98**	**608.65**

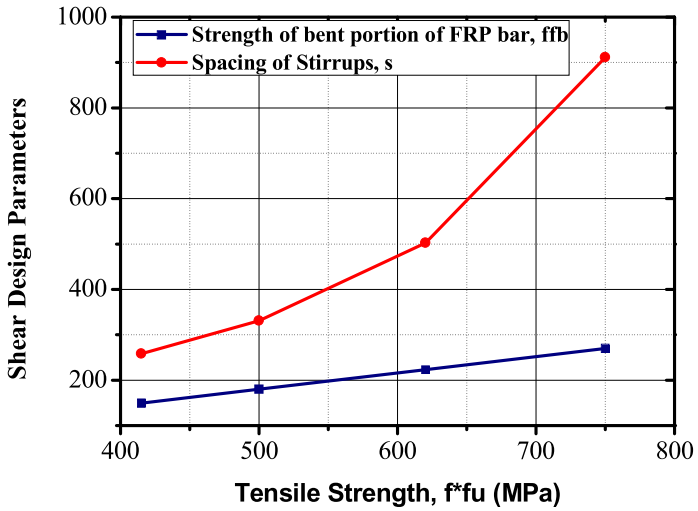

FIGURE D.1 Effect of tensile strength on shear design parameters

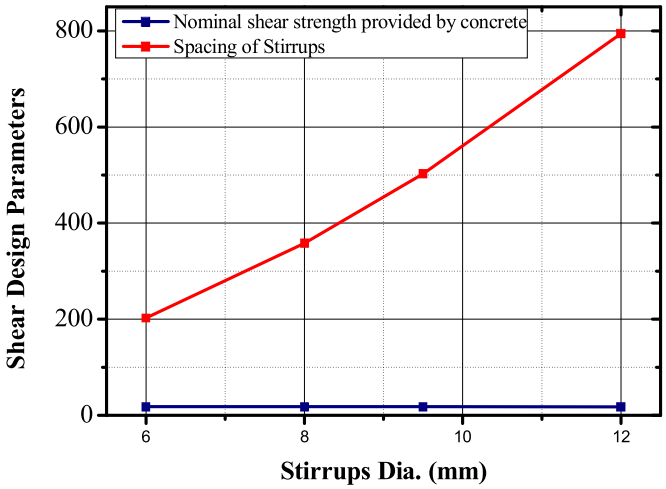

FIGURE D.2 Effect of stirrup diameter on shear design parameters

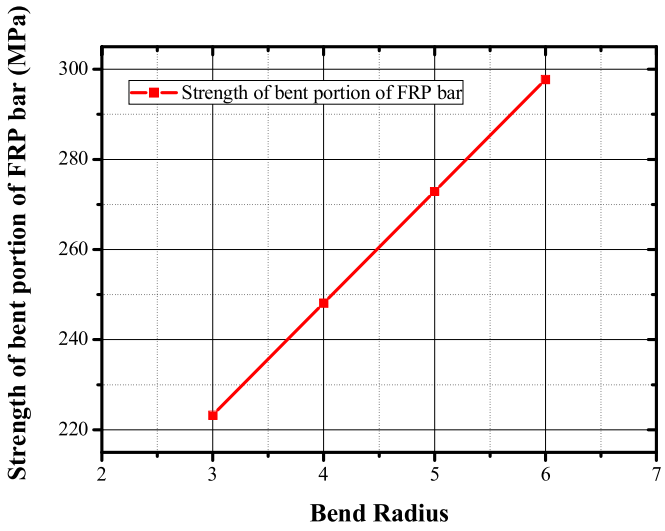

FIGURE D.3 Effect of bend radius on shear design parameters

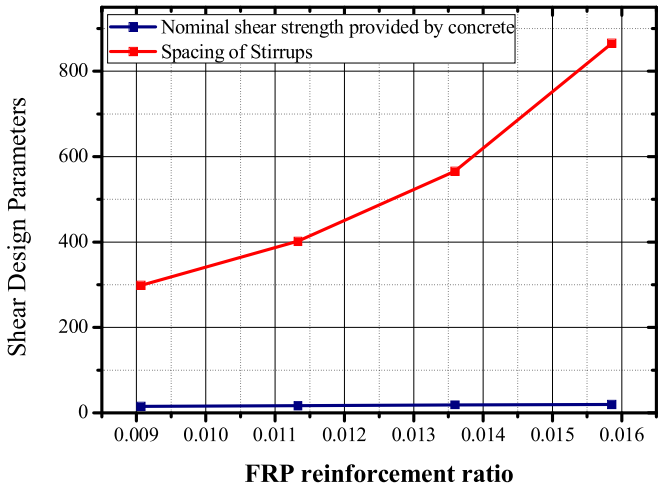

FIGURE D.4 Effect of FRP reinforcement ratio on shear design parameters

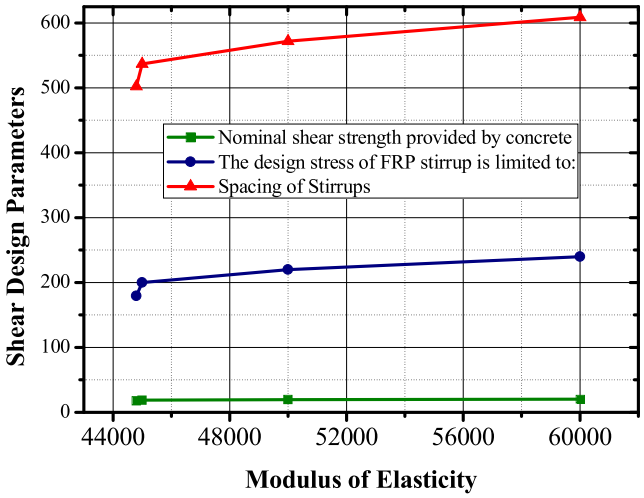

FIGURE D.5 Effect of modulus of elasticity on shear design parameters

Appendix E : Data Observation

E.1 Specimen SB.2.1

TABLE E.1 Data observation of specimen SB.2.1.

Sr. No.	Shear Force (kN)	Stirrup Strain (μStrain)	Flexural Strain (μStrain)	Concrete Strain (μStrain)	Deflection (mm)
1	6.97	3	96	67	1.56
2	13.94	20	113	134	3.48
3	20.91	32	256	195	4.84
4	27.88	56	289	264	5.48
5	34.85	70	447	320	6.12
6	41.82	123	765	379	7.08
7	48.79	159	888	444	7.24
8	55.76	212	976	520	7.88
9	62.73	267	1189	584	8.32
10	69.7	343	1378	641	9.32
11	76.67	534	1563	665	10.76
12	83.64	669	1987	705	10.99
13	**90.61**	**823**	**2289**	**755**	**11.45**
14	97.58	1908	2568	836	11.98
15	104.55	2290	2832	890	12.96
16	111.52	2726	2980	896	13.24
17	118.49			952	13.56
18	125.46			981	13.8
19	132.43			1092	14.56
20	139.4			1625	15.24
21	146.37			2180	15.6
22	153.34			2748	17.24
23	160.31			3106	17.77
24	167.28			9760	18.2
25	174.25			10830	19.6
26	181.22			23893	32.2

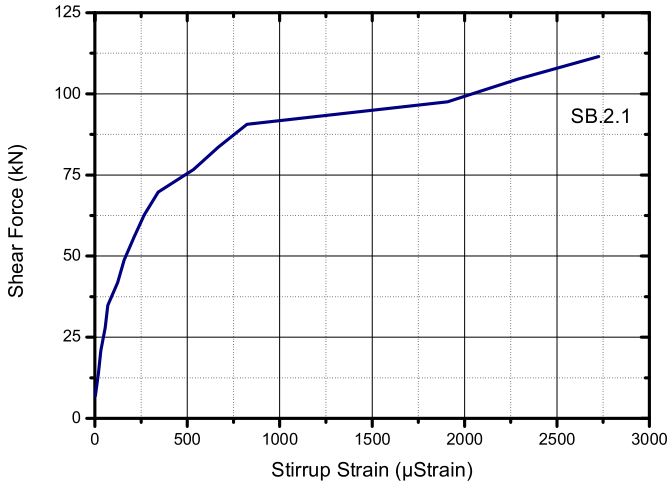

FIGURE E.1 Experimental shear force vs stirrup strain relationship of specimen SB.2.1.

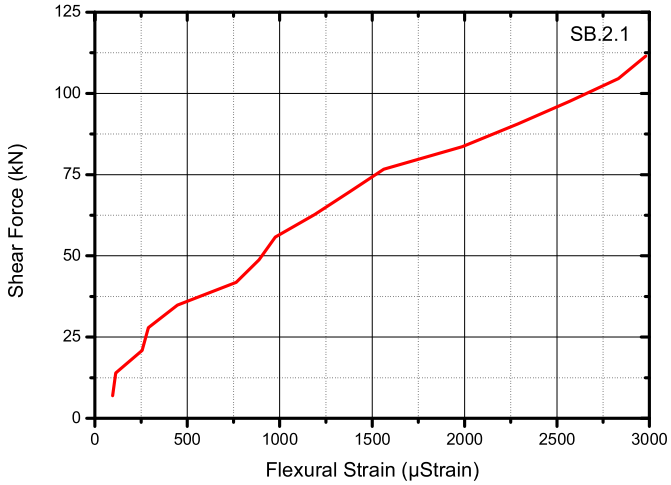

FIGURE E.2 Experimental shear force vs flexural strain relationship of specimen SB.2.1.

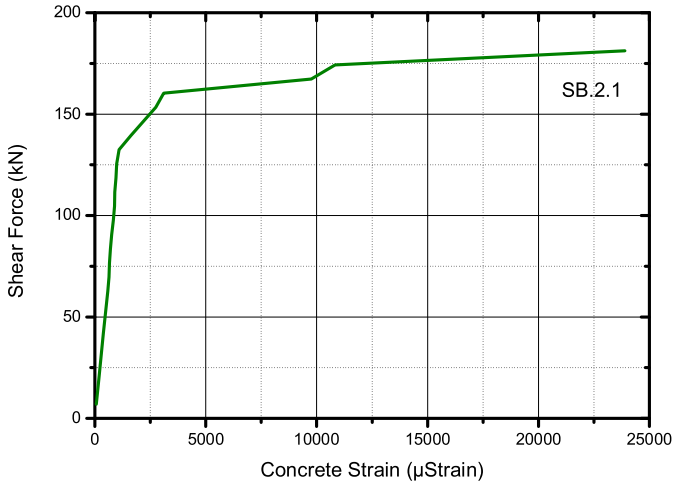

FIGURE E.3 Experimental shear force vs concrete surface strain relationship of specimen SB.2.1.

E.2 Specimen GA.1.1

TABLE E.2 Data observation of specimen GA.1.1

Sr. No.	Shear Force (kN)	Stirrup Strain (μStrain)	Flexural Strain (μStrain)	Concrete Strain (μStrain)	Deflection (mm)
1	6.97	4	142	68.33	1.08
2	13.94	16	192	136.66	2.64
3	20.91	22	234	204.99	3.12
4	27.88	46	298	273.32	3.44
5	34.85	70	518	341.65	3.64
6	41.82	236	714	409.98	5.2
7	48.79	280	938	478.31	8.84
8	55.76	338	1172	546.64	10.72
9	62.73	370	1392	614.97	11.68
10	69.7	388	1992	683.3	12.92
11	76.67	756	2556	716.63	14
12	83.64	1220	2914	749.96	15.08
13	90.61	1490	3232	783.29	16.48
14	97.58	2010	3798	816.62	18.28
15	104.55	2270	4090	889.95	20.32
16	111.52	2902	4250	1080	22.4
17	118.49	3290	4254	2538	23.96
18	125.46	3389	5186	2856	25.28
19	132.43	3490	5172	3378	26.36
20	139.4	3609	5298	4228	27.4
21	**146.37**	**3689**	**5638**	**6350**	**31**
22	153.34	3754	6478	7472	32.16
23	160.31	3826	6690	8286	33.24
24	167.28	3962	7156	10912	37.24
25	174.25	4073	7396	11470	37.88
26	181.22	4232	7578	11920	38.48
27	188.19	4290	7758	13394	40.44
28	195.16	4689	7934	14806	41.96
29	202.13	5180	8116	16290	43.52
30	209.1	6189	8694	24364	56.76

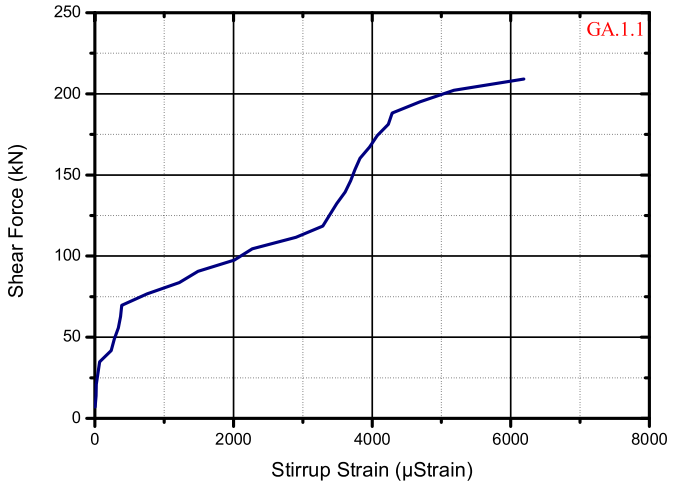

FIGURE E.4 Experimental shear force vs stirrup strain relationship of specimen GA.1.1.

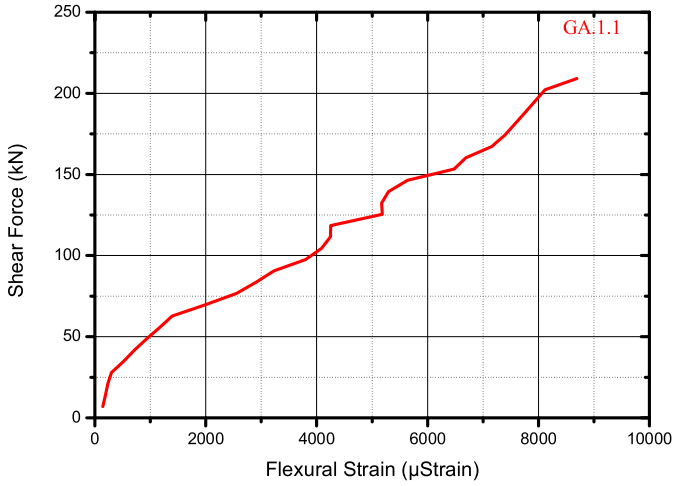

FIGURE E.5 Experimental shear force vs flexural strain relationship of specimen GA.1.1.

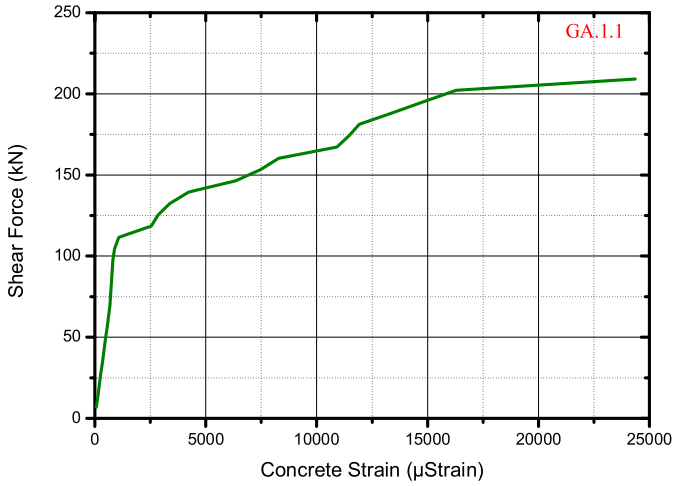

FIGURE E.6 Experimental shear force vs concrete surface strain relationship of specimen GA.1.1.

E.3 Specimen GA.1.2

TABLE E.3 Data observation of specimen GA.1.2.

Sr. No.	Shear Force	Stirrup Strain	Flexural Strain	Concrete Strain	Deflection
	(kN)	(μStrain)	(μStrain)	(μStrain)	(mm)
1	6.97	12	128	64.41	0.8
2	13.94	12	168	128.82	1.72
3	20.91	30	316	193.23	2.72
4	27.88	45	366	257.64	2.88
5	34.85	50	420	322.05	3.2
6	41.82	140	776	386.46	4.48
7	48.79	245	970	450.87	6.64
8	55.76	335	1026	515.28	7.84
9	62.73	369	1056	579.69	8.4
10	69.7	410	1448	644.1	9.04
11	76.67	876	1958	673.51	9.72
12	83.64	1090	2064	702.92	10.32
13	90.61	1629	2294	732.33	11.72
14	97.58	1762	2590	761.74	13.32
15	104.55	2027	2990	791.15	15.24
16	111.52	2493	3001	820.56	16
17	118.49	2798	3228	971.97	19.32
18	125.46	2798	3400	1670	20.68
19	132.43	2874	3567	2716	23.76
20	**139.4**	**2946**	**3698**	**7728**	**24.92**
21	146.37	3097	3867	9694	25.52
22	153.34	3500	4072	13158	26.4
23	160.31	3700	4340	14108	27.72
24	167.28	3810	4354	14812	29.44
25	174.25	4134	4670	15662	30.64
26	181.22	4136	4824	17138	31.24
27	188.19	4606	4998	19138	34.28
28	195.16	4790	5020	20236	36.88
29	202.13	4974	5180	21260	49.84
30	209.1	5586	5558	24366	
31	216.07	6070	6246		
32	223.04	6363	6748		

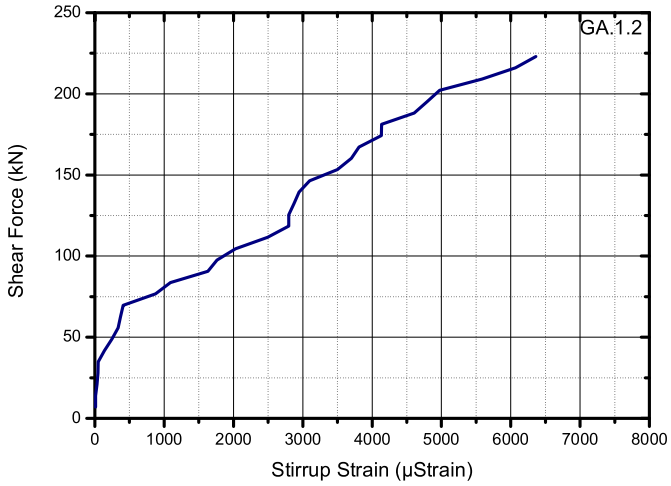

FIGURE E.7 Experimental shear force vs stirrup strain relationship of specimen GA.1.2.

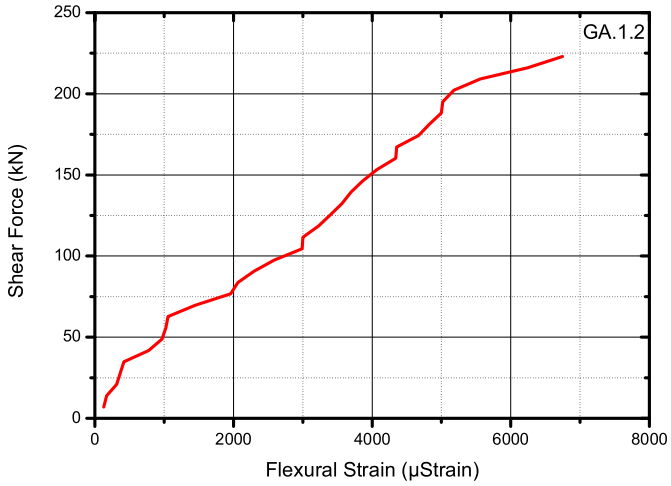

FIGURE E.8 Experimental shear force vs flexural strain relationship of specimen GA.1.2.

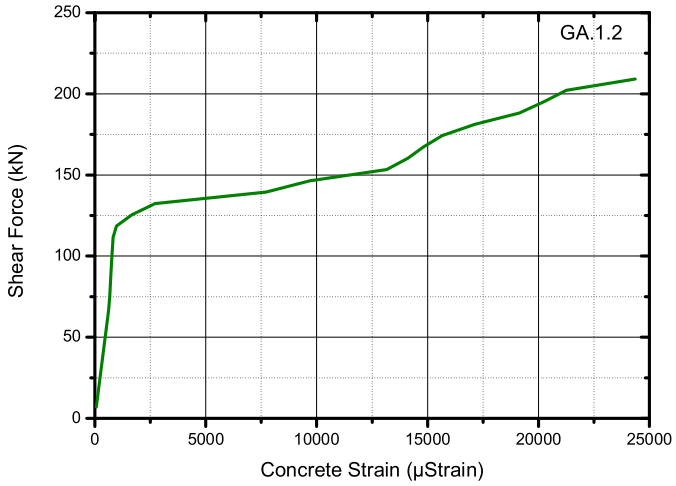

FIGURE E.9 Experimental shear force vs concrete surface strain relationship of specimen GA.1.2.

E.4 Specimen GA.2.1.

TABLE E.4 Data observation of specimen GA.2.1.

Sr. No.	Shear Force	Stirrup Strain	Flexural Strain	Concrete Strain	Deflection
	(kN)	(μStrain)	(μStrain)	(μStrain)	(mm)
1	6.97	20	220	64.41	2.44
2	13.94	30	320	128.82	2.96
3	20.91	75	450	193.23	3.32
4	27.88	178	690	257.64	3.92
5	34.85	183	592	322.05	4.2
6	41.82	222	704	386.46	4.96
7	48.79	256	1238	450.87	5.72
8	55.76	339	1486	515.28	6.96
9	62.73	458	1746	579.69	7.56
10	69.7	1874	1874	644.1	10.52
11	76.67	1994	1994	673.51	11.08
12	83.64	2000	2000	702.92	12.76
13	90.61	2452	2452	732.33	14.04
14	97.58	3044	3044	761.74	14.4
15	104.55	3510	3510	791.15	15.88
16	111.52	4146	4146	820.56	18
17	118.49	5186	5186	943.97	20.16
18	125.46	5262	5262	1198	21.04
19	132.43	5272	5272	3174	23.2
20	139.4	5330	5330	3380	24.88
21	**146.37**	**5506**	**5606**	**3390**	**25.24**
22	153.34	5774	5774	3394	27.28
23	160.31	5796	5746	8516	30.16
24	167.28	6128	6128	10694	32.2
25	174.25	8250	8250	11616	33.4
26	181.22	8436	8436	13252	35.64
27	188.19	8642	8642	14998	38.56
28	188.19			19032	

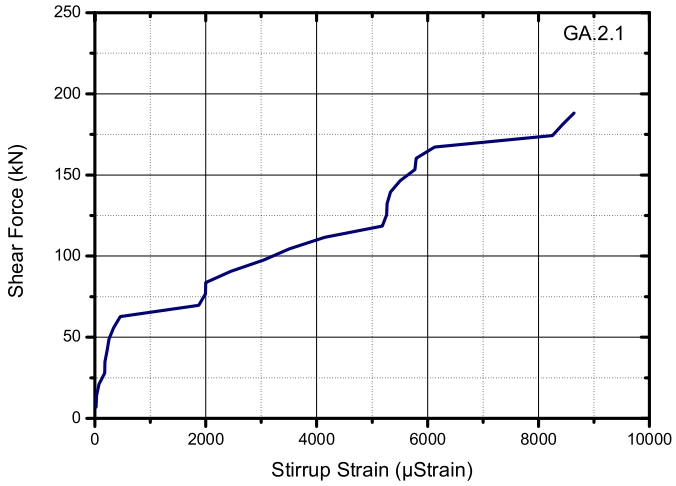

FIGURE E.10 Experimental shear force vs stirrup strain relationship of specimen GA.2.1.

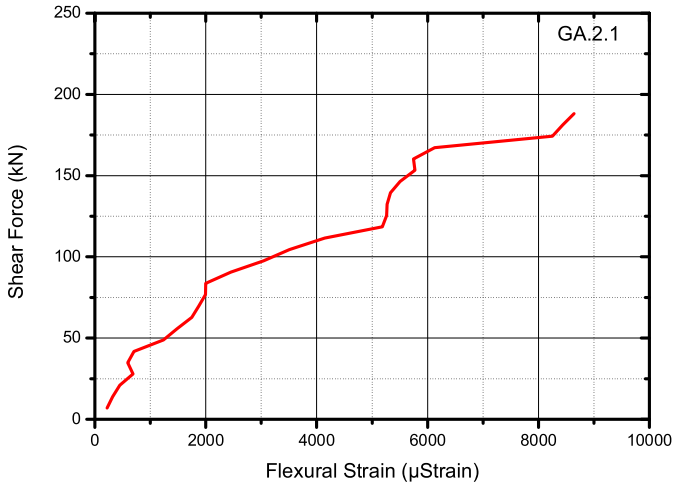

FIGURE E.11 Experimental shear force vs flexural strain relationship of specimen GA.2.1.

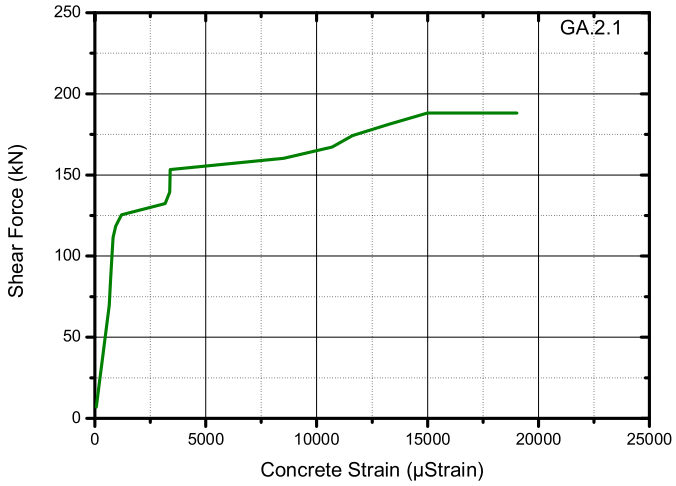

FIGURE E.12 Experimental shear force vs concrete surface strain relationship of specimen GA.2.1.

E.5 Specimen GA.2.2

TABLE E.5 Data observation of specimen GA.2.2.

Sr. No.	Shear Force	Stirrup Strain	Flexural Strain	Concrete Strain	Deflection
	(kN)	(μStrain)	(μStrain)	(μStrain)	(mm)
1	6.97	22	454	66.25	1.44
2	13.94	56	494	132.5	2.8
3	20.91	80	646	198.75	3.56
4	27.88	138	748	265	4.64
5	34.85	156	946	331.25	5.4
6	41.82	324	986	397.5	6.2
7	48.79	458	1040	463.75	6.8
8	55.76	679	1112	530	7.2
9	62.73	1149	1176	596.25	8
10	69.7	1800	1208	662.5	10.88
11	76.67	1980	1248	693.75	12.08
12	83.64	2088	1416	725	12.96
13	90.61	2599	2134	756.25	13.84
14	97.58	3277	2604	787.5	14.92
15	104.55	2698	3244	818.75	16.56
16	111.52	4489	3280	876	18.68
17	118.49	5497	3248	1358	19.44
18	125.46	5532	3338	1726	20.24
19	132.43	5678	3960	3204	22.48
20	139.4	5738	4010	4166	23.44
21	**146.37**	**5890**	**4383**	**6246**	**26.4**
22	153.34	5920	4404	6932	27.72
23	160.31	6390	4656	7808	29
24	167.28	6422	4828	8716	30.12
25	174.25	6622	5072	9770	31.52
26	181.22	6829	5986	11798	33.24
27	188.19	6932		12764	35.16
28	195.16	7290		13084	35.72
29	202.13	7492		13416	36.12
30	209.1	7688		14814	38.12
31	216.07	7763		17248	41.16
32	223.04	7792		18686	43.12
33	230.01	8112		19972	44.88
34	236.98	8122		21430	46.92
35	243.95	8201		23016	48.84
36	250.92	8204			49.8

37	250.92				65.12
38	250.92				65.04

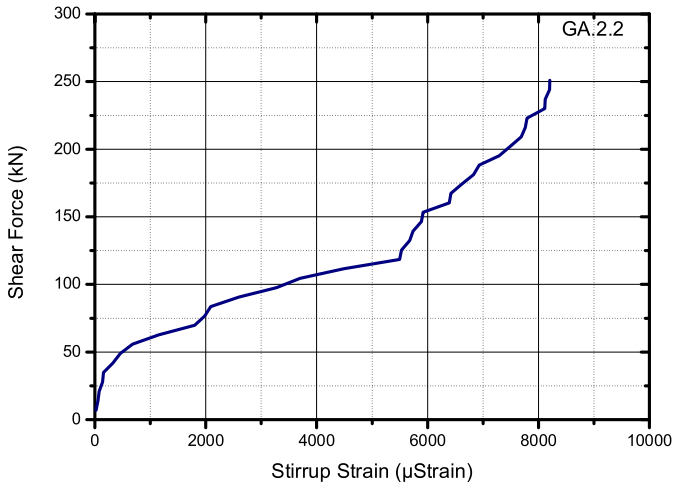

FIGURE E.13 Experimental shear force vs stirrup strain rel ationship of specimen GA.2.2.

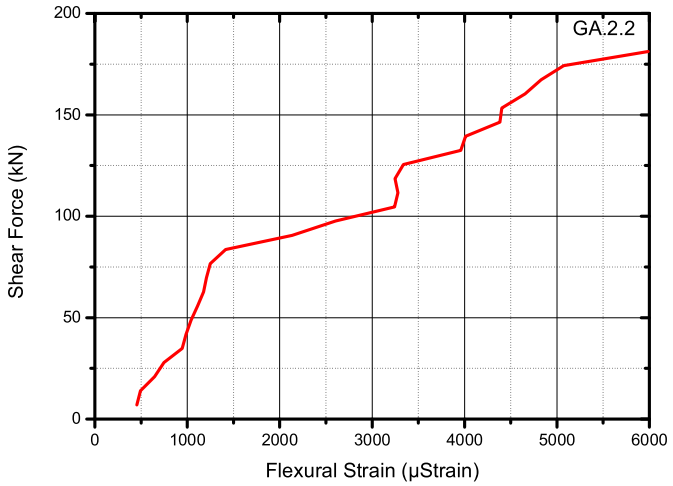

FIGURE E.14 Experimental shear force vs flexural strain relationship of specimen GA.2.2.

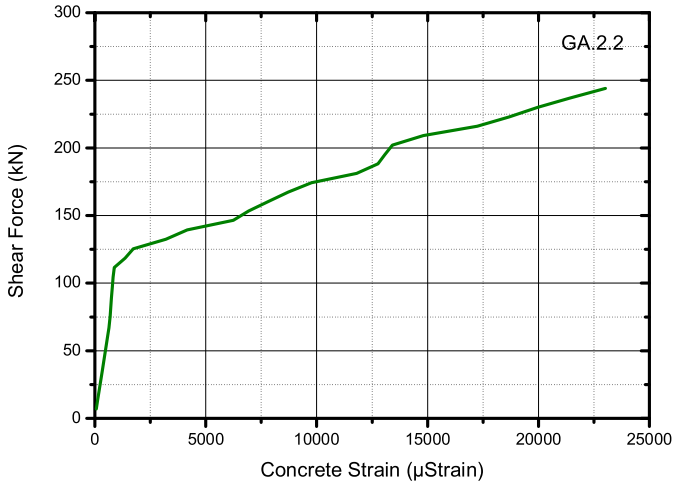

FIGURE E.15 Experimental shear force vs concrete surface strain relationship of specimen GA.2.2.

E.6 Specimen GB.2.1

TABLE E.6 Data observation of specimen GB.2.1.

Sr. No.	Shear Force	Stirrup Strain	Flexural Strain	Concrete Strain	Deflection
	(kN)	(μStrain)	(μStrain)	(μStrain)	(mm)
1	6.97	70	178	85	2.88
2	13.94	86	186	170	3.16
3	20.91	101	438	255	3.52
4	27.88	110	464	340	3.96
5	34.85	114	588	425	4.8
6	41.82	222	650	510	6.32
7	48.79	423	886	595	7.72
8	55.76	678	964	680	8.44
9	62.73	734	1606	765	10.6
10	69.7	1551	2298	1076	12
11	76.67	2222	2430	1290	14.12
12	83.64	2348	3116	1758	16.32
13	90.61	2496	3510	3502	19.04
14	97.58	4286	3866	4480	20.76
15	**104.55**	**5184**	**4370**	**5532**	**22.12**
16	111.52	5652	4876	6260	23.2
17	118.49	5820	4922	7688	23.4
18	118.49			22568	

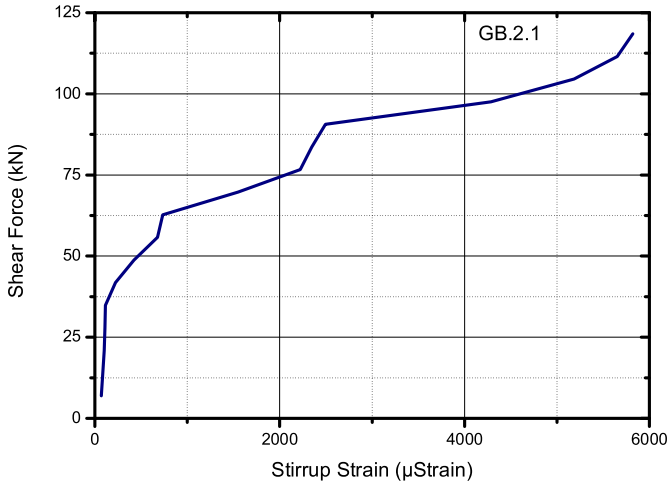

FIGURE E.16 Experimental shear force vs stirrup strain relationship of specimen GB.2.1.

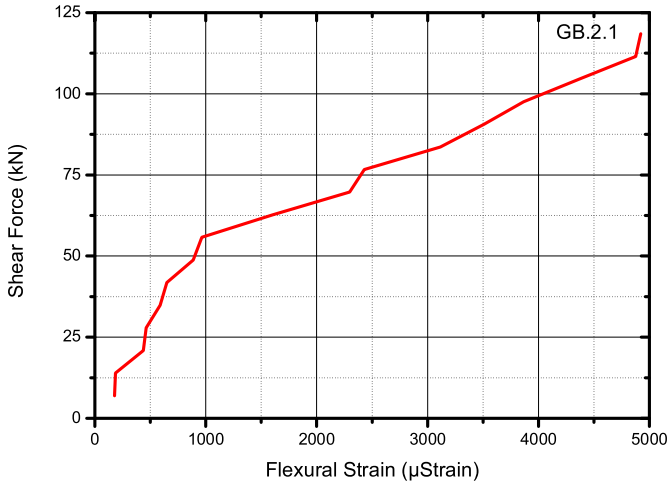

FIGURE E.17 Experimental shear force vs flexural strain relationship of specimen GB.2.1.

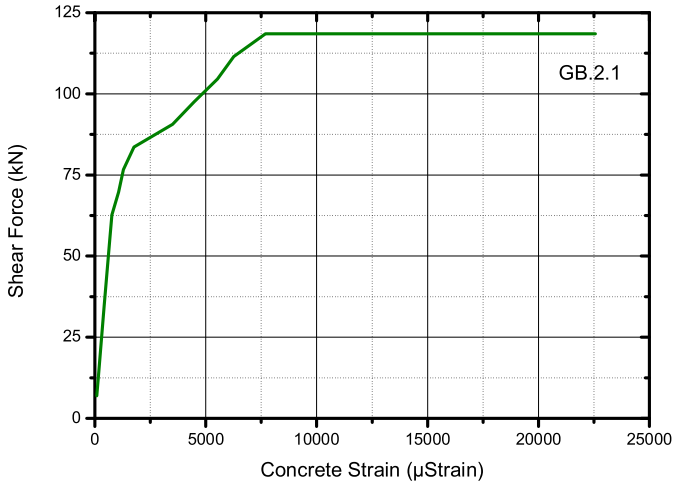

FIGURE E.18 Experimental shear force vs concrete surface strain relationship of specimen GB.2.1.

E.7 Specimen GB.2.2

TABLE E.7 Data observation of specimen GB.2.2.

Sr. No.	Shear Force	Stirrup Strain	Flexural Strain	Concrete Strain	Deflection
	(kN)	(μStrain)	(μStrain)	(μStrain)	(mm)
1	6.97	12	98	80.45	1.16
2	13.94	95	250	160.9	1.88
3	20.91	107	396	241.35	2.44
4	27.88	110	512	321.8	3.52
5	34.85	116	738	402.25	4.56
6	41.82	287	852	482.7	5.08
7	48.79	389	988	563.15	5.8
8	55.76	770	1260	643.6	6.48
9	62.73	873	1456	724.05	7.56
10	69.7	1930	2130	804.5	11.12
11	76.67	2109	2764	881.95	14.48
12	83.64	2467	3020	884	15.6
13	90.61	3345	3040	884	16.28
14	97.58	3657	3744	1242	19
15	104.55	3890	3796	1434	19.68
16	**111.52**	**3987**	**4430**	**4358**	**23.8**
17	118.49	4020	4500	4764	25.24
18	125.46	4136	4718	5118	25.8
19	132.43	4252	5158	8958	31
20	139.4	4368	5410	10406	32.48
21	146.37	4484	5854	12692	35.44
22	153.34	4567	6184	14182	37.12
23	160.31	4650	6306	16074	38.24
24	167.28	4733	6542	17702	39.92
25	174.25	4875	6908	19510	42.16
26	181.22	5037	7350	21304	44.56
27	188.19	5234	7532	22214	46.8
28	195.16	5567	7568	24174	48.04
29	202.13	5906	8120	24342	51.44
30	209.1	6386	8678		55.8

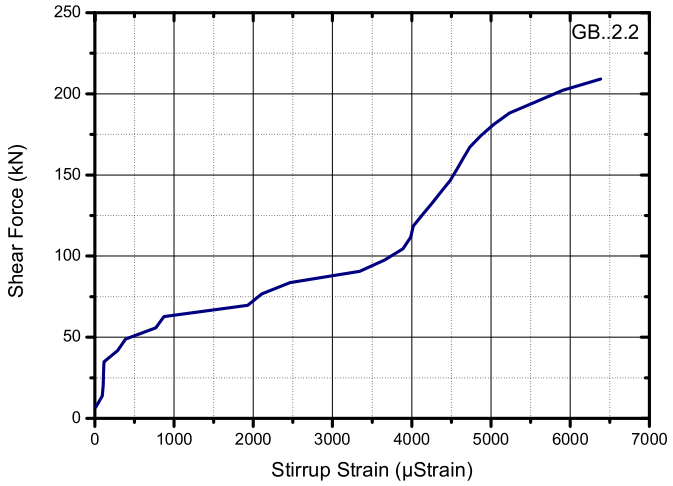

FIGURE E.19 Experimental shear force vs stirrup strain relationship of specimen GB.2.2.

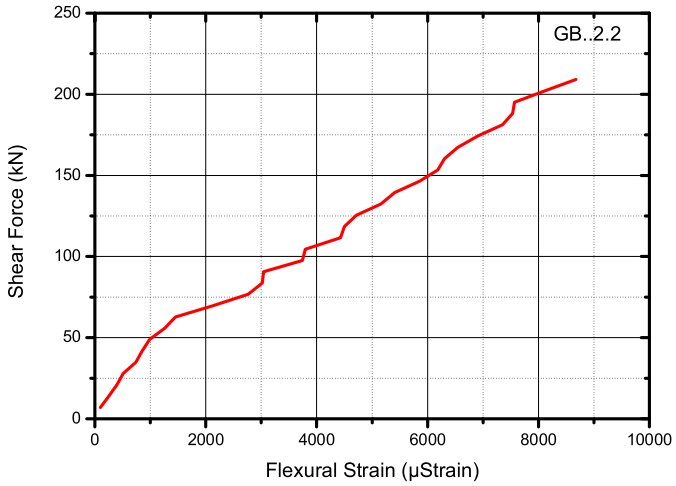

FIGURE E.20 Experimental shear force vs flexural strain relationship of specimen GB.2.2.

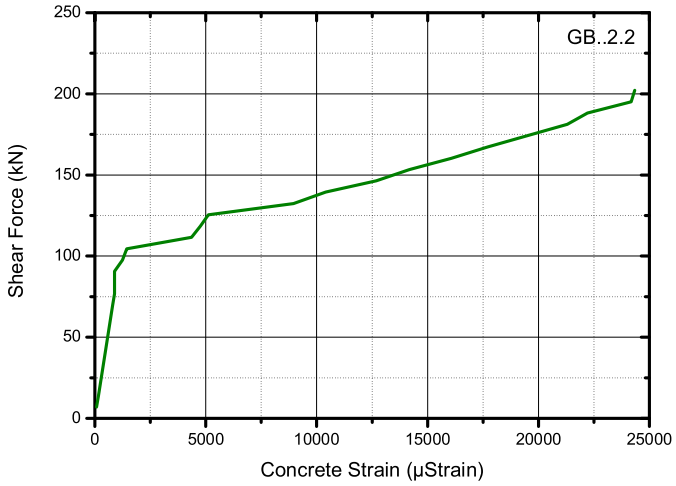

FIGURE E.21 Experimental shear force vs concrete surface strain relationship of specimen GB.2.2.

E.8 Specimen GB.3.1

TABLE E.8 Data observation of specimen GB.3.1

Sr. No.	Shear Force	Stirrup Strain	Flexural Strain	Concrete Strain	Deflection
	(kN)	(μStrain)	(μStrain)	(μStrain)	(mm)
1	6.97	34	268	90.55	2.8
2	13.94	84	522	181.1	3.16
3	20.91	112	656	271.65	3.44
4	27.88	146	758	362.2	3.68
5	34.85	168	892	452.75	3.92
6	41.82	201	1054	543.3	6.92
7	48.79	379	1140	633.85	8.56
8	55.76	679	1442	724.4	9.56
9	62.73	1023	1942	854.95	10.12
10	69.7	1576	2230	1340	12.28
11	76.67	1808	3008	2118	13.72
12	83.64	1956	3838	2390	15.56
13	90.61	2234	4276	3276	17.4
14	97.58	2675	4326	4262	18.88
15	104.55	3163	4452	5690	19.6
16	111.52	3327	4658	6582	20.44
17	**118.49**	**3578**	**4684**	**7234**	**24.88**
18	125.46	3654	4794	10510	29.4
19	132.43	3876	5084	11181	32
20	139.4	3953	5118	12176	
21	146.37	4032	5208	13788	
22	153.34	4260	5040	14201	
23	160.31	4527	5004	14738	
24	167.28	4826	4868	16326	
25	174.25	5322	4988	17574	
26	181.22	5578	4948	24352	

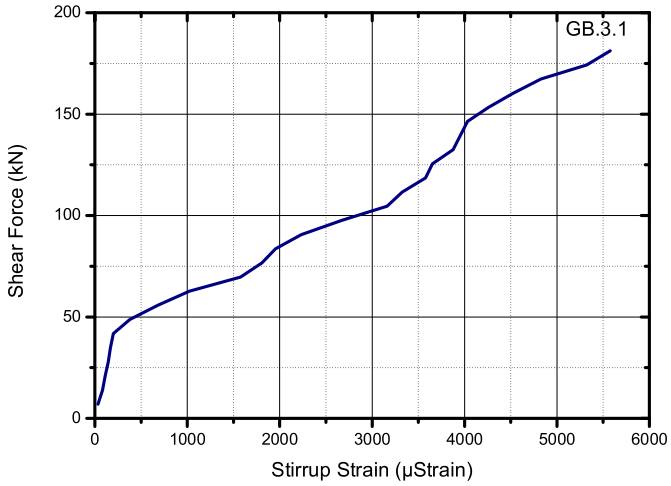

FIGURE E.22 Experimental shear force vs stirrup strain relationship of specimen GB.3.1.

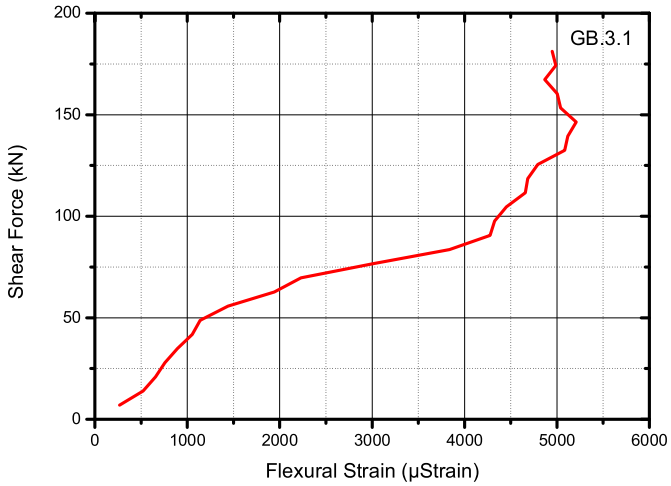

FIGURE E.23 Experimental shear force vs flexural strain relationship of specimen GB.3.1.

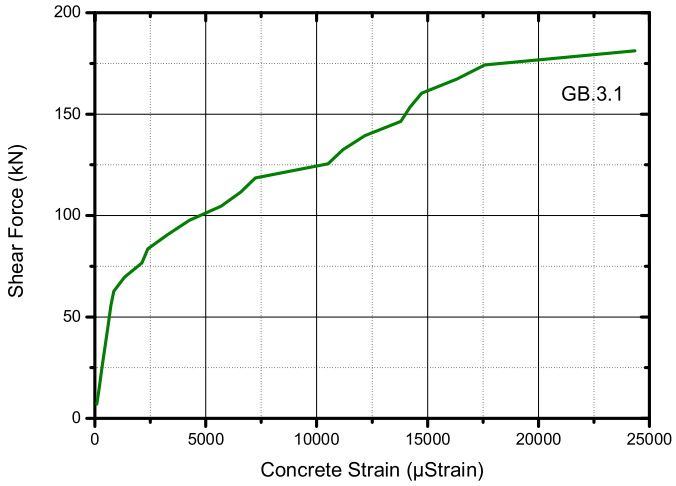

FIGURE E.24 Experimental shear force vs concrete surface strain relationship of specimen GB.3.1.

E.9 Specimen GB.3.2

TABLE E.9 Data observation of specimen GB.3.2

Sr. No.	Shear Force	Stirrup Strain	Flexural Strain	Concrete Strain	Deflection
	(kN)	(μStrain)	(μStrain)	(μStrain)	(mm)
1	6.97	46	36	93	1.96
2	13.94	95	126	186	3.48
3	20.91	109	268	279	3.92
4	27.88	127	526	372	4.88
5	34.85	148	1302	465	6
6	41.82	273	1540	558	7.08
7	48.79	396	2014	651	8.32
8	55.76	701	2272	744	10.44
9	62.73	1178	2676	837	11.76
10	69.7	1563	3116	1138	13.48
11	76.67	1857	3394	1894	15.08
12	83.64	2040	3666	2039	16.72
13	90.61	2378	3880	2686	17.32
14	97.58	2786	4010	3784	18.6
15	104.55	3866	4412	4671	21.04
16	**111.52**	**4522**	**4468**	**5815**	**21.96**
17	118.49	5028	4572	7106	24.84
18	125.46	5530	4838	9281	29.48
19	132.43	5634		10183	33.43
20	132.43			11987	
21	132.43			12345	
22	132.43			12654	
23	132.43			13252	
24	132.43			15921	
25	132.43			16999	
26	132.43			23772	

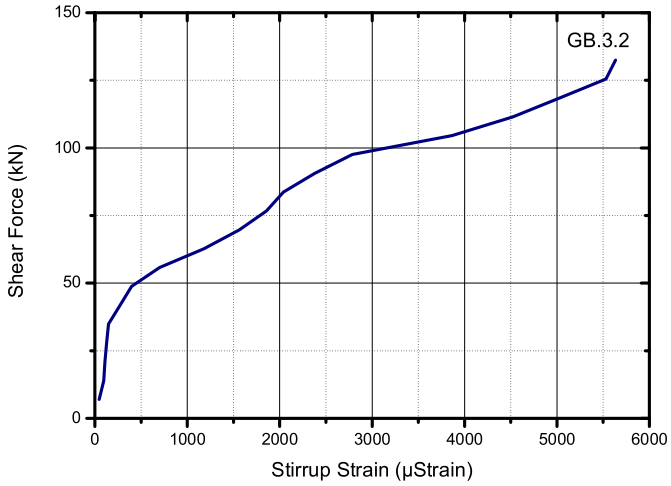

FIGURE E.25 Experimental shear force vs stirrup strain relationship of specimen GB.3.2.

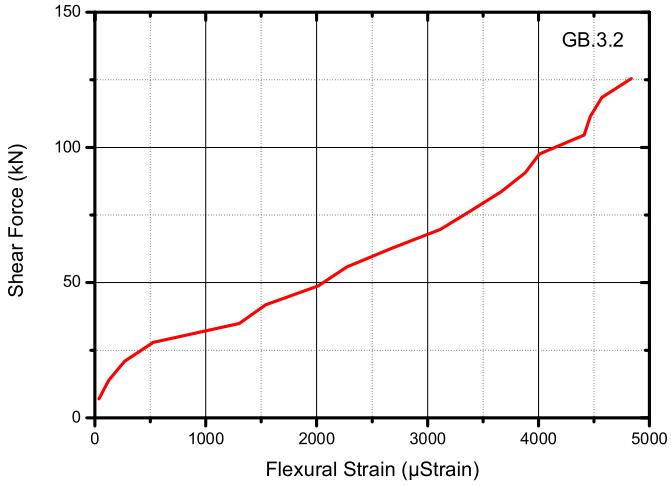

FIGURE E.26 Experimental shear force vs flexural strain relationship of specimen GB.3.2.

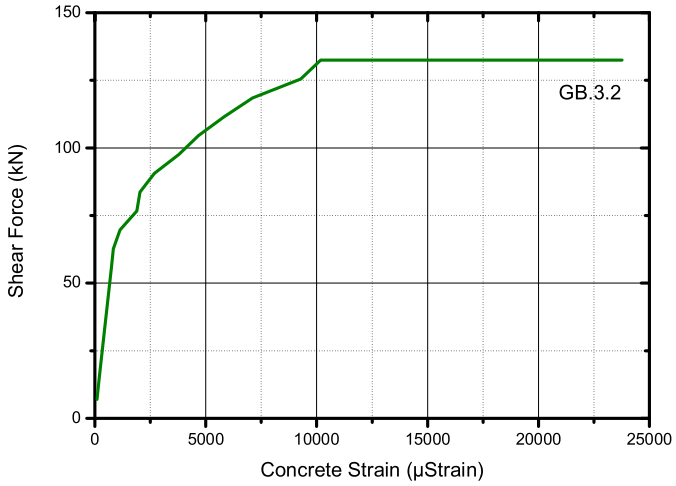

FIGURE E.27 Experimental shear force vs concrete surface strain relationship of specimen GB.3.2.

E.10 Specimen GC.4.1

TABLE E.10 Data observation of specimen GC.4.1

Sr. No.	Shear Force	Stirrup Strain	Flexural Strain	Concrete Strain	Deflection
	(kN)	(μStrain)	(μStrain)	(μStrain)	(mm)
1	6.97	87	350	80.45	2.16
2	13.94	86	432	160.9	2.68
3	20.91	127	672	241.35	3.36
4	27.88	141	970	321.8	4.32
5	34.85	158	1538	402.25	5.44
6	41.82	268	1812	482.7	6.6
7	48.79	429	2330	563.15	6.92
8	55.76	745	3142	643.6	8.24
9	62.73	976	3464	724.05	8.64
10	69.7	2289	3618	804.5	13.08
11	76.67	2802	3742	849.95	14.08
12	83.64	3897	3940	968	15.64
13	**90.61**	**4639**	**4186**	**1351**	**17.88**
14	97.58	5499	4802	1806	20.56
15	104.55		4838	2135	22.45
16	111.52		5246	3310	
17	118.49		5314	3614	
18	125.46		5500	5690	
19	132.43		5928	5910	
20	139.4		7156	7288	
21	146.37		7466	9376	
22	153.34		7698	10098	
23	160.31		8294	11290	
24	167.28		8482	20709	
25	174.25		8716	21695	
26	181.22			22440	

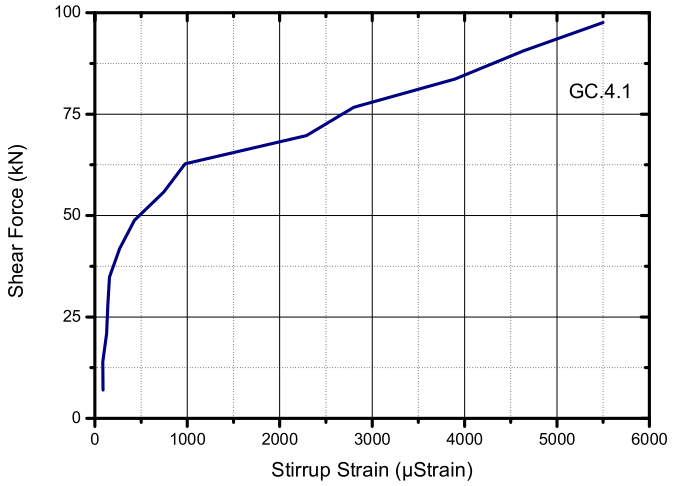

FIGURE E.28 Experimental shear force vs stirrup strain relationship of specimen GC.4.1.

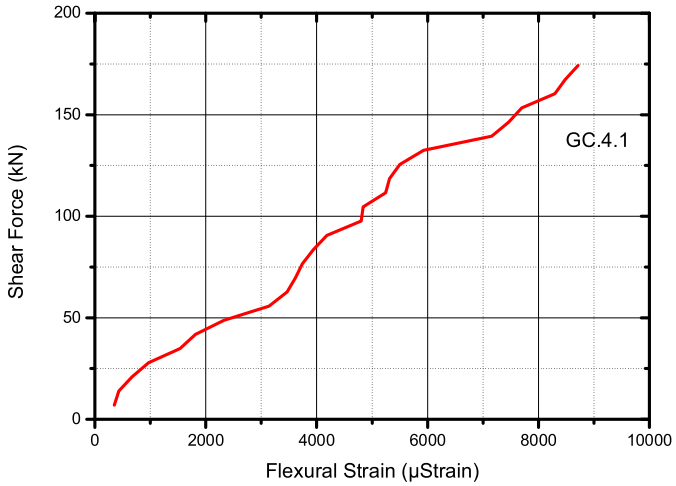

FIGURE E.29 Experimental shear force vs flexural strain relationship of specimen GC.4.1.

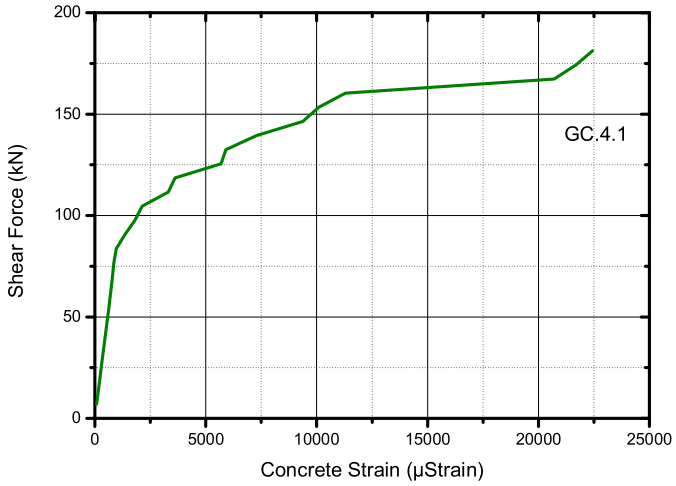

FIGURE E.30 Experimental shear force vs concrete surface strain relationship of specimen GC.4.1.

E.11 Specimen GC.4.2

TABLE E.11 Data observation of specimen GC.4.2

Sr. No.	Shear Force	Stirrup Strain	Flexural Strain	Concrete Strain	Deflection
	(kN)	(μStrain)	(μStrain)	(μStrain)	(mm)
1	6.97	45	180	85	1.92
2	13.94	98	335	170	2.92
3	20.91	124	555	255	3.72
4	27.88	131	654	340	4.8
5	34.85	149	773	425	5.28
6	41.82	254	1278	510	5.84
7	48.79	378	1434	595	8.92
8	55.76	634	2280	680	9.32
9	62.73	832	3812	765	10.08
10	69.7	1732	4226	850	11.16
11	76.67	2357	4742	890	14.24
12	83.64	2690	5089	1064	16.24
13	90.61	3634	5186	1420	17.72
14	97.58	3945	5277	1836	18.48
15	104.55	4045	5344	2084	20.04
16	**111.52**	**4246**	**5980**	**3208**	**23.36**
17	118.49	4455	6090	4464	25.96
18	125.46	4511		4970	27.4
19	132.43	4522		5218	27.96
20	139.4	4629		7178	30.76
21	146.37	4728		9346	32.72
22	153.34	4987		10068	36.88
23	160.31	5272		11260	38.8
24	167.28	5398		23120	54.36
25	174.25	5488			

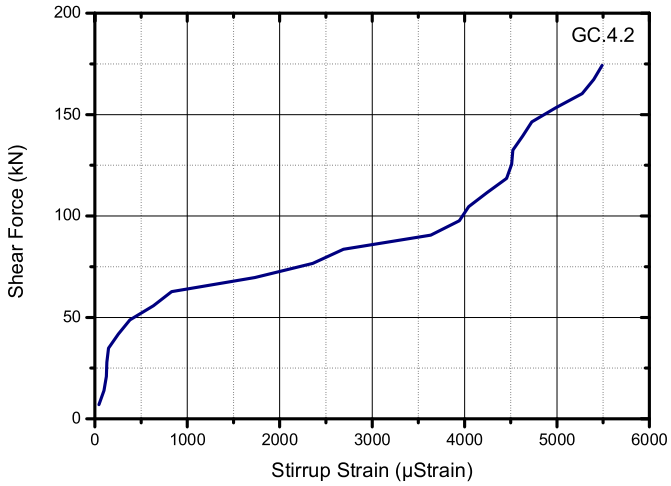

FIGURE E.31 Experimental shear force vs stirrup strain relationship of specimen GC.4.2.

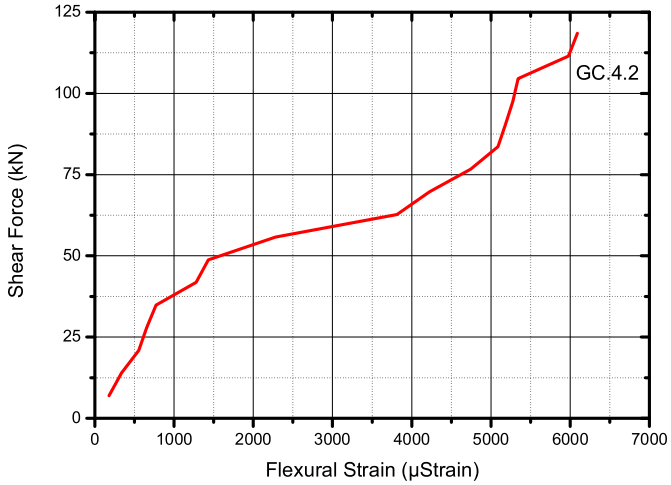

FIGURE E.32 Experimental shear force vs flexural strain relationship of specimen GC.4.2.

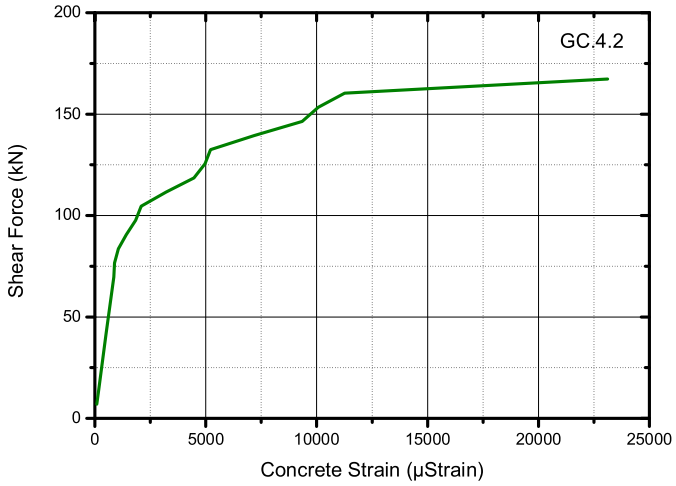

FIGURE E.33 Experimental shear force vs concrete surface strain relationship of specimen GC.4.2.

E.12 Specimen GC.5.1

TABLE E.12 Data observation of specimen GC.5.1

Sr. No.	Shear Force	Stirrup Strain	Flexural Strain	Concrete Strain	Deflection
	(kN)	(μStrain)	(μStrain)	(μStrain)	(mm)
1	6.97	43	348	90.55	2.6
2	13.94	78	445	181.1	3.08
3	20.91	111	665	271.65	3.8
4	27.88	176	978	362.2	4.08
5	34.85	185	1446	452.75	4.64
6	41.82	220	1745	543.3	7.36
7	48.79	489	2290	633.85	9.44
8	55.76	720	3050	724.4	10.16
9	62.73	910	3333	814.95	10.6
10	69.7	1876	3610	850	12.64
11	76.67	2235	3730	953	16.04
12	83.64	3490	3890	1128	16.72
13	90.61	4590	4090	1301	18.44
14	97.58	5290	4750	1391	18.88
15	**104.55**	**5820**	**4790**	**2893**	**21.04**
16	111.52	6228	5220	4394	22.04
17	118.49		5342	7198	25.11
18	125.46		5687	22451	
19	132.43		6303	23761	
20	132.43		7520		
21	132.43		7856		
22	132.43		8188		
23	132.43		8580		
24	132.43		8883		

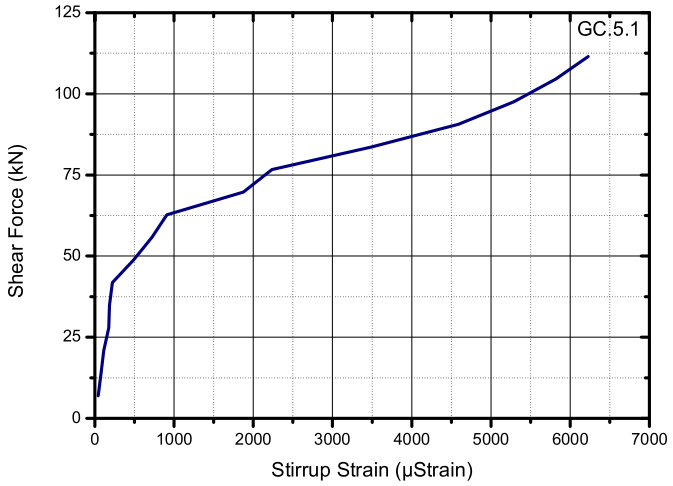

FIGURE E.34 Experimental shear force vs stirrup strain relationship of specimen GC.5.1.

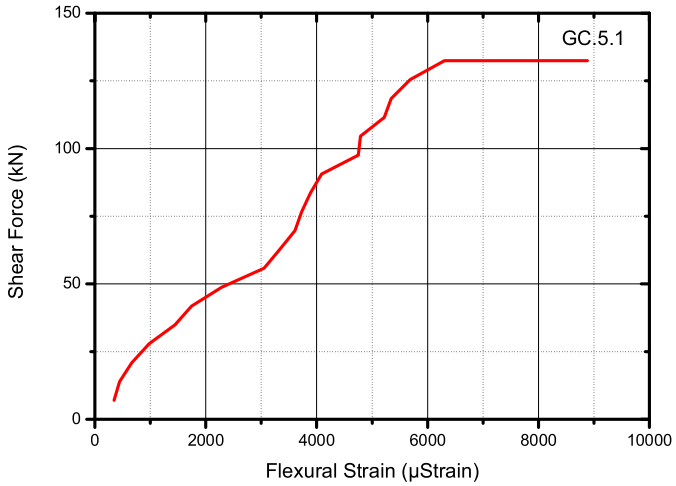

FIGURE E.35 Experimental shear force vs flexural strain relationship of specimen GC.5.1.

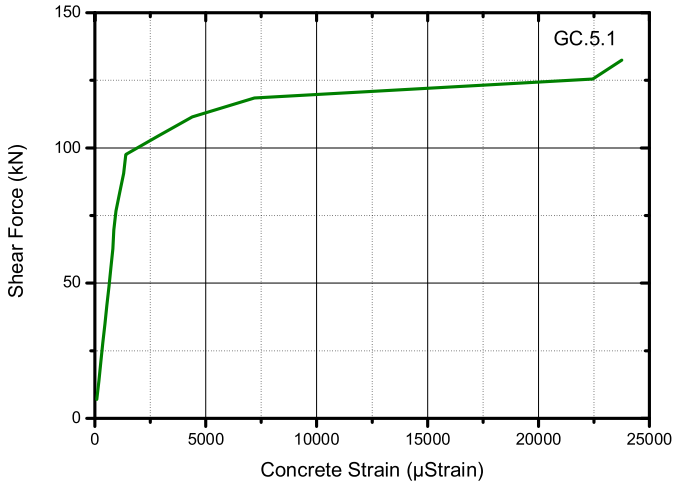

FIGURE E.36 Experimental shear force vs concrete surface strain relationship of specimen GC.5.1.

E.13 Specimen GC.5.2

TABLE E.13 Data observation of specimen GC.5.2

Sr. No.	Shear Force	Stirrup Strain	Flexural Strain	Concrete Strain	Deflection
	(kN)	(μStrain)	(μStrain)	(μStrain)	(mm)
1	6.97	74	248	70.71	1.88
2	13.94	88	342	141.42	3.4
3	20.91	99	546	212.13	3.84
4	27.88	146	656	282.84	4.8
5	34.85	185	748	353.55	5.32
6	41.82	239	1382	424.26	7.96
7	48.79	337	1502	494.97	9.12
8	55.76	723	2324	565.68	9.12
9	62.73	839	3922	636.39	9
10	69.7	1587	4334	707.1	9.68
11	76.67	2048	4874	742.81	11.72
12	83.64	3327	5134	778.52	14.16
13	90.61	4590	5238	814.23	14.96
14	97.58	5309	5384	1033.94	16.52
15	104.55	6038	5488	2782	19.6
16	**111.52**	**6534**	**6104**	**7288**	**22.36**
17	118.49	7027		11034	25.04
18	125.46	8936		24306	

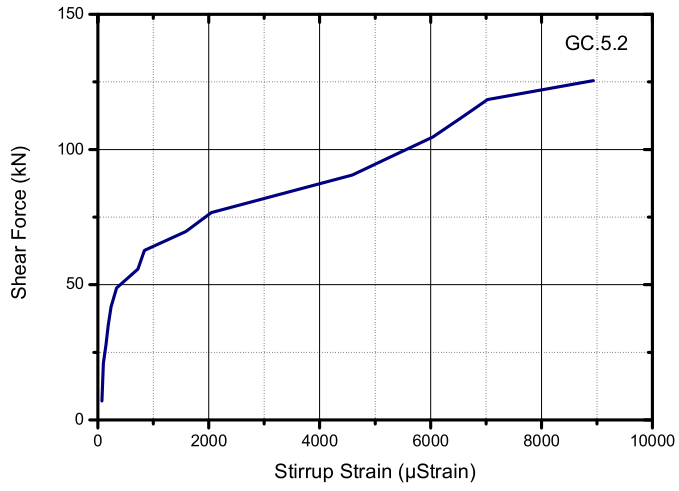

FIGURE E.37 Experimental shear force vs stirrup strain relationship of specimen GC.5.2.

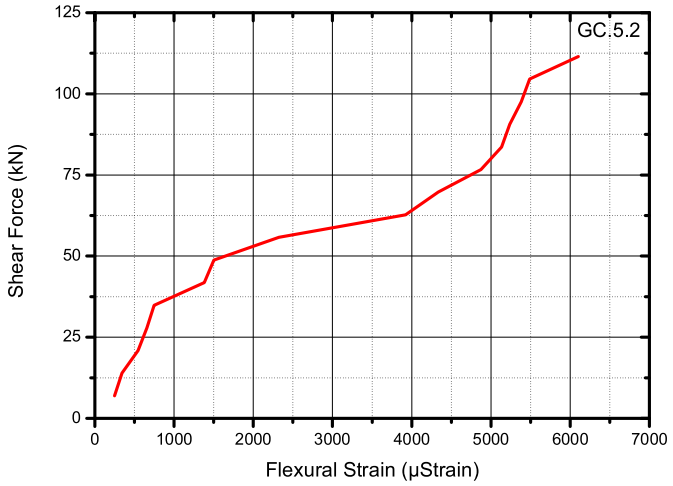

FIGURE E.38 Experimental shear force vs flexural strain relationship of specimen GC.5.2.

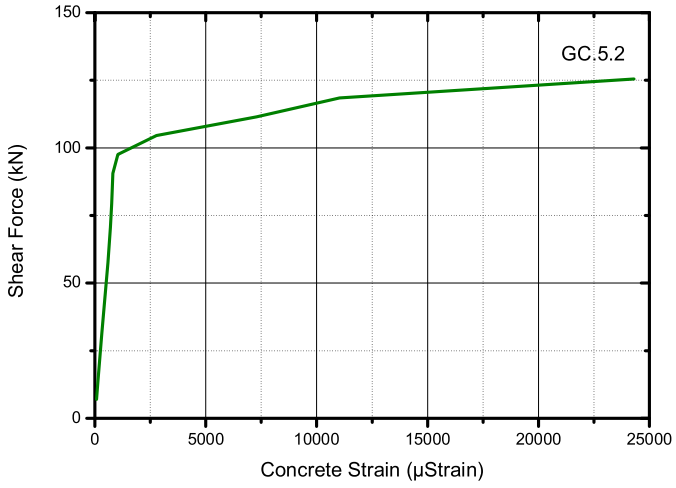

FIGURE E.39 Experimental shear force vs concrete surface strain relationship of specimen GC.5.2.

Appendix F : Calculation Sheets for Reverse Shear Capacity Evaluation of Shear Deficit Beams

TABLE F.1 Shear capacity evaluation of shear deficit beams as per ISIS Canada 2007.

Design of FRP-RC Beam ISIS Method					
Design Data					
	Span (m)	1.8	1.8	1.8	
	LL (kN/m)	35	30	29	
	Sustained load (kN/m)	0	0	0	
f'_c	Specified compressive strength of concrete (MPa)	30	30	30	
ε_{cu}	Ultimate strain in concrete	0.003	0.003	0.003	
f^*_{fu}	Tensile Strength (Mpa)	905	905	905	
ε^*_{fu}	Rupture Strain	0.0152	0.0152	0.0152	
E_f	Modulus of Elasticity (Mpa)	47300	47300	47300	
C_E	Reduction Factor Table 7.1 (ACI-440.1R-06)	0.8	0.8	0.8	
β_1	Factor	0.85	0.85	0.85	
a	Distance of loading	0.5	0.65	0.75	
h	Overall Height of Member	300	300	300	
S	Spacing of stirrup	250	300	325	
Assumptions					
b	Width of beam (mm)	112.84	112.84	150.26	
	Width of beam provided (mm)	230	230	230	
D	Depth of beam (mm)	300	300	300	
	Cover (mm)	25	25	25	
	Longi. Bar Dia. (mm)-1	18.71	18.71	18.71	
	Longi. Bar Dia. (mm)-2	15.25	15.25		
	No of Longi. Bar-1	2	2	3	
	No of Longi. Bar-2	1	1		
	Stirrups Dia. (mm)	**9.5**	**9.5**	**9.5**	
	Density of Concrete (kN/m^3)	24	24	24	
	Load Factor (DL)	1	1	1	
	Load Factor (LL)	1	1	1	

k_b	for deformed FRP bars	1.4	1.4	1.4	
A_f	area of FRP reinforcement (mm^2)	733	733	825	
A_{fv}	area of FRP stirrups reinforcement (mm^2)	71	71	71	
d	Effective Depth	256	256	256	
Load Calculation					
	Self Wt. Of Beam(KN/m)	1.66	1.66	1.66	
W_{DL}	Dead Load (kN/m)	1.66	1.66	1.66	
MU	Total Moment	18.33	20.33	22.58	
Design Rupture Stress of FRP Bars					
f_{fu}	Design Rupture Stress	724.00	724.00	724.00	$f^*_{fu}\ C_E$
Determine the Area of FRP Bars Required for Flexural Strength					
ρ_{fb}	FRP reinforcement ratio producing balanced strain conditions	0.0049	0.0049	0.0049	$\rho_{fb} = 0.85\frac{f'_c}{f_{fu}}\beta_1\frac{E_f\varepsilon_{cu}}{E_f\varepsilon_{cu}+f_{fu}}$
					$\rho_f = \frac{A_f}{bd}$
ρ_f	FRP reinforcement ratio	0.0124	0.0124	0.0140	
f_f	Stress in FRP reinforcement in tension (Mpa)	431.44	431.44	403.09	$f_f = \left[\sqrt{\frac{(E_f\varepsilon_{cu})^2}{4}+\frac{0.85\beta_1 f'_c}{\rho_f}E_f\varepsilon_{cu}}-0.5E_f\varepsilon_{cu}\right]$
M_n	Nominal moment capacity (kN. M)	72.41	72.41	75.71	$M_n = \rho_f f_f\left(1-0.59\frac{\rho_f f_f}{f'_c}\right)bd^2$
					$\phi = 0.30+\frac{\rho_f}{4\rho_{fb}}$ for $\rho_{fb} < \rho_f \le 1.4\rho_{fb}$
ϕ	Strength reduction factor	0.93	0.93	1.01	
	$\phi\ M_n$	67.60	67.60	76.73	
	Check $\phi\ M_n \ge M_u$	OK	OK	OK	
Design of Shear					
V_c		20.4001	20.4001	20.4001	$V_c = 0.2\lambda\Phi_c\sqrt{f'_c}b_w d\sqrt{\frac{E_{frp}}{E_s}}$

σ_v		181	181	181	$\sigma_v = \frac{\left(0.05\frac{r_b}{d_b} + 0.3\right) f_{frpv}}{1.5}$
ε_v		0.00125	0.00125	0.00132	$\varepsilon_{fv} = 0.0001\sqrt{f'_c \frac{\rho_{frp} E_{frp}}{\rho_{frpv} E_{frpv}}\left[1 + 2\left(\frac{\sigma_N}{f'_c}\right)\right]} \leq 0.0025$
σ_v		58.8914	58.8914	62.491	$\sigma_v = E_{frpb}\varepsilon_v$
	Minimum σ_v	58.8914	58.8914	62.491	
V_{frp}		6.41544	5.3462	5.23659	$V_{FRP} = \varphi_{frp}\frac{A_{fv}\,\sigma_v d_v \cot\theta}{s}$
V_r		26.8156	25.7463	25.6367	

TABLE F.2 Shear capacity evaluation of shear deficit beams as per JSCE 1997.

Design of FRP-RC Beam JSCE Method					
Design Data					
	Span (m)	1.8	1.8	1.8	
	LL (kN/m)	35	30	29	
	Sustained load (kN/m)	0	0	0	
f'_c	Specified compressive strength of concrete (MPa)	30	30	30	
ε_{cu}	Ultimate strain in concrete	0.003	0.003	0.003	
f^*_{fu}	Tensile Strength (Mpa)	905	905	905	
ε^*_{fu}	Rupture Strain	0.0152	0.0152	0.0152	
E_f	Modulus of Elasticity (Mpa)	47300	47300	47300	
C_E	Reduction Factor Table 7.1 (ACI-440.1R-06)	0.8	0.8	0.8	
β_1	Factor	0.85	0.85	0.85	
a	Distance of loading	0.5	0.65	0.75	
h	Overall Height Of Member	300	300	300	
S	Spacing of stirrup	250	275	325	
Assumptions					
b	Width of beam (mm)	112.84	112.84	150.26	
	Width of beam provided (mm)	230	230	230	
D	Depth of beam (mm)	300	300	300	
	Cover (mm)	25	25	25	
	Longi. Bar Dia. (mm)-1	18.71	18.71	18.71	
	Longi. Bar Dia. (mm)-2	15.25	15.25		
	No of Longi. Bar-1	2	2	3	
	No of Longi. Bar-2	1	1		
	Stirrups Dia. (mm)	**9.5**	**9.5**	**9.5**	
	Density of Concrete(kN/m^3)	24	24	24	
	Load Factor (DL)	1	1	1	
	Load Factor (LL)	1	1	1	
k_b	for deformed FRP bars	1.4	1.4	1.4	
A_f	Area of FRP reinforcement (mm^2)	733	733	825	

A_{fv}	area of FRP stirrups reinforcement (mm^2)	71	71	71	
d	Effective Depth	256	256	256	
Load Calculation					
	Self Wt. Of Beam(KN/m)	1.66	1.66	1.66	
W_{DL}	Dead Load (kN/m)	1.66	1.66	1.66	
MU	Total Moment	18.33	20.33	22.58	
Design Rupture Stress of FRP Bars					
f_{fu}	Design Rupture Stress	724.00	724.00	724.00	$f^*_{fu}\ C_E$
Determine the Area of FRP Bars Required for Flexural Strength					
ρ_{fb}	FRP reinforcement ratio producing balanced strain conditions	0.0049	0.0049	0.0049	$\rho_{fb} = 0.85\frac{f'_c}{f_{fu}}\beta_1\frac{E_f\varepsilon_{cu}}{E_f\varepsilon_{cu}+f_{fu}}$
ρ_f	FRP reinforcement ratio	0.0124	0.0124	0.0140	$\rho_f = \frac{A_f}{bd}$
f_f	Stress in FRP reinforcement in tension (Mpa)	431.44	431.44	403.09	$f_f = \left[\sqrt{\frac{(E_f\varepsilon_{cu})^2}{4}+\frac{0.85\beta_1 f'_c}{\rho_f}E_f\varepsilon_{cu}}-0.5E_f\varepsilon_{cu}\right]$
M_n	Nominal moment capacity (kN. M)	72.41	72.41	75.71	$M_n = \rho_f f_f\left(1-0.59\frac{\rho_f f_f}{f'_c}\right)bd^2$
ϕ	Strength reduction factor	0.93	0.93	1.01	$\phi = 0.30+\frac{\rho_f}{4\rho_{fb}}$ for $\rho_{fb} < \rho_f \le 1.4\rho_{fb}$
	$\phi\ M_n$	67.60	67.60	76.73	
	Check $\phi\ M_n \ge M_u$	OK	OK	OK	
Design of Shear					
f_{cvd}		0.62145	0.62145	0.62145	$f_{cvd} = 0.2(f'c)^{1/3} \le 0.72\ N/mm^2$
β_d		1.40565	1.40565	1.40565	$\beta_d = (1000/d)^{1/4} \le 1.5$
β_p		0.66499	0.66499	0.69182	$\beta_p = (100\,\rho_{fl}E_{fl}/E_s)^{1/3} \le 1.5$

					$\beta_n = 1 + M_o/M_d\ \beta_n \le 2\ for\ N_f \ge 0$
β_n		2	3	4	$\beta_n = 1 + 2\ M_o/M_d\ \beta_n \le 2\ for\ N_f \ge 0$
V_c		26.325	26.325	27.387	$V_c = \beta_d \beta_p \beta_n f_{cvd}\ bd\ /\ \gamma_b$
f_{mcd}		30	30	30	$f'_{mcd} = \left(\frac{h}{300}\right)^{-1/10} f'_{cd}$
σ_N		4.58032	4.58032	4.81854	$\sigma_N = N_f\ /\ A_g \le 0.4\ f'_{mcd}$
ε_{fv}		0.00123	0.00129	0.00149	$\varepsilon_{fv} = 0.0001 \sqrt{f'_{mcd} \frac{\rho_f E_{fv}}{\beta_p E_{fv}} \left[1 + 2\left(\frac{\varepsilon_p}{f'_{mcd}}\right)\right]} \le f_{FRPbend} / E_{fv}$
ε_{fv}		0.003827	0.003827	0.003827	$\varepsilon_{fv} = f_{FRPbend}\ /\ E_{fv}$
V_{FRP}		6.38993	6.09256	5.94689	$V_{FRP} = [A_{fv}\ E_{fv}\ \varepsilon_{fv}\ (\sin\alpha s + \cos\alpha s)\ /\ s]\ z\ /\ \gamma_b$
V_r		32.7149	32.4175	33.3339	

TABLE F.3 Shear capacity evaluation of shear deficit beams as per ACI 2006.

Design of FRP-RC Beam ACI Method					
Design Data					
	Span (m)	2	2	2	
	LL (kN/m)	35	30	29	
	Sustained load (kN/m)	0	0	0	
f'_c	Specified compressive strength of concrete (MPa)	30	30	30	
ε_{cu}	Ultimate strain in concrete	0.003	0.003	0.003	
f^*_{fu}	Tensile Strength (Mpa)	905	905	905	
ε^*_{fu}	Rupture Strain	0.0152	0.0152	0.0152	
E_f	Modulus of Elasticity (Mpa)	47300	47300	47300	
C_E	Reduction Factor Table 7.1 (ACI-440.1R-06)	0.8	0.8	0.8	
β_1	Factor	0.85	0.85	0.85	
a	Distance of loading	0.5	0.65	0.75	
h	Overall Height Of Member	300	300	300	
S	Spacing of stirrup	250	275	325	
Assumptions					
b	Width of beam (mm)	112.84	112.84	150.26	
	Width of beam provided (mm)	230	230	230	
D	Depth of beam (mm)	300	300	300	
	Cover (mm)	25	25	25	
	Longi. Bar Dia. (mm)-1	18.71	18.71	18.71	
	Longi. Bar Dia. (mm)-2	15.25	15.25		
	No of Longi. Bar-1	2	2	3	
	No of Longi. Bar-2	1	1		
	Stirrups Dia. (mm)	**9.5**	**9.5**	**9.5**	
	Density of Concrete(kN/m^3)	24	24	24	
	Load Factor (DL)	1	1	1	
	Load Factor (LL)	1	1	1	
k_b	for deformed FRP bars	1.4	1.4	1.4	
A_f	area of FRP reinforcement (mm^2)	733	733	825	
A_{fv}	area of FRP stirrups reinforcement (mm^2)	71	71	71	
d	Effective Depth	256	256	256	
r_b		40	40	40	

Load Calculation					
	Self Wt. Of Beam(KN/m)	1.66	1.66	1.66	
W_{DL}	Dead Load (kN/m)	1.66	1.66	1.66	
MU	Total Moment	18.33	20.33	22.58	
Design Rupture Stress of FRP Bars					
f_{fu}	Design Rupture Stress	724.00	724.00	724.00	$f^*_{fu}\ C_E$
Determine the Area of FRP Bars Required for Flexural Strength					
ρ_{fb}	FRP reinforcement ratio producing balanced strain conditions	0.0049	0.0049	0.0049	$\rho_{fb} = 0.85\frac{f'_c}{f_{fu}}\beta_1\frac{E_f\varepsilon_{cu}}{E_f\varepsilon_{cu}+f_{fu}}$
ρ_f	FRP reinforcement ratio	0.0124	0.0124	0.0140	$\rho_f = \frac{A_f}{bd}$
f_f	Stress in FRP reinforcement in tension (Mpa)	431.44	431.44	403.09	$f_f = \left[\sqrt{\frac{(E_f\varepsilon_{cu})^2}{4}+\frac{0.85\beta_1 f'_c}{\rho_f}E_f\varepsilon_{cu}}-0.5E_f\varepsilon_{cu}\right]$
M_n	Nominal moment capacity (kN. M)	72.41	72.41	75.71	$M_n = \rho_f f_f\left(1-0.59\frac{\rho_f f_f}{f'_c}\right)bd^2$
ϕ	Strength reduction factor	0.93	0.93	1.01	$\phi = 0.30+\frac{\rho_f}{4\rho_{fb}}$ for $\rho_{fb} < \rho_f \le 1.4\rho_{fb}$
	$\phi\ M_n$	67.60	67.60	76.73	
	Check $\phi\ M_n \ge M_u$	OK	OK	OK	
Design for Shear					
V_u	Factored shear force at section	36.23	31.23	30.23	$V_u = \frac{w_u\ell}{2}-w_u d$
c		48.98	48.98	51.64	c = kd
V_c	Nominal shear strength provided by concrete	24.68	24.68	26.02	$V_c = \frac{2}{5}\sqrt{f'_c}\,b_w c$
f_{fb}	Strength of bent portion of FRP bar	325.8	325.8	325.80	$f_{fb} = \left(0.05\frac{r_b}{d_b}+0.3\right)f_{fu}$

f_{fv}	The design stress of FRP stirrup is limited to:	212.85	212.85	212.85	$f_{fv} = 0.004E_f \leq f_{fb}$
s	Spacing provided	275	300	350	
V_r		39.59	37.83	36.08	